SANDIA REPORT
SAND2009-0874
Unlimited Release
Printed March 2009

Analyses to Support Development of Risk-Informed Separation Distances for Hydrogen Codes and Standards

Jeffrey LaChance[1], William Houf[1], Bobby Middleton[1], and Larry Fluer[2]

[1]Sandia National Laboratories
[2]Fluer, Inc.

Prepared by
Sandia National Laboratories
Albuquerque, New Mexico 87185 and Livermore, California 94550

Sandia is a multi-program laboratory operated by Sandia Corporation,
a Lockheed Martin Company, for the United States Department of Energy's
National Nuclear Security Administration under Contract DE-AC04-94AL85000.

Issued by Sandia National Laboratories, operated for the United States Department of Energy by Sandia Corporation.

Available to DOE and DOE contractors from
U.S. Department of Energy
Office of Scientific and Technical Information
P.O. Box 62
Oak Ridge, TN 37831

Telephone: (865)576-8401
Facsimile: (865)576-5728
E-Mail: reports@adonis.osti.gov
Online ordering: http://www.osti.gov/bridge

Available to the public from
U.S. Department of Commerce
National Technical Information Service
5285 Port Royal Rd
Springfield, VA 22161

Telephone: (800)553-6847
Facsimile: (703)605-6900
E-Mail: orders@ntis.fedworld.gov
Online order: http://www.ntis.gov/help/ordermethods.asp?loc=7-4-0#online

SAND2008-0874
Unlimited Release
Printed March 2009

Analyses to Support Development of Risk-Informed Separation Distances for Hydrogen Codes and Standards

Jeffrey LaChance[1], William Houf[2], Bobby Middleton[1],
and Larry Fluer[3]

[1]Sandia National Laboratories, P.O. Box 5800, Albuquerque, NM, 87185-0748
[2]Sandia National Laboratories, P.O. Box 969, Livermore, CA, 94551-0969
[3]Fluer, Inc., 2550 Niderer Road, Paso Robels, CA, 93446-8603

Abstract

The development of a set of safety codes and standards for hydrogen facilities is necessary to ensure they are designed and operated safely. To help ensure that a hydrogen facility meets an acceptable level of risk, code and standard development organizations are utilizing risk-informed concepts in developing hydrogen codes and standards.

This report describes the application of a risk-informed process to establish one code requirement: the separation distances between a bulk gaseous hydrogen storage facility and the public at large. A risk-informed process, as opposed to a risk-based process, utilizes risk insights obtained from quantitative risk assessments (QRAs) combined with other considerations to establish code requirements. The QRAs are used to identify and quantify scenarios for the unintended release of hydrogen, identify the significant risk contributors at different types of hydrogen facilities, and to identify potential accident prevention and mitigation strategies to reduce the risk to acceptable levels. Other considerations used in this risk-informed process include the results of deterministic analyses of selected accidents scenarios, the frequency of leakage events at hydrogen facilities, and the use of safety margins to account for uncertainties.

The risk-informed approach results in a defensible technical basis for specifying separation distances for hydrogen facilities. The results also demonstrate that separation distances for hydrogen facilities can be significantly affected by facility design parameters such as the system operating pressure and available mitigating features, component leakage frequency data, and the selected consequence measures and risk guidelines used in the evaluation. The separation distances generated in this report have been accepted for incorporation into revisions of several hydrogen facility standards.

Acknowledgements

This work was supported by the U. S. Department of Energy, Office of Energy Efficiency and Renewable Energy, Hydrogen, Fuel Cells and Infrastructure Technologies Program. The authors wish to thank Marty Gresho for his guidance of the NFPA 2 Technical Group 6 (TG6) charged with establishing the basis for the separation distances incorporated into NFPA 2. In addition, the authors wish to also acknowledge the other members of NFPA 2 TG6 who provided guidance on the selected methodology and critical input into the analysis. The study could not have been performed without the data and facility design information provided by David Farese and Peter Steiner of Air Products and Chemicals, Inc.

Contents

Figures

Tables

Acronyms

API	American Petroleum Institute
BLEVE	Boiling Liquid Expanding Vapor Explosion
CDF	Cumulative Distribution Function
CG	Compressed Gas
CNG	Compressed Natural Gas
DOE	Department of Energy
EIGA	European Industrial Gas Association
EIHP	European Integrated Hydrogen Project
HSE	Health and Safety Executive
ICC	International Code Council
ID	Inside Diameter
IFC	International Fire Code
ISO	International Organization for Standardization
LD50	Lethal Dose 50
LFL	Lower Flammability Limit
MLE	Maximum Likelihood Estimate
NFPA	National Fire Protection Association
NRC	Nuclear Regulatory Commission
OSHA	Occupational Safety and Health Administration
P&ID	Piping and Instrumentation Diagram
QRA	Quantitative Risk Assessment
SDO	Standards Development Organization
SNL	Sandia National Laboratories

Nomenclature

b	Coefficient for hydrogen in the Abel-Nobel equation of state (7.691 x 10^{-3} m^3/kg)
Btu	British thermal unit
C*	Non-dimensional radiant power
CH_4	Methane
C_2H_2	Acetylene
C_2H_4	Ethylene
C_3H_8	Propane
d_{eff}	The effective diameter, m
d_j	Jet exit diameter, m
d*	Jet momentum diameter, m
D_{rad}	Radiation distance, m
FLA	Fractional leak area (ratio of the leak area to the total flow area of the pipe)
Fr_f	Froude number (dimensionless parameter based on the ratio of momentum effects to buoyancy effects)
f_s	Mass fraction of fuel at stoichiometric conditions
g	Acceleration due to gravity (9.8 m/sec^2)
H_2	Molecular hydrogen
hr	hour
K	The entrainment constant
K_c	The entrainment constant for a round jet
L_{vis}	Visible flame length, m
L*	Non-dimensional flame length
LF	Leak frequency
LFL	Lower flammability limit
LFL_{DPF}	Lower flammability limit for a downward propagating flame
LFL_{UPF}	Lower flammability limit for an upward propagating flame
m_{fuel}	Total fuel mass flow rate, kg/sec
$m_{fuel}\triangle H_c$	Total heat released due to chemical reaction, W
p_j	The jet exit pressure, bar
p_{supply}	The pressure in the supply, bar
p_{tank}	The pressure in the tank, bar
p_∞	The ambient pressure, bar
$q_{rad}(x,r)$	The radiant heat flux measured at a particular axial location, x, and radial location, r, W/m^2
r	Radial position, m
R_{H2}	Gas constant for hydrogen (4124.18 J/kg/K)
R_u	Universal gas constant (8314.34 J/kmol/K)
R_{max}	The maximum radial position from the flame centerline for the given heat flux level, m
S_{rad}	The total emitted radiative power, W
T_{ad}	Adiabatic flame temperature of hydrogen in air (2390K)
u_j	Jet exit velocity, m/sec

u_{eff}	The effective velocity at the end of expansion, m/sec
x	Axial position, m
x_o	The virtual origin of the jet, m
$X(R_{max})$	The axial location at which the maximum heat flux level occurs, m
X_{rad}	The radiant fraction or the fraction of the total chemical heat release that is radiated to the surroundings
W_f	Flame width, m
W_{mix}	Mean molecular weight of the products of stoichiometric combustion of hydrogen in air (24.54 kg/kmol)
Z	The compressibility factor [$Z = p/(\rho RT)$]
$\triangle H_c$	Heat of combustion, J/kg
$\triangle T_f$	Peak flame temperature rise due to combustion heat release, K
α_2	Parameter relating mean leak frequency to FLA
α_1	Scaling parameter for the exponential function relating μ_{LF} and FLA.
π	Pi
ρ_f	Flame density, kg/m^3
ρ_{gas}	The density of the exiting gas evaluated at ambient temperature and pressure, kg/m^3
ρ_j	Jet exit density, kg/m^3
(ρ_j/ρ_∞)	Ratio of jet gas density to ambient gas density
ρ_∞	Density of the ambient fluid, kg/m^3
$\overline{\eta}_{cl}$	Volume fraction (mole fraction) along the centerline of the jet
μ_{LF}	Mean of the recorded leak frequency
τ	Precision of the distribution describing the recorded leak frequency
τ_f	Global flame residence time, sec
$\chi^2_{.r}(A)$	r^{th} percentile of the Chi-square distribution with A degrees of freedom

Analyses to Support Development of Risk-Informed Separation Distances for Hydrogen Codes and Standards

1. Introduction

The development of a set of safety codes and standards for hydrogen facilities is necessary to ensure that those facilities are designed and operated safely. To help ensure that a hydrogen facility meets an acceptable level of risk, code and standard development are utilizing risk-informed concepts in developing hydrogen codes and standards.

1.1 Background

The use of hydrogen as an energy carrier on a large-scale commercial basis, while integral to the future hydrogen economy, is currently underdeveloped. The development of an infrastructure for the future hydrogen economy will require the simultaneous development of a set of codes and standards to establish guidelines for building this structure. Such codes and standards are necessary to assure that related products and systems are safe and perform as designed.

Several standard development organizations (SDOs) are working to modify existing codes and standards and draft new ones related to the use of hydrogen as an automobile fuel and also for other electrical generation applications (i.e., stationary fuel cell applications). The SDOs include the National fire Protections Association (NFPA), the International Code Council (ICC), and the International Organization for Standardization (ISO). Their efforts include re-establishing the bases for some requirements in existing standards such as separation distances. For example, the NFPA has launched an effort to compile all requirements for hydrogen applications into one model code, NFPA 2, Hydrogen Technologies. The Technical Committee for NFPA 2 is systematically reviewing all NFPA model codes and standards related to hydrogen as part of this compilation. In addition, the Committee has created a number of task groups to assess the technical foundations of requirements in these codes and standards. One of these task groups (Task Group 6) is examining the technical bases for separation distances and is applying recent research on hydrogen behavior and quantitative risk assessments (QRA) techniques as part of this examination.

In addition, several groups have been established to coordinate the development and implementation of a consistent set of hydrogen-related codes and standards. Three examples in the U.S. are the National Hydrogen and Fuel Cells Codes and Standards Coordinating Committee, managed by the National Renewable Energy Laboratory, the National Hydrogen Association, and the U.S. Fuel Cell Council, and the independent Hydrogen Industry Panel on Codes, which focuses on harmonizing requirements in NFPA and the ICC model codes. In addition, the U.S. FreedomCAR and Fuel

Partnership have created a Codes and Standards Technical Team to coordinate the research and development needed to establish a scientific foundation for requirements in hydrogen and fuel codes and standards. The Codes and Standards Working Group of the Canadian Transportation Fuel Cell Alliance has a similar charter in Canada. A common theme in the efforts of the SDOs and industry cooperation groups is the establishment of science-based codes and standards that will ensure public safety from the use of hydrogen as a fuel. The use of a risk-informed process is one way to establish the requirements in these new codes and standards necessary to ensure public safety.

As part of the U.S. Department of Energy (DOE) Hydrogen, Fuel Cells & Infrastructure Technologies Program, Sandia National Laboratories is developing the technical basis for assessing the safety of hydrogen-based systems for use in the development/modification of relevant codes and standards. The project impacts most areas of hydrogen utilization, including bulk transportation and distribution, storage, production and utilization. Sandia is developing benchmark experiments and a defensible analysis strategy for risk and consequence assessment of unintended releases from hydrogen systems. This work includes experimentation and modeling to understand the fluid mechanics and dispersion of hydrogen for different release scenarios, including investigations of hydrogen combustion and subsequent heat transfer from hydrogen flames. The resulting technical information is incorporated into engineering models that are used for assessment of different hydrogen release scenarios and for input into QRAs of hydrogen facilities.

The QRAs are used to quantify the risk associated with unintended releases of hydrogen, to identify the significant risk contributors at different types of hydrogen facilities, and to identify potential accident prevention and mitigation strategies to reduce the risk to acceptable levels. The performance and use of the QRA analysis requires modeling of different types of accident scenarios, selection of appropriate component failure data, the selection and evaluation of different consequence measures, and the selection of risk criteria for use in making decisions. In addition, parametric and uncertainty studies are performed to identify the effect of selected parameters and assumptions on the resulting separation distances. The results of the QRAs are one input into a risk-informed codes and standards development process that can also include other considerations by the code and standard developers.

1.2 Objectives and Scope

This report describes the application of QRA methods to help establish one key code requirement: the minimum separation distances between a bulk gaseous hydrogen storage facility and other facilities and the public at large that help reduce the potential for injury and facility damage. Hydrogen facilities usually must comply with these separation distances (also referred to in the literature as setback or safety distances) in order to be permitted for operation. The results of this QRA application demonstrated the utility of a risk-informed approach to help establish separation distances and identified key facility design parameters and important modeling parameters that can influence those distances. The analysis helped focus the efforts of NFPA 2 Task Group 6 (TG6) and the results have been used to help establish separation distances for incorporation

into a new NFPA hydrogen code - NFPA 2 and into a revision of the existing NFPA 55 [1]. The developed methods, data, and results are available for use by other SDOs to help achieve one of the goals of the U.S. DOE Hydrogen, Fuel Cells & Infrastructure Technologies Program, harmonization of the technical requirements in the different codes and standards.

The existing analysis performed to support separation distances was limited to releases from hydrogen gas storage facilities located outside. The external location was assumed to preclude hydrogen buildup leading to explosions. Thus, only the consequences associated with hydrogen jets were considered in this assessment. Releases resulting from human errors or external events such as earthquakes were not explicitly included but are implicitly included by the use of actual leakage events in gaseous hydrogen facilities. Furthermore, releases from liquid hydrogen components have not been analyzed.

1.3 Summary of Analysis Methods

A risk-informed process was used to establish the separation distances for bulk gaseous hydrogen storage areas. This process follows guidance by the Fire Protection Research Foundation published in March 2007 that encourages NFPA Technical Committees to use risk concepts in their decision making process [2]. A risk-informed process, as opposed to a risk-based process, utilizes risk insights obtained from QRAs combined with other considerations to establish code requirements. The QRAs are used to identify and quantify scenarios for the unintended release of hydrogen, identify the significant risk contributors at different types of hydrogen facilities, and to identify potential accident prevention and mitigation strategies to reduce the risk to acceptable levels. Other considerations used in this risk-informed process include the results of deterministic analyses of selected accident scenarios, the frequency of leakage events at hydrogen facilities, and the use of safety margins to account for uncertainties. The risk-informed approach resulted in a defensible technical basis for specifying the separation distances in NFPA 2 and NFPA 55 and is available for use in other hydrogen standards.

1.4 Report Organization

Background information on separation distances is presented in Section 2 of this report. Example separation distances and the parameters used to define them and options for establishing new separation distances are provided. Section 3 provides a description of the risk-informed approach used for determining separation distances. The basis for this approach involves a deterministic evaluation of separation distances as a function of hydrogen pressure and leak diameters for different components. Selection of the appropriate leak diameter is based on statistical analysis (presented in Section 4) of component leakage rates and risk evaluations (presented in Section 5). Failure data for hydrogen components and typical gaseous storage facility descriptions that were used in the analysis were provided by industry participants. Uncertainty in the data analysis and risk evaluations is also addressed in Sections 4 and 5. A summary of the results are provided in Section 6. Details on the deterministic consequence model, example facility

used in the evaluations, leak frequency calculations, and the QRA risk models are provided in the appendices.

2. Hydrogen Facility Separation Distances

Separation or safety distances are used to protect the public and other facilities from the consequences of potential accidents related to the operation of a facility. Separation distances are also used to reduce the potential that a minor accident at one portion of a facility propagates to another part of the facility thus increasing the resulting consequences. Specified separation distances may not provide protection against all potential accidents but they generally should address likely events initiated by a hazard located on the facility and by external hazards (e.g., automobiles), some of which can occur outside the boundary of the facility (e.g., a fire at an adjacent building). The latter case implies that separation distances can be two-way measures that protect adjacent structures from the hazards of the facility and also protect the facility against the hazards from adjoining facilities.

2.1 Current Separation Distances in Hydrogen Codes, Standards, and Regulations

The separation distances currently defined in the different codes and standards for hydrogen facilities vary according to the target that can be exposed to accident phenomena. Typical targets include members of the public, adjacent facilities, onsite structures, other flammable or combustible material, air intake openings, and ignition sources. In addition, the separation distances can vary from one code or standard to another in addition to how they are specified. These facts are illustrated in Table 2-1, which provides examples of the separation distances for gaseous hydrogen storage provided in the ICC International Fire Code (IFC) [3] and two currently published standards from the NFPA: NFPA 55 [1] and NFPA 52 [4]. Separation distances are also specified in governmental regulations such as those specified by the Occupational Safety and Health Administration (OSHA) [5].

While both the IFC and NFPA 52 currently present single separation distances for each target or exposure, NFPA 55 (and OSHA) currently provides different separation distance as a function of the total gaseous hydrogen volume. The Canadian Hydrogen Installation Code [29] provides separation distances as a function of the total mass for gaseous hydrogen and total volume for liquid hydrogen. The ISO in their standard for gaseous hydrogen fuelling stations (ISO/TS 20100:2008(E) [6]) currently provides separation distances (not shown in Table 1) as a function of the gas pressure, gas volume, and stored quantity. The separation distances in ISO/TS 20100:2008(E) range from 1 to 12 m depending on the type of exposure and the pressure, volume, and quantity of hydrogen gas that is stored. Whether the parameters currently being used to differentiate separation distances in these codes are adequate for future hydrogen refueling stations and other hydrogen facilities is an issue that is being addressed by the codes and standards groups. Specifically, higher gas storage and dispensing pressures than contemplated during the creation of the current codes are being considered for hydrogen refueling stations (gas storage cylinders with pressures of 70 MPa or greater are being incorporated into facility

designs). A consequence of these higher pressures is that the required separation distances may be significantly larger than currently specified.

Table 2-1. Example separation distances for gaseous hydrogen storage currently specified in codes and standards.

Type of Exposure	Separation Distance (m)				
	ICC International Fire Code (2003)	NFPA 55 (2005)			NFPA 52 (2006)
		Volume of H_2 <99 m^3	Volume of H_2 = 99 m^3 to 425 m^3	Volume of H_2 >425 m^3	
Lot line	3.1	1.5	1.5	1.5	3.1
Outdoor public assembly	7.6	7.6	15.2	15.2	-
Offsite sidewalks and parked vehicles	4.6	4.6	4.6	4.6	3.1
Ignition sources	3.1	7.6	7.6	7.6	-
Building – Noncombustible walls	1.5[a] or 3.1[b]	0[b]	1.5[c] or 3.1[d]	1.5[c] or 7.6[d]	-
Building – Combustible walls	7.6[b]	3.1	7.6	15.2	3.1
Above ground flammable or combustible liquid storage	6.1[e] or 15.2[f]	3.1[g] or 7.6[h]	3.1[g] or 7.6[h]	3.1[g] or 7.6[h]	6.1
Below ground flammable or combustible liquid storage- vent or fill opening	6.1	7.6[g,h]	7.6[g,h]	7.6[g,h]	-
Flammable gas storage above ground (other than hydrogen)	7.6[i] or 15.2[j]	3.1[k] or 7.6[l]	7.6[k] or 15.2[l]	7.6[k] or 15.2[l]	-

Notes:

a. Two-hour fire barrier interrupts line of site.
b. Either with sprinklers or without sprinklers in the building.
c. With sprinklers in the building, or without sprinklers and greater than 2-hour fire rating.
d. Without sprinklers in the building and less than 2-hour fire rating.
e. Area under tank is diked.
f. Area under storage tank is not diked.
g. Volume of stored liquid ranges from 0 to 3785 L.
h. Volume of stored liquid >3785 L.
i. The storage cylinders/tanks have a common shutoff valve.
j. The storage cylinders/tanks do not have a common shutoff valve.
k. Either high pressure or low pressure gas cylinders, 0 to 255 m^3 capacity.
l. Either high pressure or low pressure gas cylinders, >255 m^3 capacity.

The parameters that are important for establishing separation distances for gaseous hydrogen facilities were determined by deterministic analysis of hydrogen releases. The models developed by Houf and Schefer [7], which are described in detail in Appendix A, were exercised in this effort. The models consider either the concentration decay of an un-ignited high-momentum hydrogen leak or in the case where the mixture ignites, a

high-momentum hydrogen jet flame, its visible length, and the radiation heat flux from the flame. The results described below indicate that facility parameters such as the pressure and volume of the hydrogen gas can be important in determining harm distances. In addition, the selected leak diameter or leak rate is also critical. The harm criteria used to set the separation distance between the hydrogen source and a selected target or exposure is also important.

Figure 2-1 provides an example of safety distances based on one possible consequence of a hydrogen leakage event: the radiant heat flux from an ignited hydrogen jet. The figure shows the distances required to limit the exposure of a person to a radiant heat flux of 1.6 kW/m^2 which is generally accepted as a level that will not result in harm to an individual even for long exposures. The values shown are for a constant leak rate, assume an infinite volume (the effect of gas volume is addressed later in this section), and ignore any transient effects that may occur immediately after leak initiation. They are also based on the free-forming jet fires that are not affected by the ground or structures and are orientated towards the target (jet fires that are orientated upwards result in harm distances that are roughly half the distance shown in Figure 2-1). The calculated values are conservative because of these facts. As indicated in Figure 2-1, the harm distances are significantly affected by the pressure of the hydrogen gas and the leak diameter. These results clearly indicate the gas storage pressure is an important parameter that should be considered when specifying separation distances and that the selection of a specified leak size and orientation is critical in determining the separation distances.

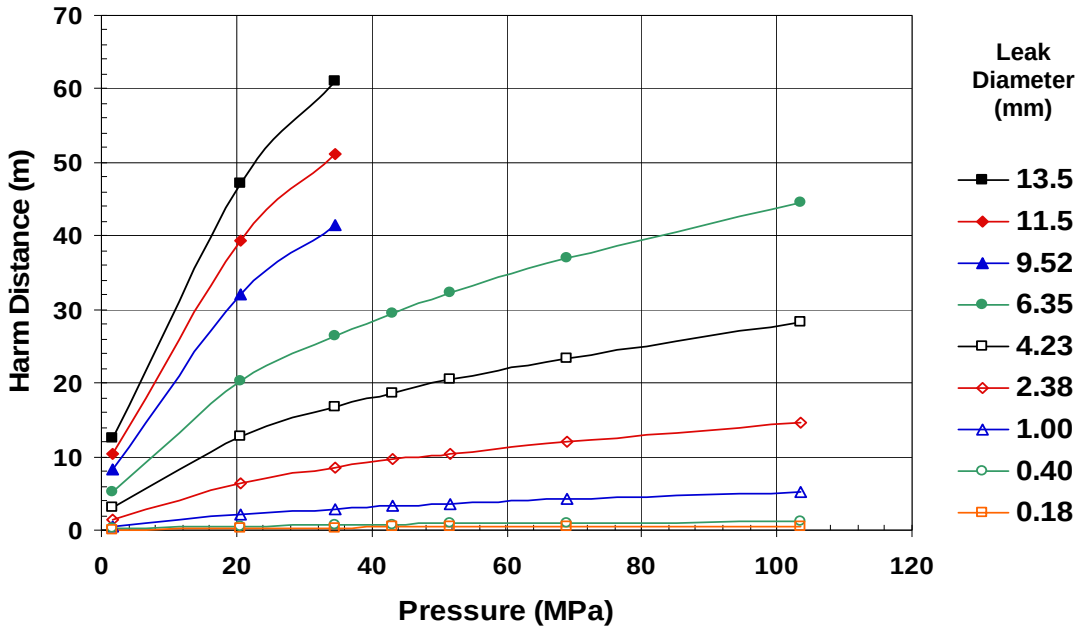

Figure 2-1. No-harm distances associated with a radiant heat flux of 1.6 kW/m^2 generated by a jet fire.

The no-harm distances shown in Figure 2-1 are generally larger than the separation distances shown in Table 2-1 for the current ICC and NFPA codes and standards if the leak diameters are greater than approximately 2.38 mm. One way to reduce

consequence-based separation distances is to use a higher consequence level that introduces the potential for injuring the public or damaging structures. This is illustrated in Figure 2-2, which shows the harm distances associated with different radiant heat flux levels and hydrogen gas pressures. The harm distances were evaluated for a specified leak diameter of 2.38 mm and only consequences related to hydrogen jets are included in Figure 2-2.

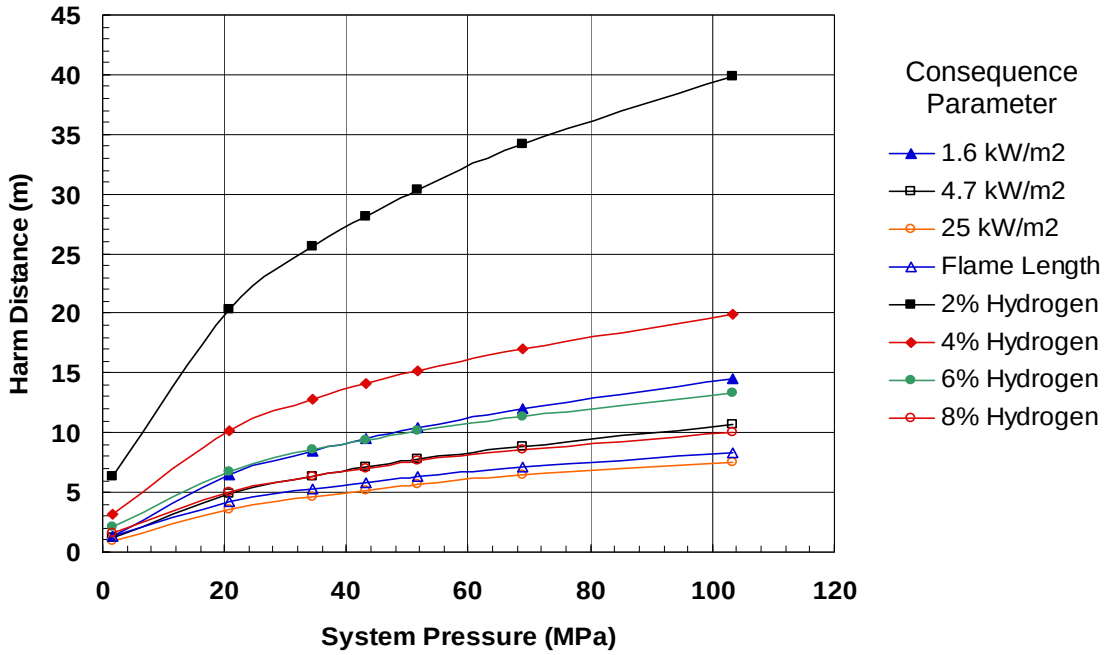

Figure 2-2. Harm distances required for a jet fire from a 2.38 mm diameter leak using different consequence parameters.

Although a variety of radiant heat flux levels and associated injury or damage levels are quoted in the literature [8,9,10], only three levels are shown in Figure 2-2: the 1.6 kW/m^2 no-harm level discussed previously, and two higher levels that can result in more harm to individuals and structures. A three minute exposure to 4.7 kW/m^2 could result in a low probability of a fatality and is used as a protection criterion by the American Petroleum Institute (API) in API 521 [11] for emergency response personnel and as a criterion in the IFC for protecting employees from releases through hydrogen vent lines. A radiant heat flux of 4.5 to 5 kW/m^2 is also specified in regulations in several countries including the United States [5] and in NFPA 59A [12] as an acceptable radiation hazard level for public exposure to hydrocarbon fires. An extended exposure to 25 kW/m^2 is used in the IFC as a criterion for damage to structures and components. Figure 2-3 illustrates how different exposure times to the three heat flux levels can result in different levels of burns from the resulting thermal dose (a thermal dose is the product of the heat flux to the 4/3 power and the exposure time). As indicated in Figure 2-3, short exposures to a 25 kW/m^2 heat flux level would also result in third degree burns that could lead to a fatality. It should be noted that the harm distances predicted by the Houf and Schefer model for a 25

kW/m^2 heat flux are approximately the same as those for the visible flame length of a hydrogen jet (also shown in Figure 2-2). Thus, the selection of this heat flux level provides an indication of the harm distances associated with direct flame contact. Direct contact with a flame is generally assumed to result in severe burns and a high probability of a fatality. In conclusion, the information presented in Figures 2-2 and 2-3 indicate that harm distances vary significantly with the selected harm criteria and consequence parameter.

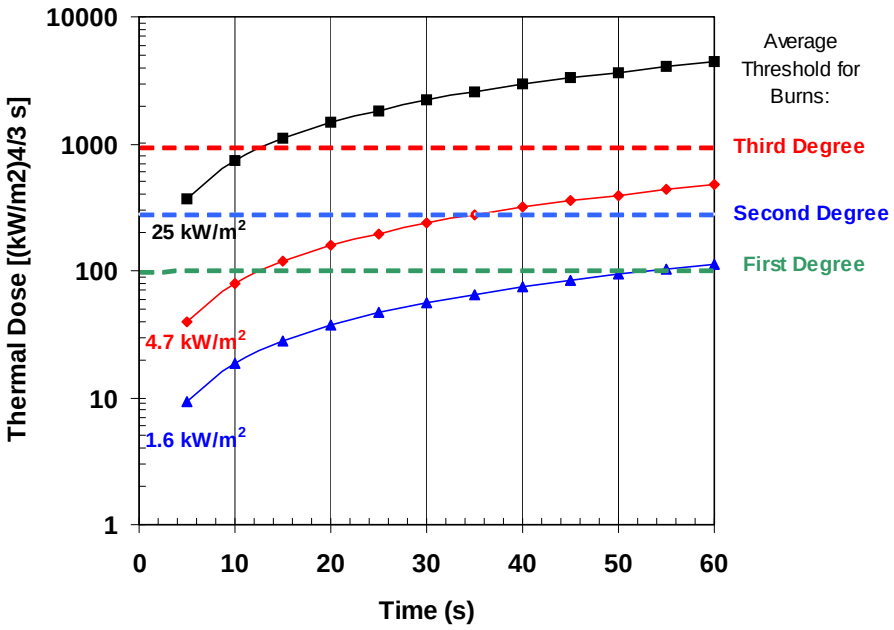

Figure 2-3. The potential for burns from different exposure times to radiant heat fluxes.

Figure 2-2 also illustrates the separation distances required for hydrogen concentrations ranging from 2% to 8%. The distances corresponding to the lower flammability limit (LFL) of hydrogen (4%) are important to consider since a delayed ignition of a hydrogen jet can injure people within the radius bounded by the LFL. The distances for a 2% hydrogen concentration (i.e., half of the LFL) are also shown since it has been used in other applications to provide a safety margin in establishing separation distances. The 6%, and 8% concentration contours are provided to reflect the uncertainty in the experimental literature on the ignitable concentration of hydrogen in turbulent flows [7]. The hydrogen concentration in an un-ignited hydrogen jet can be used as a basis to establish the separation distance from a hydrogen storage area to the public, ignition sources, and ventilation intakes.

The harm distances shown in Figure 2-2 indicate that it is possible to establish reasonable deterministic-based separation distances from jet fires even for high pressure systems if some level of personnel injury or property damage (represented in the figure by the higher radiant heat fluxes and hydrogen concentrations) is acceptable and if the evaluations are based on justifiably low leakage sizes.

As mentioned previously, several existing standards also differentiate separation distances based on the system volume. The volume of gaseous hydrogen can influence the duration of the hydrogen release and the potential consequences from hydrogen jets. Figure 2-4 illustrates the effect of both the gaseous volume and leak size on the duration of a hydrogen release from a 104 MPa (15000 psig) system with a pipe diameter of 7.16 mm calculated using the TOPAZ fluid flow computer code [12]. For a leak equal to 10% of the flow area in a small volume system containing 11.3 m^3 (400 standard cubic feet (scf)), the system pressure decreases to atmospheric pressure within 55 seconds. For a smaller leak equal to 1% of the flow area, it takes approximately 480 s before the system pressure decreases to atmospheric pressure. For a larger volume system equal to 99 m^3 (3500 scf), the system blow down is slower. A leak equal to 1% of the flow area takes approximately 4200 s for the system pressure to reach atmospheric pressure. Similar pressure decay rates were obtained for systems at the other operating pressures (1.72 MPa, 20.7 MPa, and 51.7 MPa) and which use different size piping (52.5 mm, 24.31 mm, and 7.16 mm, respectively).

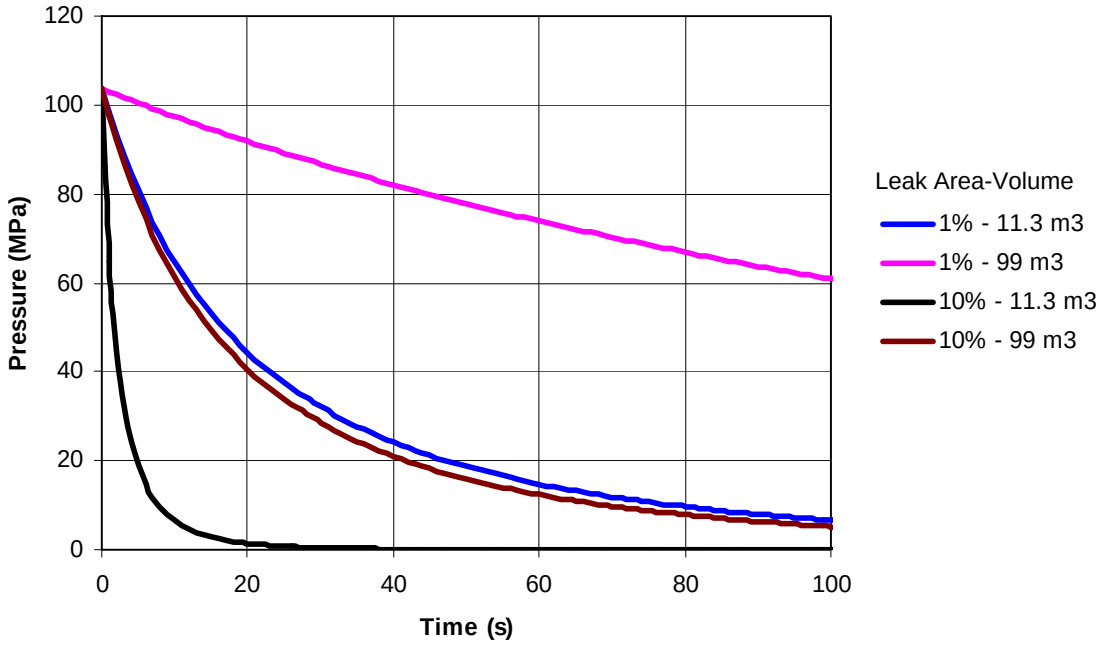

Figure 2-4. Pressure response for leaks from 104 MPa gaseous hydrogen systems containing different gas volumes.

The time behavior of the hazards experienced by a target can also be significantly affected by the system volume and leak size. This is illustrated in Figure 2-5, which shows impact on the radiation heat flux level that would occur 3 m from the location of a 1% flow area leak in a 104 MPa system. The radiation heat flux decreases rapidly for a small 11.3 m^3 system but much slower for a 99 m^3system. For a person standing at a distance 3 m from this leak, the thermal dose received over a 40 s period would be approximately 500 $(kW/m^2)^{4/3}$s for a release from the 11.3 m^3 system and 2000 $(kW/m^2)^{4/3}$s for a release from the 99 m^3 system. Using the Tsao and Perry probit

function described in Section 5.2, thermal doses of 500 and 2000 $(kW/m^2)^{4/3}s$ represent a 5% and 95% probability of fatality, respectively. Thus, the difference in volumes can have an effect on the consequences from the exposure to a radiation heat flux. However, if one assumes the radiation heat flux does not decrease with time (equivalent to assuming an infinite gas volume), the thermal dose for a 40 s exposure to a 25 kW/m^2 heat flux is 2900 $(kW/m^2)^{4/3}s$, which results in a 99.5% probability of fatality based on the Tsao and Perry probit function. Thus, for systems with volumes greater than 99 m^3, the probability of a fatality from exposure to radiation heat fluxes is not significantly affected by the system volume (this conservatively assumes the exposure begins at the time of leak initiation). It should be noted that use of the more optimistic Eisenberg probit function (see Section 5.2) would not substantially change this conclusion.

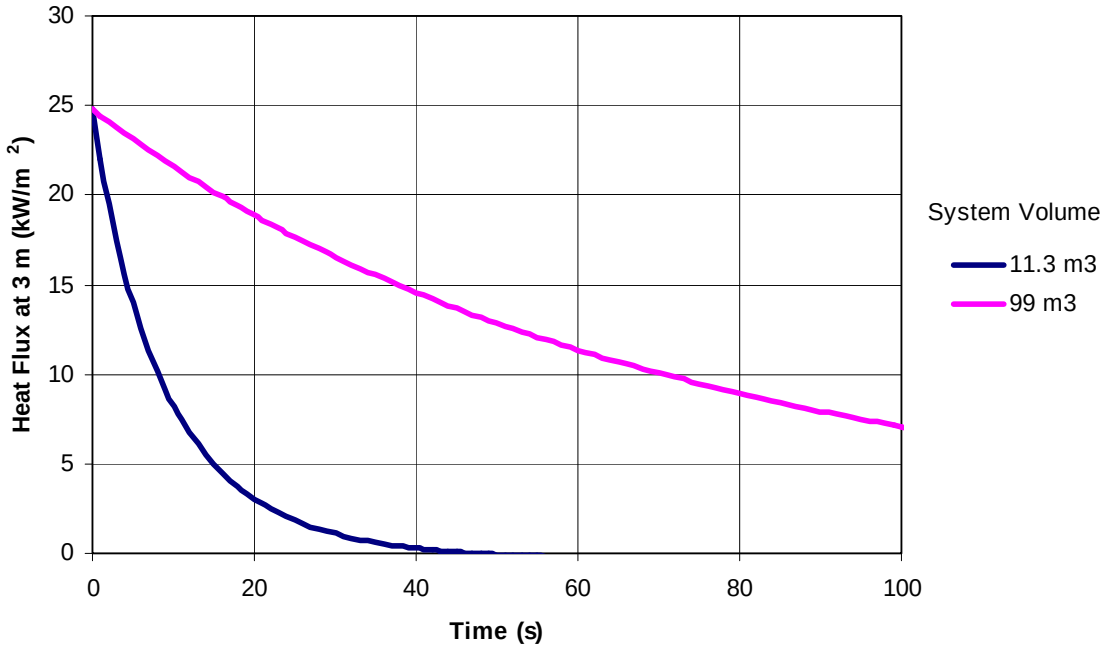

Figure 2-5. Radiation heat flux at 3 m for a 1% leak in a 104 MPa gaseous hydrogen system with a pipe diameter of 7.16 mm.

The consequences from direct contact with a self-ignited hydrogen flame could also be affected by the system volume. However, the affect would be minimal if one conservatively assumes the contact occurs immediately after the hydrogen jet is ignited and that only a short duration contact with a flame is required to result in significant third-degree burns. For an un-ignited hydrogen jet, the extent of the jet would also be affected by the system volume and leak area. However, as indicated in Figure 2-6, the extent of the 4% hydrogen envelope for the example problem described above would not change substantially over 5 minutes for system volumes greater than 99 m^3 and for small leak areas. In conclusion, it is conservative to assume the exposure to the flame or the radiation heat flux from an ignited hydrogen jet, or the hydrogen envelope from an un-ignited jet occurs immediately after leak initiation, especially for small leak diameters. Furthermore, ignoring the decreasing flame length and hydrogen envelope that can occur

with small system volumes is also conservative for small leaks. The amount of conservatism decreases dramatically for systems with large volumes.

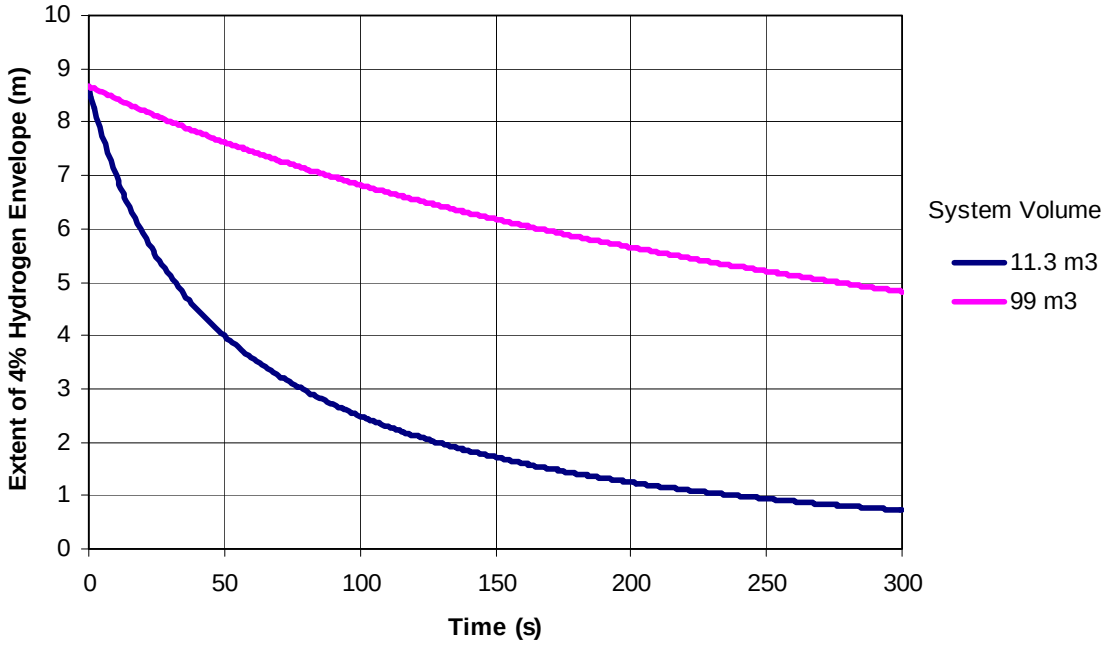

Figure 2-6. Extent of the 4% hydrogen envelope in a hydrogen jet for a 1% leak in a 104 MPa gaseous hydrogen system with a pipe diameter of 7.16 mm.

2.2 Approaches for Establishing Separation Distances

The development of separation distances for hydrogen facilities can be determined in several ways. The first is to use expert judgment utilizing available information. For the most part, SDOs in the past have relied upon expert panels to establish necessary code requirements. The bases for the expert judgments are not documented but likely reflect a combination of good engineering practices to address the potential hazards associated with hydrogen, historical precedence based on requirements for other fuels such as compressed natural gas (CNG), and anecdotal knowledge of past problems in hydrogen facilities. It is possible that some of the requirements are based on experimental or deterministic analyses of selected accidents that were felt to represent credible, but not worst case, accidents. It should be noted that this process appears to have worked to ensure safety in many industries primarily through the continuing process of adapting the applicable code requirements to address issues identified from an analysis of accidents. Although the expert judgment process involves the use of all available information, there is a movement to utilize more science-based approaches that utilize deterministic calculations and risk considerations to establish code and regulatory requirements. There are several possible variations of this approach ranging from purely deterministic methods to risk-based methods. The variations are discussed below.

Purely deterministic approaches utilize predictions from accepted models to determine separation distances. A conservative approach is to use the worst possible accidents in terms of consequences. Selection of large leaks would result in large separation distances. Such accidents may be of very low frequency such that they would likely never occur. Although this approach bounds separation distances, the resulting distances are generally prohibitive with regard to the available area surrounding the facility. The current separation distances do not reflect this approach. An alternative deterministic approach that is often utilized by SDOs and allowed under some regulations is to select accident scenarios that are more probable but do not provide bounding consequences. In this approach, expert opinion is generally used to select the accidents used as the basis for the prescribed separation distances. Although anecdotal experience often forms the basis for the selection of the accidents, the frequency of accidents can also be used as a selection criterion.

Anecdotal evidence of typical leak sizes or evaluation of available data is a possible method for selecting a leak size. For example, the Compressed Gas Association suggests that typical leak sizes are less than 20% of the flow area of the component [13]. An analysis of available leakage data can be used to determine expected leak sizes. Separation distances based on a probable leak diameter can introduce a high level of risk from leaks that are less probable but which result in high consequences. Thus, it is also desirable that risk considerations be included in the determination of accidents. The process of including risk considerations in developing separation distances and other code requirements is referred to as a risk-informed process.

A purely deterministic approach was tried by Sandia National Laboratories in an early effort to support the ICC Ad-Hoc Committee for Hydrogen Gas to develop new separation distances for incorporation into the IFC. The resulting separation distances were large for evaluated leak sizes of 3.175 mm, 6.35 mm, and 9.525 mm and led to the realization that a risk-informed approach was needed to provide a basis for establishing the selected leak size.

A risk-informed process utilizes risk insights combined with other considerations to establish code requirements. The risk from the operation of a facility is the product of the frequency and consequences of all credible accidents and can be estimated using QRA. A QRA is used to identify and quantify scenarios for the unintended release of hydrogen, identify the significant risk contributors at different types of hydrogen facilities, and to identify potential accident prevention and mitigation strategies to reduce the risk to acceptable levels. Examples of other considerations used in this risk-informed process can include the results of deterministic analyses of selected accident scenarios, the need for defense-in-depth for certain safety features (e.g., overpressure protection), the use of safety margins in the design of high-pressure components, and requirements identified from actual occurrences at hydrogen facilities. A key component of this process is that both accident prevention and mitigation features are included in the code and standard requirements.

A risk-informed process can help establish the baseline design and operational requirements for hydrogen fueling stations. Although separation distances are a key safety parameter specified in hydrogen codes and standards, there are other design and operational requirements that are used to ensure safe operation. Key design features currently specified in hydrogen codes and standards include interlocked leak detection and isolation capability, dilution ventilation, emergency venting, emergency manual shutoff switches, pressure relief devices and associated vent lines, process monitoring and safety interlocks, and fail safe design requirements (e.g., closure of isolation valves on loss of power). Operational requirements can include normal operating procedures, maintenance and surveillance procedures, limiting conditions of operation, and emergency procedures in the case of major accidents.

QRA can be used in several different ways to help establish the code and standard requirements for hydrogen facilities. First, by analyzing a comprehensive set of possible accidents, the risk drivers for these facilities can be identified. Accident prevention and mitigation features can then be specified to address all accidents. The number or type of specified requirements can be determined by both the cause and frequency of the accident and the associated risk. For example, one could specify that redundant or highly reliable design features be in place to address commonly occurring events such as small hydrogen leaks and that procedural requirements include inspections and emergency response plans to prevent or respond to more catastrophic accidents such as tank ruptures. The risk-reduction potential of the specified design and operational features can then be evaluated using the QRA models. Important questions that can be answered using QRA include identifying which of these design and operational features are most effective to reduce risk and determining whether additional features are necessary to achieve an acceptable level of risk.

Risk can also be used as the sole basis for determining hydrogen code requirements including separation distances. Such an approach is referred to as a risk-based approach. One risk-based approach utilizes the conceptual framework, shown in Figure 2-7, which was developed by the European Industrial Gases Association (EIGA) [8]. In this approach, the cumulative frequencies of different leak diameters resulting in one or more specified consequence are evaluated against the separation distances required to protect people, equipment, or structures from a specified level of harm. The accidental releases can occur due to random component failures such as pipe ruptures, overpressure events, unintentional venting, external events such as fires at adjoining structures, and human errors including those related to dispensing hydrogen and incorrect performance of maintenance on the facility. The availability of features to mitigate accidental releases (e.g., shutoff valves initiated by hydrogen or flame sensors) can be included in the accident frequency evaluation. A selected risk acceptance guideline is used to establish the risk-based separation distances based on the selected consequence parameters. Hydrogen leaks resulting in risk values below this criterion could be eliminated in the separation distance evaluation. In effect, this approach can provide a basis for eliminating large leakage events which have low frequencies and result in significant consequences that require large separation distances to protect the public, structures, and equipment from harm.

A consequence of a risk-based approach is that the established separation distances will present some residual level of risk that must be acceptable by affected stake holders (i.e., the public, regulators, and facility operators). That level of risk is determined by the selected consequence measures and risk threshold used in the risk-informed evaluation. A major limitation of a risk-based approach is that there can be large uncertainties in the data and models utilized in a QRA and conservative assumptions used in the analysis can affect the results. The lack of hydrogen component leakage data is an example of particular limitation for hydrogen facility QRAs. Uncertainty and sensitivity analyses can be performed to address assumptions and known concerns. However, the process of making decisions based purely on risk can be difficult in light of these uncertainties. The decisions are generally on a sounder basis in a risk-informed process where risk is only one input into the decision process and the weight given to all the input accounts for the known uncertainties.

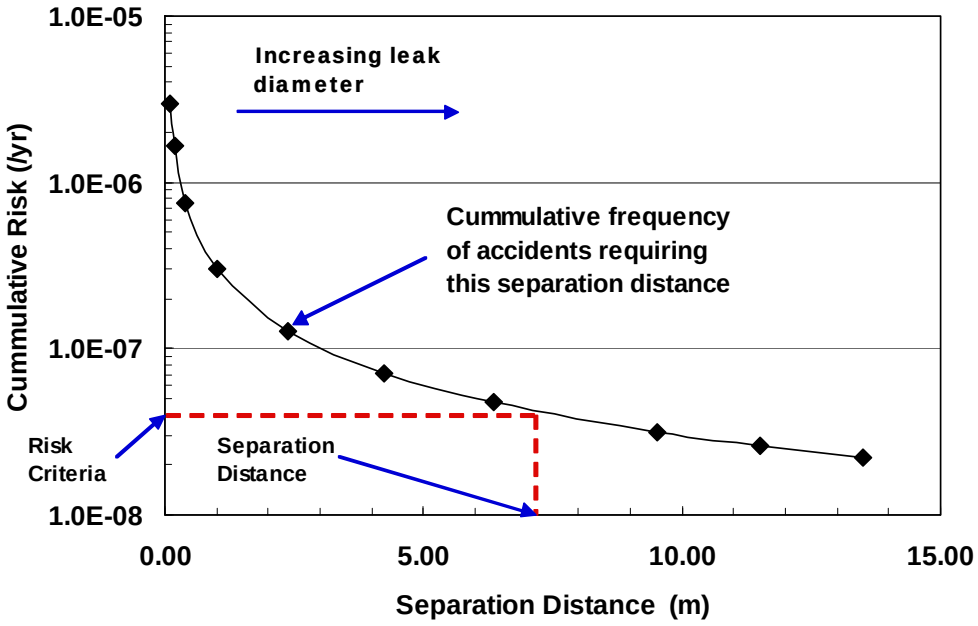

Figure 2-7. Risk-informed approach for establishing safety distances.

3. NFPA Separation Distance Approach

Based on the input provided in Section 2 by Sandia National Laboratories, the NFPA 2 TG6 selected a risk-informed approach as the means for developing the separation distances for inclusion into both the NFPA 2 and NFPA 55 standards. The selected approach for selecting the separation distances utilizes harm criteria (parameters) evaluated from deterministic analyses of hydrogen jets based on a selected leak diameter. The leak diameter is selected based on the expected frequency of different size leaks in typical gaseous hydrogen storage facilities and the associated risk from all leaks. Five harm criteria were evaluated in the deterministic analysis and used to determine the separation distances for the different exposures or targets in the separation distance table developed by TG6. The NFPA 2 TG6 also selected system pressure as an important parameter for determining the separation distances and specified four pressure ranges that are typical of different types of gaseous hydrogen storage facilities. However, system volume was not selected as a differentiating parameter except for establishing a minimum volume for which separation distances are required. As indicated in Section 2, it is conservative to ignore volume effects but the level of conservatism decreases as the gas volume increases.

3.1 NFPA 2 and NFPA 55 Separation Distance Table Format

The members of NFPA 2 TG6 established the format for the NFPA 2 and NFPA 55 separation distance tables based on the input provided in Section 2. The exposures or targets of concern, for which separation distances are required, were identified by TG6 by examining the existing exposures listed in NFPA 55. Some targets were combined, some were deleted, and some new targets were identified. A list of the exposures is provided in Table 3-1.

For each of the exposures, potential hazard scenarios associated with ignited and un-ignited hydrogen jets were identified. The number of identified hazard scenarios varied for different targets. Based on the identified hazard scenarios, a harm criteria or hazard parameter was selected for determining the associated separation distance for most of the hazards. The worst hazard scenario determined the harm criteria. The hazard parameters associated with these scenarios include specific heat flux levels that could cause some level of damage, direct flame contact, or a 4% hydrogen concentration which represents the potential for a flash fire given delayed ignition. The hazard scenarios and selected harm criteria for each exposure are listed in Table 3-1.

The NFPA 2 TG6 specified that only hazards associated with un-ignited jets or ignited jet flames from hydrogen leaks be considered in the assessment. Because the characteristics of hydrogen jets and jet flames depend on the source pressure and effective diameter of the leak, the separation distance table was broken into four pressure ranges defined by members of TG6 based on typical gaseous storage systems. For each pressure range, a pipe inside diameter (ID) was selected that is characteristic of the pipe diameter in typical

systems operating within that pressure range. The pressure ranges and characteristic diameters that were selected are provided in Table 3-2.

Table 3-1. NFPA-55 separation distance exposures.

	Exposure[1]	Hazard Scenario
1	Lot lines[greater of (a) or (b)]	1. Gas release and subsequent entrainment or accumulation by the receptor. 2. Fire spread to or from adjacent equipment or structure. 3. Gas explosion hazard on site or affecting adjacent property. 4. Threat of injuries on site or adjacent property. 5. Ignition of an un-ignited release/vented hydrogen.
2	Exposed persons other than those involved in servicing of the system. (e)	4. Threat of injuries on site or adjacent property.
3	Buildings and Structures Combustible construction(c) Noncombustible non-fire-rated construction(d) Fire rated construction with a fire resistance rating of not less than 2 hours(f)	2. Fire spread to or from adjacent equipment or structure.
4	Openings in buildings of fire-rated or non-fire-rated construction (doors, windows and penetrations) Openable(a) Fire-rated or non fire-rated Un-openable(c) Fire-rated or non fire-rated	1. Gas release and subsequent entrainment or accumulation by the receptor. 2. Fire spread to or from adjacent equipment or structure.
5	Air intakes (HVAC, compressors, other) (a)	1. Gas release and subsequent entrainment or accumulation by the receptor.
6	Fire barrier walls or structures used to shield the bulk system from exposures. (f)	2. Fire spread to or from adjacent equipment or structure. 4. Threat of injuries on site or adjacent property.
7	Unclassified electrical equipment(g)	2. Fire spread to or from adjacent equipment or structure. 5. Ignition of an un-ignited release/vented hydrogen.
8	Utilities (overhead) including electric power, building services, or hazardous materials piping. (c)	2. Fire spread to or from adjacent equipment or structure. 10. Failure of equipment exposes the hydrogen system to electrical hazard, physical or health hazard. Failure of the system exposes utilities to failure.
9	Ignition sources such as open flames and welding (a)	3. Gas explosion hazard on site or affecting adjacent property. 5. Ignition of an un-ignited release/vented hydrogen.
10	Parked cars(e)	4. Threat of injuries on site or adjacent property.

Table 3-1. NFPA-55 separation distance exposures.

	Exposure[1]	Hazard Scenario
11	Flammable gas storage systems including other hydrogen systems above ground. Non-bulk(c) Bulk(h)	2. Fire spread to or from adjacent equipment or structure.
12	Aboveground vents or exposed piping and components of flammable gas storage systems including other hydrogen systems below ground. (c) Gaseous or Cryogenic	6. Damage to exposed components of underground system that are exposed above ground. 7. Damage to above ground system due to function of explosion control system used to vent underground vault or structure.
13	Hazardous materials (other than flammable gases) storage below ground(c) Physical hazard materials or Health hazard materials	6. Damage to exposed components of underground system that are exposed above ground. 7. Damage to above ground system due to function of explosion control system used to vent underground vault or structure.
14	Hazardous materials storage (other than flammable gases) above ground. (c) Physical hazard materials or Health hazard materials	8. Fire or explosion in other hazardous materials results in a release of hydrogen. 9. Fire or explosion in hydrogen system results in a release of other hazardous materials.
15	Ordinary combustibles including fast burning solids such as ordinary lumber, excelsior, paper or combustible waste and vegetation other than that found in maintained landscaped areas. (c)	2. Fire spread to or from adjacent equipment or structure.
16	Heavy timber, coal or other slow burning combustible solids(c)	2. Fire spread to or from adjacent equipment or structure.

[1]The basis for establishing the separation distance for each exposure are identified by the superscripted letters and are listed below:

(a) Un-ignited Jet concentration decay distance to 4% mole fraction (volume fraction) hydrogen.
(b) D_{rad} – Radiation Heat Flux Level of 1577 W/m^2 (500 Btu/hr ft^2).
(c) The greater of D_{rad} for combustible heat flux level of 20,000 W/m^2 (6340 Btu/hr ft^2) or the visible flame length.
(d) The greater of D_{rad} for non-combustible equipment heat flux level of 25,237 W/m^2 (8000 Btu/hr ft^2) or the visible flame length.
(e) D_{rad} for heat flux level of 4732 W/m^2 (1500 Btu/hr ft^2) exposure to employees for a maximum of 3 minutes.
(f) The minimum clearance between the structure and the system required for access for service related activities.
(g) Equipment classified as meeting Class I, Division 2, Group B requirements of NFPA 70 *National Electrical Code* when the area is in accordance with NFPA 497 *Recommended Practice for the Classification of Flammable Liquids, Gases, or Vapors and of Hazardous (Classified) Locations for Electrical Installations in Chemical Process Areas* .
(h) Bulk hydrogen storage systems are allowed to integrate (co-locate) other non-liquefied flammable gas systems when the output of the system is designed to deliver a product in which the gases are mixed or blended for delivery

Table 3-2. Pressure ranges for NFPA 2 and NFPA 55 separation distances tables and the associated system characteristic pipe diameter.

Storage Pressure Range	Characteristic Pipe Diameter (I.D.)
>0.103 to ≤ 1.72 MPa (gauge) (>15 to ≤250 psig)	52.50 mm (2.07 in)
>1.72to ≤ 20.68MPa (gauge) (>250 to ≤3000 psig)	18.97 mm (0.75 in)
>20.68 ≤ 51.71 MPa (gauge) (>3000 to ≤7500 psig)	7.92 mm (0.31 in)
>51.71 ≤ 103.42 MPa (gauge) (>7500 to ≤15000 psig)	7.16 mm (0.28 in)

The storage pressure in the NFPA separation distance tables is defined as the maximum pressure of a storage array with volume greater than 11.3 m^3 (400 scf) in the system. The system pipe diameter is based on the largest inside diameter (I.D.) of the piping within the system or portion of the system downstream of the stored volume. If a system contains multiple storage arrays with volumes greater than 11.3 m^3 at different pressures, then the storage pressures and largest pipe diameters must be determined for each storage array in the system. Separation distances must be determined for each storage array in the system and the largest separation distance for each storage array defines the value of the separation distance for the overall system.

The effective leak diameter for each pressure range was based on a fraction of the flow area using the characteristic pipe diameters listed in Table 3-2. For a round leak the effective diameter of the leak is

$$d_{leak} = (x)^{1/2} d_{pipe(I.D.)} \tag{3.1}$$

where x is the fraction of the system flow area selected as the leak area, d_{leak} is the effective leak diameter and $d_{pipe(I.D.)}$ is the inside diameter of the pipe. Table 3-3 illustrates the harm distances for the four pressure ranges and five harm criteria utilized in the NFPA separation table for a variety of leak sizes. The harm distances were evaluated for the highest pressure in each of the four ranges using the models generated by Houf and Schefer [7] that are described in Appendix A and the characteristic pipe diameters provided in Table 3-2. As indicated in Table3-3, the harm distances can vary substantially for leak sizes ranging from 1% to 20% of the largest system flow area. The leak size selected by NFPA 2 TG6 was determined using the risk-informed method described in the following section.

3.2 Risk-Informed Method

It is generally accepted that separation distances are not used to provide protection against rare events such as large, catastrophic ruptures. Separation distances should be selected to cover events that may be expected to occur during the facility lifetime,

especially small leaks that may occur frequently. It is also desirable to establish separation distances that do not result in unacceptable risk levels. In particular, the associated risk from leakage events that would result in consequences beyond the designated separation distances should be acceptable. The risk-informed process approved by the NFPA 2 TG6 for selecting the leak size included consideration of both the frequency of the selected leak size and the risk from larger leaks.

Table 3-3. Harm distances for different leak areas, harm criteria, and pressures.

Harm Criteria	Harm Distance (Leak Area)			
	>0.10 to 1.72 MPa (>15 to 250 psig)	**>1.72 to 20.68 MPa (>250 to 3000 psig)**	**>20.68 to 51.71 MPa (>3000 to 7500 psig)**	**>51.71 to 103.43 MPa (>7500 to 15000 psig)**
Un-ignited jet concentration – 4% mole fraction of hydrogen	31.2 m (20% Area) 22.1 m (10% Area) 15.7 m (5% Area) 12.1 m (3% Area) 7.0 m (1% Area)	36.1m (20% Area) 25.6 m (10%Area) 18.1 m (5% Area) 14.0 m (3% Area) 8.1 m (1% Area)	22.6 m (20% Area) 16.0 m (10% Area) 11.3 m (5% Area) 8.8m (3% Area) 5.0 m (1% Area)	26.8 m (20% Area) 19.0 m (10% Area) 13.4 m (5% Area) 10.4 m (3% Area) 6.0 m (1% Area)
Radiation heat flux level of 1577 W/m^2 (500 Btu/hr-ft^2)	23.4 m (20% Area) 15.9 m (10% Area) 10.7 m (5% Area) 7.9m (3% Area) 4.1 m (1% Area)	28.1 m (20% Area) 19.0 m (10% Area) 12.8m (5% Area) 9.5 m (3% Area) 4.8 m (1% Area)	16.6 m (20% Area) 11.2 m (10% Area) 7.8 m (5% Area) 5.5 m (3% Area) 2.6 m (1% Area)	20.5 m (20% Area) 13.8 m (10% Area) 9.6 m (5% Area) 6.8 m (3% Area) 3.3 m (1% Area)
Radiation heat flux level of 4.7 kW/m^2 (1500 Btu/hr-ft^2)	17.0 m (20% Area) 11.6 m (10% Area) 7.9 m (5% Area) 5.9 m (3% Area) 3.1 m (1% Area)	20.2m (20% Area) 13.8m (10% Area) 9.4m (5% Area) 7.0 m (3% Area) 3.7m (1% Area)	12.2 m (20% Area) 8.2 m (10% Area) 5.5 m (5% Area) 4.1 m (3% Area) 2.1 m (1% Area)	14.9 m (20% Area) 10.0 m (10% Area) 6.7 m (5% Area) 5.1 m (3% Area) 2.6 m (1% Area)
Greater of radiation heat flux level of 25237 W/m^2 (8000 Btu/hr-ft^2) or visible flame length[1]	13.0 m (20% Area) 9.2 m (10% Area) 6.5 m (5% Area) 5.0 m (3% Area) 2.9 m (1% Area)	15.0 m (20% Area) 10.6 m (10% Area) 7.5m (5% Area) 5.8 m (3% Area) 3.4 m (1% Area)	9.4 m (20% Area) 6.7 m (10% Area) 4.7 m (5% Area) 3.6m (3% Area) 2.1 m (1% Area)	11.1 m (20% Area) 7.9 m (10% Area) 5.6 m (5% Area) 4.3m (3% Area) 2.5 m (1% Area)
Greater of radiation heat flux level of 20000 W/m^2 (6340 Btu/hr-ft^2) or visible flame length[1]	13.0 m (20% Area) 9.2 m (10% Area) 6.5 m (5% Area) 5.0 m (3% Area) 2.9 m (1% Area)	15.0 m (20% Area) 10.6 m (10% Area) 7.5m (5% Area) 5.8 m (3% Area) 3.4 m (1% Area)	9.4 m (20% Area) 6.7 m (10% Area) 4.7 m (5% Area) 3.6m (3% Area) 2.1 m (1% Area)	11.1 m (20% Area) 7.9 m (10% Area) 5.6 m (5% Area) 4.3m (3% Area) 2.5 m (1% Area)

[1]The largest harm distances are predicted for the visible flame length.

The leak diameter used to select the separation distance for each exposure was selected to encompass 95% of the expected leakage events in typical hydrogen gas storage facilities. A 95th percentile was selected based on the fact that high percentiles ranging from 90% to 99% are often used in other applications as a basis for decision making. The process of generating the component and system leakage frequencies used in this effort is described in Section 4. The typical hydrogen storage facilities used in the analysis were defined by industrial members of TG6 and are described in Appendix B. Based on this frequency analysis, a leak size equal to 0.1% of the largest pipe area downstream of the hydrogen storage array could be justified.

The cumulative risk to the public from leaks was then evaluated using the framework shown in Figure 2-7 and compared to a risk guideline selected by TG6. The results of risk analysis for the facilities are provided in Section 5. Section 5 also provides the basis for the selected risk guideline and harm criteria that were used in the risk analysis.

The results indicate that the cumulative risk to a person located at a separation distance determined by a leak equal to 0.1% of the system flow area would exceed the selected risk guidelines. Specifically, a person located at the resulting separation distances would be exposed to deadly consequences from larger leaks, which would result in an unacceptable level of risk. To reduce the risk, the separation distance must be larger than that associated with a 0.1% leak. The risk results in Section 5 indicate that separation distances associated with component leak sizes ranging from 1% to 10% of the component flow area provide risk estimates close to the risk guidelines. The risk from this range of leaks is acceptable when the uncertainties and conservative assumptions used in the risk assessment are considered.

Based on the data and risk analysis inputs, a leak size of 3% of the system flow area was selected by TG6 as the basis for determining separation distances including the lot line distance used to protect members of the public from potential accidents. The 3% leak area value actually represents 97% of the expected leakage events in the example facilities. In addition, leaks greater than 3% would not present an unacceptable level of risk to persons located at the lot line. The resulting separation distances for the five harm criteria used in the NFPA tables are highlighted in red in Table 3.3.

4. Leak Frequency Analysis

In order to begin quantifying the overall risk associated with a hydrogen facility, it is necessary to establish the types of accidents that can occur. Currently, the assessment performed to support gas storage-related separation distances only includes contributions from component leakage events. To utilize the methodology for determining separation distances described in Section 3, component leakage frequencies representative of hydrogen components must be expressed as a function of the leak size and system pressure.

Unfortunately, there is little available data on hydrogen-specific component leakage events that can be utilized in a QRA. Although major events are recorded in databases such as the DOE Hydrogen Incident Reporting database [14] for lessons learned, the failure to record all events (e.g., small leakage events) and the number of operating hours represented in the database makes utilization of the data for analysis difficult if not impossible. Most QRAs for hydrogen facilities have utilized published values from other non-hydrogen sources. In general, the process for selecting failure frequencies has involved a review of data sources and a selection of values that are felt to be most representative of hydrogen components. For example, EIGA provides recommended leak rates in Reference 8 for various components including pipes, valves, joints and unions, hoses, and flanges. The recommend values were chosen after a review of leak frequencies presented in five different sources (none of which are hydrogen data) and then used for the hydrogen facility assessment documented in Reference 8.

Rather than selecting a value from different generic sources, a different approach was utilized in this assessment. Data from different sources were collected and combined using statistical analysis. The types of data analysis methods that could be used are described in Section 4.1. A Bayesian statistical method [15] was selected for use in the data analysis. This approach has three major advantages over the approach utilized by EIGA and other QRA guidance documents. First, it allows for the generation of leakage rates for different amounts of leakage. Second, it generates uncertainty distributions for the leakage rates that can be propagated through the QRA models to establish the uncertainty in the risk results. Finally, it provides a means for incorporating limited hydrogen-specific leakage data with leakage frequencies from other sources to establish estimates for leakage rates for hydrogen components. Sources of leakage frequencies used in this study are listed in Section 4.2. The Bayesian model used to generate hydrogen-specific leakage frequencies from this data is described in Section 4.3.

The generated component leakage frequencies were then used to generate estimates for the total leakage frequency for typical hydrogen gas storage facilities. The cumulative system leakage frequencies were used to select the leak size used as the basis for determining the NFPA 2 and NFPA 55 separation distances. The system leakage frequency analysis is documented in Section 4.4. Uncertainties in the data analysis are addressed in Section 4.5.

4.1 Data Analysis Methods

There are two general approaches to analyzing data: traditional statistical methods and Bayesian statistics. In cases where data are limited, such as for hydrogen facilities, Bayesian techniques are superior to traditional frequentist techniques. Traditional frequentist approaches to statistical analysis do not allow analysts to distinguish among multiple types of data. Leak frequency data for a component (e.g. pipe) *other than those in hydrogen systems* cannot be included in the specific analysis unless one chooses to agglomerate all of the generic and hydrogen-specific data into a single information set. Any other type of information related to the leak frequency would also have to be modified so that the tailored information would be treated equally to the other leak frequency data that are available. The consequences of this restriction include the inability to determine useful values for uncertain variables in many cases. For example, the exact pipe leakage sizes were not provided for the hydrogen-specific data. Based on this lack of information, there is no consistent way to estimate the leak frequency.

With Bayesian analysis, however, these problems are somewhat mitigated. Using Bayes' rule, information from multiple sources may be combined. For the case concerning the pipes used in a hydrogen system, data from generic sources may be used to form "first guess" values for the parameters that define the distributions of the leak frequency. In Bayesian analysis, the leak frequency will not be a point value, but rather have a distribution associated with it. The distribution described by the parameters obtained in this manner can be called "prior" distributions. These priors can then be "updated" with the hydrogen-specific data in order to obtain "posterior" distributions. These posterior distributions may then be used in order to make decisions about the system. The hierarchical Bayesian approach used in this study allows one to attach different "layers" of significance to all the data used in the modeling process. This significance may be assigned either explicitly or implicitly within the model. It also allows multiple levels of uncertainty. For a very useful, detailed explanation of the process, see Reference 16.

In cases where large amounts of data are available, traditional methods are usually preferred. A typical traditional statistical analysis would involve calculating a maximum likelihood estimate (MLE) and a central 90% confidence interval. For an observation period of 't' with 'x' events (in our case, "events" would be synonymous with "leaks"), the following equations would be used to calculate these values.

$$\text{MLE} = \frac{x}{t}$$

$$\text{90\% Confidence Interval} = \left(\frac{\chi^2_{.05}(2x)}{2t}, \frac{\chi^2_{.95}(2x+2)}{2t} \right) \qquad (4.1)$$

where $\chi^2_{.r}(A)$ is the r^{th} percentile of the Chi-square distribution with A degrees of freedom.

Note that the lower bound of the interval is not defined if x = 0. In this case, the MLE is zero and the lower bound of the confidence interval is also set to zero [16].

There are some major advantages to using traditional statistical analysis methods. From formal education and professional experience, most engineers and scientists have some basic knowledge and training in traditional statistical techniques. Since the math involved is typically quite simple, users may utilize the equations without significant computational time. When the analysis becomes more detailed (i.e. with the Bayesian method), the computational power required to solve the series of equations turn out to be more prohibitive. With a sufficient amount of data available, the results from traditional analysis are informative enough to be useful. In this case, the differences between the two specific statistical results should be minimal.

When using traditional methods, there are some disadvantages that should be recognized. If there are only a few data values or poorly identified information that is available, the results are not typically useful. Also, when multiple types of data are available, there is no consistent way to combine the data to obtain reasonable results since all data must be treated equally. Any time new data are obtained, the results must be re-calculated. There is no way to easily update the model in order to incorporate newly obtained data.

In some cases, only small amounts of data can be found that are relevant to the problem at hand. In these cases, Bayesian techniques have proven to be superior to traditional analyses. Bayesian analysis utilizes Bayes' theorem which is illustrated in Equation 4.2.

$$P(\theta = \theta_i \mid \varepsilon) = \frac{P(\varepsilon \mid \theta = \theta_i)P(\theta = \theta_i)}{P(\varepsilon)} = \frac{P(\varepsilon \mid \theta = \theta_i)P(\theta = \theta_i)}{\sum_i P(\varepsilon \mid \theta = \theta_i)P(\theta = \theta_i)} \tag{4.2}$$

where:

- $P(\varepsilon \mid \theta = \theta_i)$ - The conditional probability that the value ε will be observed for the random variable X in a given trial, *assuming the value* θ_i *for the parameter* θ.
- $P(\theta = \theta_i)$ - The **prior distribution** – prior to observing the value ε for X; can also be stated as "prior to obtaining the evidence" – probability that the value of θ is equal to θ_i.
- $P(\varepsilon)$ - The total probability that the value ε will be observed for the random variable X, *summed over all possible values* θ_i *for the parameter* θ.
- $P(\theta = \theta_i \mid \varepsilon)$ - The **posterior distribution** – after observation of the value ε for X – probability that the value of θ is equal to θ_i.

There are many advantages to using Bayesian techniques for statistical analysis. One of the greatest strengths of Bayesian techniques is the ability to consistently modify a given analysis any time new evidence is gathered. The term for this process is "Bayesian updating." Every time new data are obtained, they may be used to update the existing distribution without changing any of the previous data or the system model. The new

information is simply added as extra points and the distributions are updated through the use of Equation 4.2. It is important to note that in this updating process, what was previously defined as the posterior now becomes the prior and the updated distribution becomes the posterior.

Another advantage of Bayesian analysis with respect to traditional analysis is the inherent uncertainty measures associated with Bayesian results. A traditional analysis typically produces a point value for parameters such as the mean, median, and standard deviation. A Bayesian analysis produces a distribution for each of these parameters; this distribution essentially identifies necessary information about the parameter, including a central tendency and the uncertainty associated with it.

There are two major drawbacks to Bayesian analyses. The first drawback involves the use of prior distributions. Since prior distributions are subjective, the results of a Bayesian analysis are also somewhat subjective. In situations where little or no data are available, the results are strongly dependent upon the subjective prior distributions. This has left Bayesian techniques open to some criticism. However, very few alternatives have been proposed and the ones that have been proposed have problems of their own, which seem to be more extensive than any of the issues associated with Bayesian analysis. One method to address this issue is to perform sensitivity studies where different prior distributions are assumed.

The second drawback to Bayesian analyses is the fact that the computational power required is greater than that required for traditional analyses. Due to this fact and the fact that any results of a Bayesian analysis should approach the results of a traditional analysis if large amounts of data are available, the benefits of using Bayesian techniques are much greater if used when there are little or no historical data available.

By comparing the two methods of statistical analysis for use in the QRAs of the hydrogen fueling process, it is apparent that, based on the currently available data, Bayesian techniques should be used rather than traditional means. Having the ability to generate uncertainty distributions presents larger confidence to the calculated values. The use of this method will provide more flexibility when additional data is presented. And additionally, Bayesian analysis will allow greater consideration to be placed on more applicable or specific data sets. These reasons illustrate the decision to use the Bayesian approach for this assessment.

4.2 Data Sources

Because data on hydrogen systems is extremely limited, sources from commercial operations may be used as a baseline for a Bayesian statistical analysis. Component leakage frequencies have been historically gathered by the chemical processing, compressed gas, nuclear power plant, and offshore petroleum industries; however, there has been little consistency across the disciplines and studies performed. Variances in leakage definitions, component classification, and data reliability make it difficult to directly apply the information to hydrogen specific processes. Unique physical

challenges, such as hydrogen embrittlement, provide additional uncertainty when applying statistically determined leakage frequencies to the risk assessment. Nevertheless, the identification of the component failure rates and severity of ensuing leaks by performing an extensive review of industrial sources is an appropriate initial phase to the Bayesian process described above.

Sources used in data analysis were obtained from a narrow range of available data and studies. They varied in nomenclature, component specifics, and data determination; however, at the present time it was the most widely accessible information. The existing frequencies may be found in reports and studies from the chemical processing, compressed gas, nuclear power plant, and offshore petroleum industries. It was important to consider the origin of this data and determine whether the information was derived from actual component failures or based on expert judgment. Making this distinction should provide a greater amount of confidence through the assessment process. The following sources were used to develop the component leakage frequencies:

- CPR 18E ed. 1, "Guidelines for Quantitative Risk Assessment: The Purple Book," Committee for the Prevention of Disasters, The Hague, The Netherlands, 1999.
- Center for Chemical Process Safety of the American Institute of Chemical Engineers, "Guidelines for Process Equipment Reliability Data with Data Tables," 1989.
- S.A Eide, S.T.,Khericha. M.B. Calley, D.A. Johnson, M.L. Marteeny, "Component External Leakage and Rupture Frequency Estimates," EGG-SSRE-9639, Nov 1991.
- NUREG/CR-6928, "Industry-Average Performance for Components and Initiating Events at U.S. Commercial Nuclear Power Plants," February 2007.
- NUREG-75/014, "Reactor Safety Study: An Assessment of Accident Risks in U.S. Commercial Nuclear Power Plants," WASH-1400, Oct 1975.
- Rijnmond, Openbaar Lichaam; "Risk Analysis of Six Potentially Hazardous Industrial Objects in the Rijnmond Area, A Pilot Study," COVO, 1982.
- Savannah River Site, "Generic Data Base Development," WSRC-TR-93-263, June 1993.
- Canadian Hydrogen Safety Program, "Quantitative Risk Comparison of Hydrogen and CNG Refueling Options," Presentation, IEA Task 19 Meeting, 2006.
- A.J.C.M. Matthijsen, E.S. Kooi, "Safety Distances for Hydrogen Filling Stations," Journal of Loss Prevention in the Process Industries 19, pp. 719 - 723, 2006.
- R. E. Melchers, W. R Feutrill, "Risk Assessment of LPG Automotive Refueling Facilities," Reliability Engineering and System Safety, 74, 2001.
- Rosyid, Oo Abdul, "System-Analytic Safety Evaluation of the Hydrogen Cycle for Energetic Utilization," Dissertation, 2006.

These multiple sources provided the raw generic data for the various components used in the hydrogen fueling process. The data is provided in Appendix C. A large variation in the leakage frequencies may be observed from this collection of data. Although many data sources provide leak rates as a function of leak size, vary few provide leak rates as a

function of pressure. Thus, the analysis performed in this study does not differentiate leak rates for systems operating at different pressures.

Limited hydrogen-specific leakage data was obtained through the efforts of members of NFPA 2 TG6 from the Compressed Gas Association. Due to the proprietary nature of the data, it is not presented in this report. The results of traditional statistical analysis of that data are shown in Table 4-1. For many components the fact that there are no reported failures prohibits estimating the MLE or the lower confidence bound (5th percentile). However, an upper confidence bound (95th percentile) can still be estimated but is not useful for evaluating realistic risk values. As shown in Table 4-1, the available hydrogen data is not sufficient for the application of traditional statistical analysis, thus the Bayesian model described in the following section was used to combine this limited data with generic estimates of component leakage rates.

Table 4-1. Traditional statistical analysis of hydrogen data.

		MLE	5.0%	95.0%			MLE	5.0%	95.0%
Compressor	Very Small	8.7E-02	4.5E-02	1.5E-01	Joints	Very Small	3.5E-05	2.3E-05	5.1E-05
	Minor	1.9E-02	3.4E-03	6.1E-02		Minor	0.0E+00	0.0E+00	6.1E-06
	Medium	1.9E-02	3.4E-03	6.1E-02		Medium	4.1E-06	7.3E-07	1.3E-05
	Major	0.0E+00	0.0E+00	2.9E-02		Major	2.1E-06	1.1E-07	9.7E-06
	Rupture	0.0E+00	0.0E+00	2.9E-02		Rupture	2.1E-06	1.1E-07	9.7E-06
Cylinders	Very Small	0.0E+00	0.0E+00	1.8E-06	Pipes	Very Small	0.0E+00	0.0E+00	1.9E-05
	Minor	0.0E+00	0.0E+00	1.8E-06		Minor	0.0E+00	0.0E+00	1.9E-05
	Medium	0.0E+00	0.0E+00	1.8E-06		Medium	0.0E+00	0.0E+00	1.9E-05
	Major	0.0E+00	0.0E+00	1.8E-06		Major	0.0E+00	0.0E+00	1.9E-05
	Rupture	0.0E+00	0.0E+00	1.8E-06		Rupture	0.0E+00	0.0E+00	1.9E-05
Hoses	Very Small	5.9E-04	2.6E-04	1.2E-03	Valves	Very Small	2.9E-03	1.8E-03	4.4E-03
	Minor	0.0E+00	0.0E+00	3.0E-04		Minor	5.8E-04	1.6E-04	1.5E-03
	Medium	0.0E+00	0.0E+00	3.0E-04		Medium	0.0E+00	0.0E+00	5.8E-04
	Major	0.0E+00	0.0E+00	3.0E-04		Major	0.0E+00	0.0E+00	5.8E-04
	Rupture	0.0E+00	0.0E+00	3.0E-04		Rupture	0.0E+00	0.0E+00	5.8E-04

4.3 Hydrogen Leak Frequency Model

A Bayesian model was developed in order to predict the probability of a leak in various components used in a hydrogen infrastructure. The model was selected based on analysis of actual leakage data from the offshore oil industry. The offshore industry data [17] shown in Figure 4-1 indicates that the leakage frequencies for components on offshore oil and gas facilities are a power function of the leak diameter with lower frequencies occurring for larger diameter leaks. Additionally, leak frequencies provided in many

sources indicated a similar relationship. Specifically, the method suggested by Cox, Lees, and Ang [18] for analyzing liquid natural gas hazards uses leak frequencies that are a power function of the leak area. Based on these sources, the component leak frequencies were modeled as a power function of the leak area. Note that other parameters may be important when characterizing the leak frequencies. In particular, the component operating pressure may be an important factor. Unfortunately, generic component leakage frequency estimates as a function of pressure are not widely available nor was there enough hydrogen-specific data to allow differentiation by pressure. Thus, the generated hydrogen-specific leakage estimates are independent of the component operating pressure.

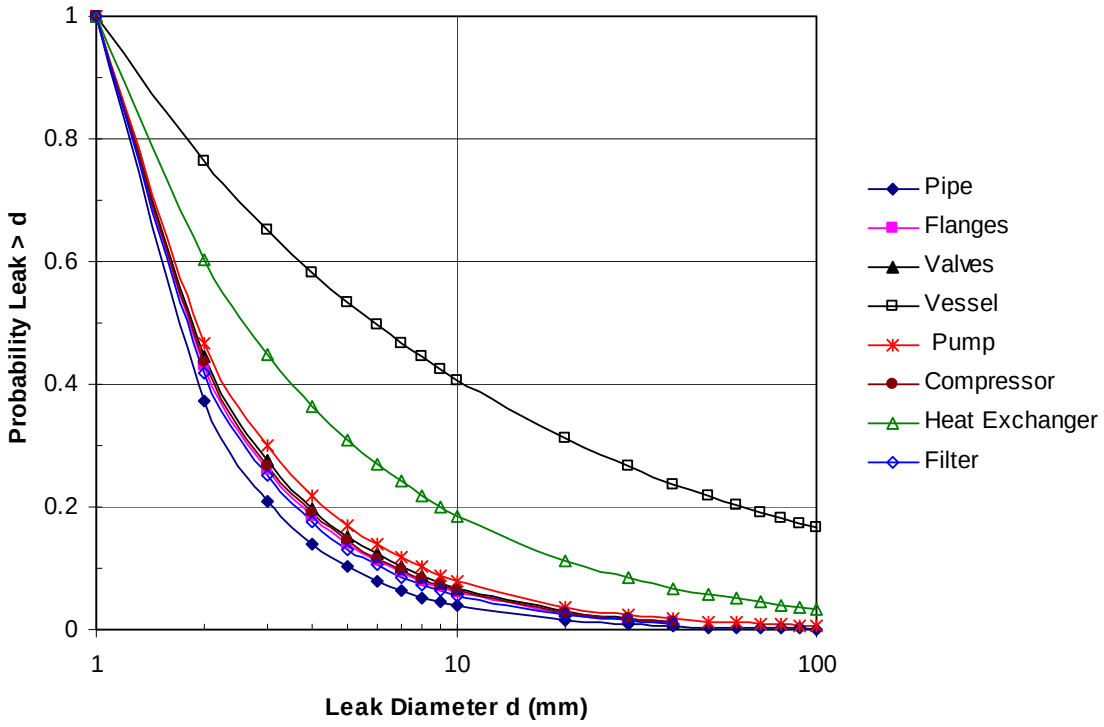

Figure 4-1. Correlation of offshore oil and gas leakage data.

The model assumes that the mean leak frequency of any component is linearly related to the logarithm of the fractional flow area of the leak. The fractional flow area is the ratio of the leak area to the total flow area of the pipe. The coefficients of the linear relationship – (α_1 and α_2) – are assumed to be normally distributed. The model is described in Equation 4.3.

$$\log\left(\mu_{LF,j}\right) = \alpha_2 \log(FLA_j) + \alpha_1 \Rightarrow \mu_{LF,j} = 10^{\alpha_1} \times FLA_j^{\alpha_2} \qquad (4.3)$$
$$\alpha_1 \sim N\left(0, 10^{-3}\right)$$
$$\alpha_2 \sim N\left(0, 10^{-3}\right)$$
$$\log\left(LF_j\right) \sim N\left(\mu_{LF,j}, \tau_j\right)$$
$$\tau_j \sim Gamma\ (1,1)$$

The variables in the model have the following descriptions:

- μ_{LF} - Mean of the recorded leak frequency (also called mean leak frequency in the subsequent discussion). In this model, it is the "true" leak frequency.
- FLA – Fractional leak area. This is the ratio of the leak area to the total cross-sectional flow area of the pipe.
- LF – The recorded leak frequency.
- α_2 - Parameter relating mean leak frequency to FLA.
- α_1 - Scaling parameter for the exponential function relating μ_{LF} and FLA.
- τ - Precision of the distribution describing the recorded leak frequency. The precision of a normal random variable is defined as the multiplicative inverse of the variance.
- j – Subscript used to enumerate the different leak sizes.

For this analysis, the leaks were divided into the following four sizes based on the data categories defined in generic data sources:

- Very Small- Leak area is 0.01 % of total flow area
- Minor – Leak area is 0.1% of total flow area
- Medium – Leak area is 1% of total flow area
- Major – Leak area is 10% of total flow area
- Rupture – Leak area is 100% of total flow area

The first phase of the Bayesian process used the data obtained from generic sources listed in Section 4.2. First, the means and standard deviations of the leak rates from these different sources were determined for each component. This data was then used to generate the parameters of the prior distributions for each component. This is appropriate since the data is an initial estimate of the distribution parameters. Additionally, non-informative prior distributions were selected for some of the parameters (α_1, α_2, and τ) in the model shown in Equation 4.3 (the prior distribution types and variable are shown in Equation 4.3). The Bayesian model and data was input into the WinBUGS program [30] to perform the hierarchical Bayesian analysis. The results of the first phase of the Bayesian analysis (estimates of generic component leakage frequencies) were then used to define the parameters of the prior distributions for the second phase of the Bayesian model. In the second phase, hydrogen-specific data were used to update the model, using WinBUGS, to provide the final posterior distribution that can be used in a hydrogen facility QRA. The results of the Bayesian analysis for each specific component are provided in Table 4-2. Note that hydrogen data was not available for some components and thus only generic leak frequencies could be generated.

Table 4-2. Results of Bayesian analysis of hydrogen component leakage frequencies.

Component	Leak size	Generic Leak Frequencies (Phase 1)				Hydrogen Leak Frequencies (Phase 2)			
		Mean	5.0%	Median	95.0%	Mean	5.0%	Median	95.0%
Compressor	Very Small	8.3E+00	1.8E-01	2.1E+00	2.6E+01	1.8E-01	1.2E-01	1.8E-01	2.5E-01
	Minor	2.3E-01	1.5E-02	1.1E-01	7.1E-01	2.2E-02	7.8E-03	2.0E-02	4.4E-02
	Medium	1.2E-02	7.9E-04	5.2E-03	3.4E-02	7.9E-03	1.4E-03	5.9E-03	2.1E-02
	Major	3.9E-04	6.6E-05	2.5E-04	1.0E-03	2.1E-04	3.5E-05	1.4E-04	5.7E-04
	Rupture	9.7E-05	1.2E-06	1.2E-05	1.3E-04	3.4E-05	1.3E-06	1.2E-05	1.1E-04
Cylinders	Very Small	2.2E+00	4.1E-02	6.4E-01	7.4E+00	1.1E-06	1.7E-07	9.8E-07	2.7E-06
	Minor	4.3E-02	2.3E-03	2.0E-02	1.3E-01	9.8E-07	1.9E-07	8.3E-07	2.3E-06
	Medium	9.5E-04	1.2E-04	6.3E-04	2.6E-03	6.7E-07	1.5E-07	5.6E-07	1.6E-06
	Major	2.7E-05	5.3E-06	1.8E-05	7.1E-05	3.9E-07	9.0E-08	3.2E-07	9.0E-07
	Rupture	8.4E-07	1.5E-07	6.1E-07	2.1E-06	2.1E-07	4.8E-08	1.7E-07	5.0E-07
Filters	Very Small	2.5E-01	2.0E-04	5.3E-03	1.4E-01	NA[1]	NA	NA	NA
	Minor	2.3E-02	4.1E-04	5.1E-03	6.1E-02	NA	NA	NA	NA
	Medium	4.2E-02	4.1E-04	4.8E-03	5.5E-02	NA	NA	NA	NA
	Major	7.7E-03	1.1E-03	4.6E-03	2.0E-02	NA	NA	NA	NA
	Rupture	5.4E-02	9.1E-04	4.4E-03	2.1E-02	NA	NA	NA	NA
Flanges	Very Small	9.0E-02	1.4E-03	2.0E-02	3.0E-01	NA	NA	NA	NA
	Minor	5.3E-03	2.8E-04	2.2E-03	1.7E-02	NA	NA	NA	NA
	Medium	5.2E-03	6.3E-06	2.4E-04	9.0E-03	NA	NA	NA	NA
	Major	4.1E-05	6.8E-06	2.6E-05	1.0E-04	NA	NA	NA	NA
	Rupture	2.5E-05	1.4E-07	2.9E-06	5.9E-05	NA	NA	NA	NA
Hoses	Very Small	3.7E+01	1.1E+00	1.2E+01	1.3E+02	1.1E-03	6.6E-04	1.1E-03	1.7E-03
	Minor	2.7E+00	2.1E-01	1.4E+00	8.1E+00	2.0E-04	3.7E-05	1.8E-04	4.4E-04
	Medium	2.4E-01	3.4E-02	1.6E-01	6.4E-01	1.7E-04	3.9E-05	1.5E-04	3.8E-04
	Major	2.4E-02	5.0E-03	1.7E-02	6.3E-02	1.6E-04	3.8E-05	1.4E-04	3.4E-04
	Rupture	8.7E-03	1.5E-04	2.0E-03	2.4E-02	7.3E-05	6.2E-06	5.2E-05	2.1E-04
Joints	Very Small	1.9E+00	5.2E-02	5.4E-01	6.4E+00	7.0E-05	5.2E-05	7.0E-05	9.1E-05
	Minor	2.1E-01	1.6E-02	1.0E-01	6.7E-01	3.4E-06	2.0E-07	2.7E-06	9.3E-06
	Medium	4.1E-02	3.4E-03	1.8E-02	1.2E-01	7.6E-06	2.4E-06	7.0E-06	1.5E-05
	Major	4.3E-03	1.2E-03	3.6E-03	9.7E-03	6.8E-06	1.6E-06	6.0E-06	1.4E-05
	Rupture	9.2E-04	2.0E-04	6.3E-04	2.3E-03	6.1E-06	1.3E-06	5.3E-06	1.3E-05
Pipes	Very Small	7.8E-04	6.1E-05	3.6E-04	2.1E-03	8.6E-06	1.6E-06	7.1E-06	2.1E-05
	Minor	1.0E-04	1.5E-05	6.2E-05	2.7E-04	4.5E-06	8.6E-07	3.6E-06	1.1E-05
	Medium	4.0E-05	8.2E-07	1.1E-05	1.4E-04	1.7E-06	9.1E-08	9.5E-07	6.1E-06
	Major	5.4E-06	2.0E-07	1.8E-06	1.8E-05	8.9E-07	5.2E-08	4.7E-07	3.1E-06
	Rupture	5.3E-06	8.3E-09	3.2E-07	1.2E-05	5.6E-07	4.8E-09	1.5E-07	2.5E-06
Valves	Very Small	2.3E-02	1.8E-03	1.1E-02	7.4E-02	5.7E-03	4.1E-03	5.6E-03	7.5E-03
	Minor	6.4E-03	4.1E-04	1.9E-03	8.8E-03	7.4E-04	3.1E-04	6.9E-04	1.3E-03
	Medium	1.4E-03	2.2E-05	3.1E-04	4.4E-03	9.6E-05	6.8E-06	6.3E-05	3.0E-04
	Major	7.2E-05	1.5E-05	5.2E-05	1.7E-04	4.1E-05	9.7E-06	3.3E-05	1.0E-04
	Rupture	3.0E-05	7.1E-07	8.4E-06	1.0E-04	1.4E-05	5.8E-07	6.2E-06	5.5E-05

[1] NA = Not available. No hydrogen-specific estimate could be calculated since no hydrogen leakage data was available.

Figure 4-2 shows the results of the Bayesian analysis for pipes. The generic prior was estimated utilizing 60 published leak frequencies (shown as blue diamonds on Figure 4-2)

that include values from the compressed gas, chemical processing, hydrocarbon industry, and nuclear sources. As indicated, the generic median (i.e., the 50th percentile) is a straight line on the log-log plot since that is the model that was assumed in the Bayesian model. The median leak frequency is at the center of the available data, which was binned as medium (1% flow area), major (10% flow area), and rupture (100% flow area) leak sizes. The Bayesian analysis resulted in estimates for small leak sizes based on these published leak frequencies. The mean leak frequencies are higher than the median values since the assumed distribution is lognormal. The 5th and 95th percentiles for the leak frequency distributions for the five leak sizes (shown as the black brackets in Figure 4-2) encompass the data except for a couple of outliers.

The hydrogen data that was available indicated that there were no leakage events of any size over a rather large operating history of pipes in hydrogen systems. The fact that there were no failures in a large operating history suggests that the upper confidence limit (95th percentile) of the hydrogen-specific leak frequencies obtained from the traditional statistical analysis, regardless of the size of the leak, are 1.9E-5/yr (see Table 4-1), which are less than the generic values for the small leak sizes.

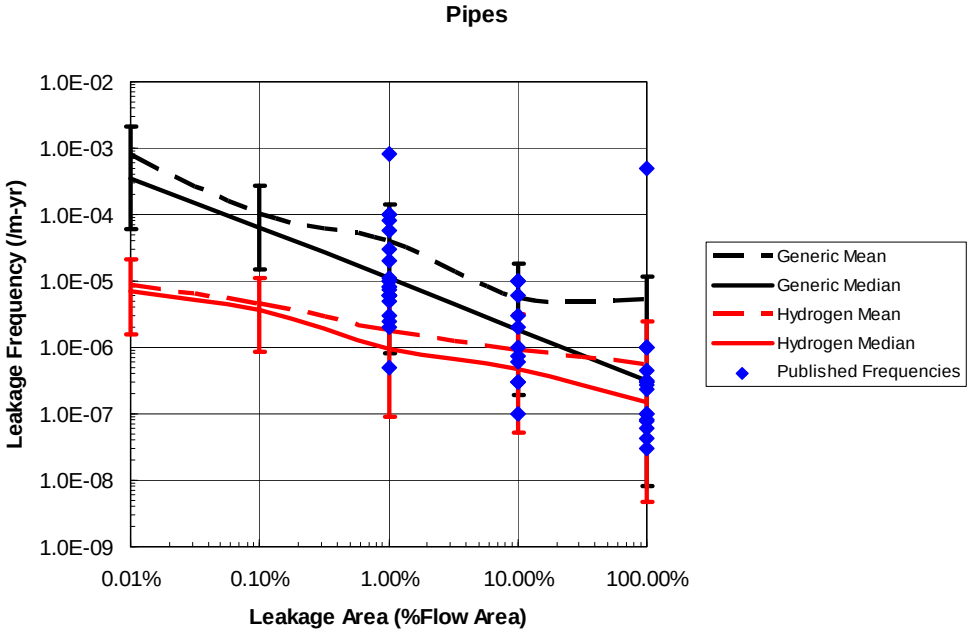

Figure 4-2. Results of Bayesian analysis for pipe leakage frequency.

Using the available hydrogen pipe information, the generic prior distributions were updated to obtain the estimated leakage frequency distributions for hydrogen pipes (shown in red in Figure 4-2). As indicated in the figure, the estimated hydrogen pipe leak frequencies for 0.1% to 1% flow area leaks are 1 to 2 orders of magnitude less than the generic estimates. For the larger leak sizes, the hydrogen estimates are much closer (a factor of 2 to 4 less).

As shown in Figure 4-3, updating from generic data only to generic and hydrogen-specific data changed both the central tendency (i.e., median value) and the precision (i.e. spread) of the leak frequency distributions. The large spread in the generic prior is due to the large range of values for the minor leak frequency that were found in the literature. The smaller width in the estimated hydrogen leak frequency distribution is due to the fact that a substantial amount of hydrogen pipe operating history was available. The lower median values for the hydrogen estimate is again due to the fact that no failures were observed in the provided data.

Figure 4-4 presents the results of the Bayesian analysis for pipe joints. Only a few generic estimates were obtained from the literature for pipe joints and that data did not specify what types of joints were considered. The generic leak frequencies are relatively high compared to the pipe leak frequencies discussed above. The hydrogen-specific failure data that was obtained indicated that different size leakages had occurred over a large operating history. The maximum likelihood estimates based on this data (included on Figure 4-4) indicate that the expected hydrogen leak frequencies for pipe joints could be substantially smaller than the values found in the literature. As indicated in Figure 4-4, the estimated hydrogen leak rates for joints obtained from the Bayesian analysis is from 2 to 5 orders of magnitude less than the generic estimates depending on the size of the leak. The width of the probability distributions were also generally smaller for the hydrogen estimates except for the 0.1% leak size since no hydrogen leakage events were identified for that leak size. It should be noted that these estimated frequencies do not differentiate between the types of joints used and thus encompass all types of joints. It is possible that specific types of joints may have higher or lower leakage potential but the data analysis performed to date does not provide that degree of resolution.

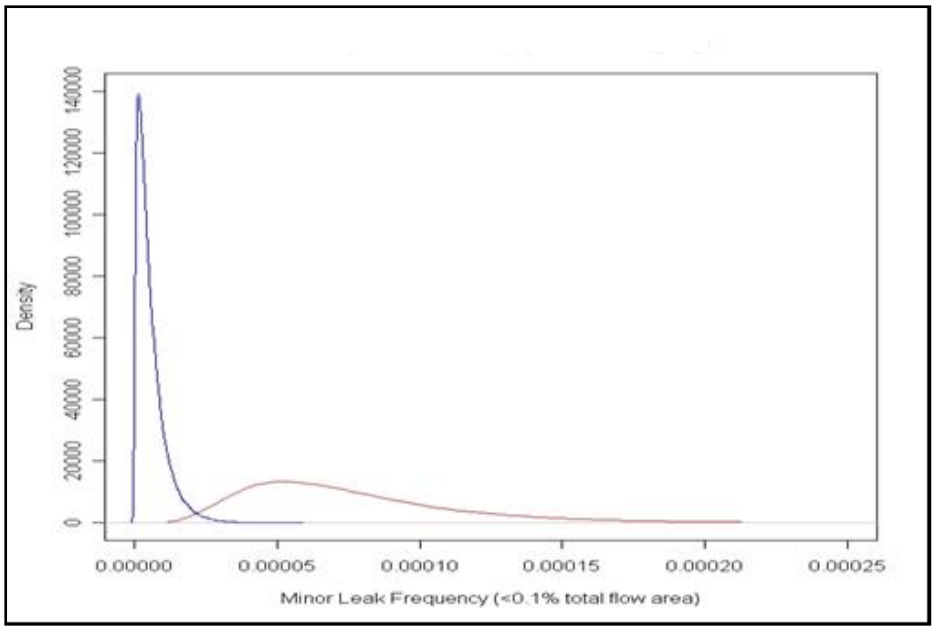

Figure 4-3. Probability density functions from the generic (red) and hydrogen (blue) Bayesian analysis for minor pipe leaks (<0.1% flow area).

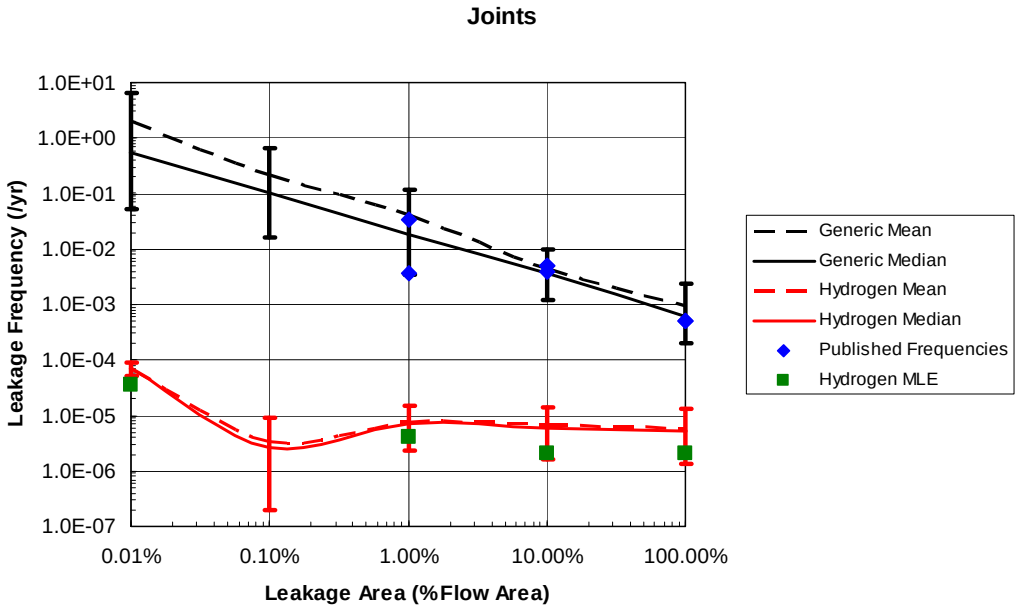

Figure 4-4. Results of Bayesian analysis for pipe joint leak frequency.

The results of the Bayesian analysis for compressors are shown in Figure 4-5. The compressor results are indicative of a component in which there are a significant number of hydrogen leakage events in a relatively short operating experience. As with pipe joints, very few leak frequencies were found for compressors in the literature and the results of the Bayesian analysis resulted in a median generic leak frequency greater than 1 for very small leaks (defined as <0.01% of the connecting pipe flow area). Even though there were a relatively large number of very small hydrogen leakage events, the MLE was below the estimated generic values. As a result of the inclusion of the hydrogen data in the Bayesian process, the estimated hydrogen-specific leakage frequencies are less than the generic estimates for leak sizes equal to 0.01% and 0.1% of the connecting pipe flow area. In contrast, the hydrogen leakage data for a 1% leak size resulted in an MLE (using traditional statistical analysis) that is greater than the estimated generic median. As a result of inclusion of the hydrogen data for 1% leaks in the Bayesian model, the estimated hydrogen-specific leak frequencies for a 1% or greater leak area are nearly the same as the estimated generic values.

Finally, the estimated leak frequencies for valves are shown graphically in Figure 4-6. A significant number of leak frequencies were found in the literature. In addition, some hydrogen-specific leak events were also identified in the 0.01% and 0.1% range. As indicated in Figure 4-6, the estimated hydrogen leak frequencies are similar to those for the generic estimates with the largest deviation occurring for the 1% leak size.

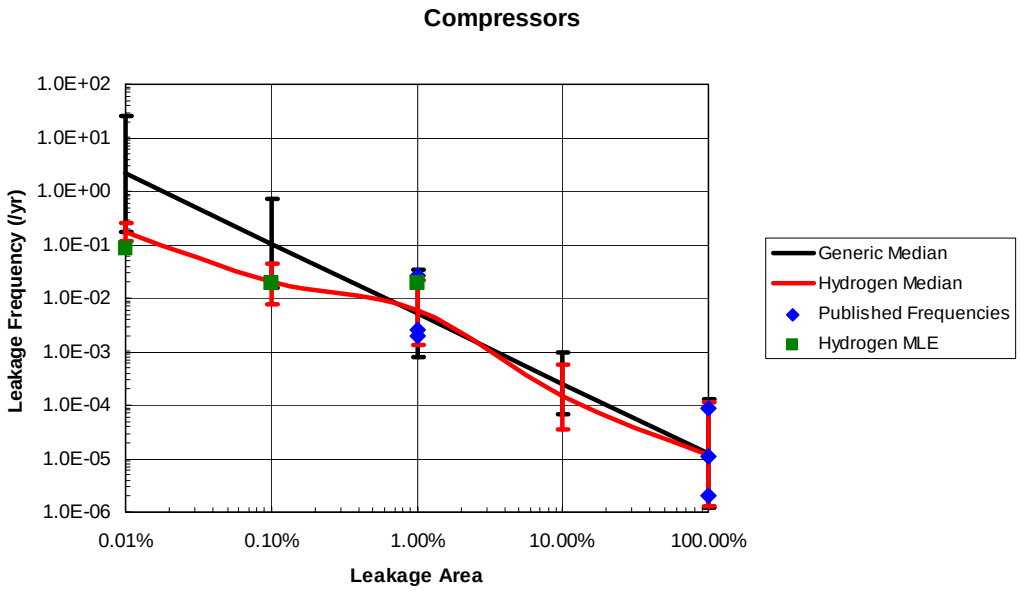

Figure 4-5. Results of Bayesian analysis for compressor leak frequency.

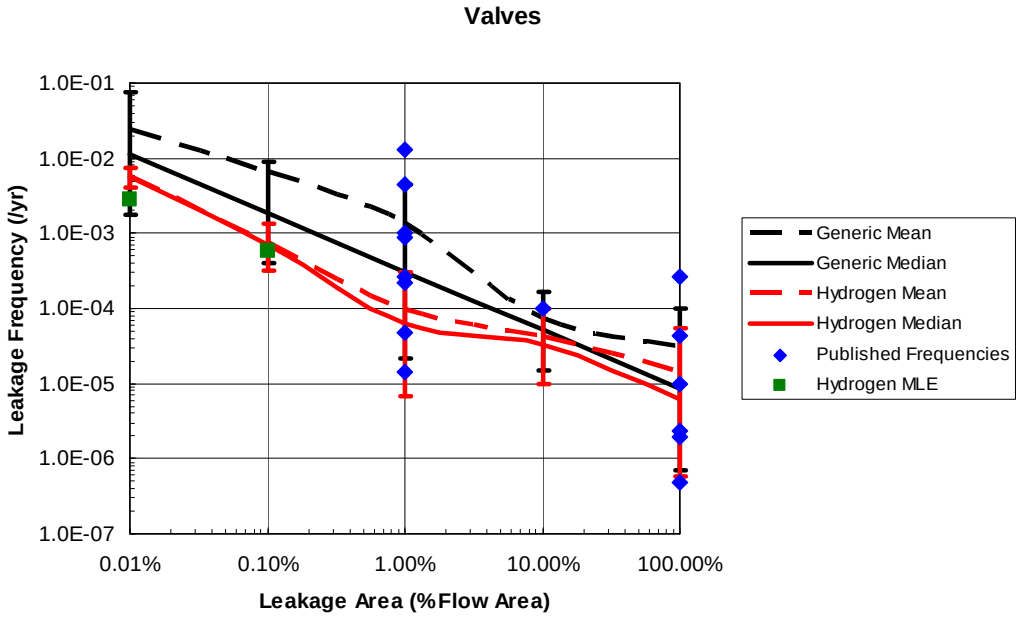

Figure 4-6. Results of Bayesian analysis for valve leak frequency.

4.4 Use of Leakage Frequencies to Establish Leak size for Determining Separation Distances

One application of the resulting component leakage rates is to help establish a basis for determining the leak size used to determine separation distances. The concept is to use the cumulative probability for different component leak sizes to identify the range of leaks that encompass the most probable leak sizes. Table 4-3 presents a first order approximation of the cumulative probability for different leak sizes for six components. Figure 4-7 graphically presents the approximate cumulative distribution functions (CDFs). The cumulative probability establishes the probability that a component leak rate will be a specific size or less. For example, the cumulative probability that the size of a hose leak will be less than or equal to 1% of the hose flow area is shown in Table 4-3 to be approximately 87% (13% of the leaks would be greater than this area). The provided cumulative probabilities are conditional on having a component leak. Thus they do not provide an indication of the actual frequency of leakage, which varies from component to component.

Table 4-3. Approximate cumulative probabilities for different leakage sizes based on Bayesian analysis of hydrogen-specific leakage data.

	Components					
Leak size	Compressors	Cylinders	Hoses	Joints	Pipes	Valves
<0.01%A	85.8%	33.8%	65.3%	74.6%	52.8%	86.4%
<0.1%A	96.2%	62.7%	76.8%	78.3%	80.4%	97.7%
<1%A	99.9%	82.5%	86.9%	86.4%	91.1%	99.2%
<10%A	100.0%	93.9%	95.8%	93.6%	96.6%	99.8%
<100%A	100.0%	100.0%	100.0%	100.0%	100.0%	100.0%

* A = cross-sectional flow area for hoses, joints, pipes, and valves. For cylinders, A is the cross-sectional area of the cylinder. For compressors, A is the area of the upper head gasket.

In order to utilize the cumulative probability information shown in Table 4-3 and Figure 4-7 to determine what leak size could be justified as the basis for selecting separation distances, several decisions are required. First, a cumulative probability percentile must be selected as the criteria for selecting the leak size. In many applications of statistical data, the use of the 95th percentile is common in decision making. Some decision makers have used lower values (e.g., 90th percentile) while other have chosen to use a more restrictive value (e.g., 99th percentile). In general, as the potential consequences of the event under consideration increases, a higher percentile is recommended. As an example, thermal-hydraulic evaluation of design basis events in nuclear power plants can be performed taking into account uncertainty in all of the design and thermal-hydraulic parameters. Whether the reactor design meets the deterministic licensing criterion is based on the 95th percentile value determined in the analysis.

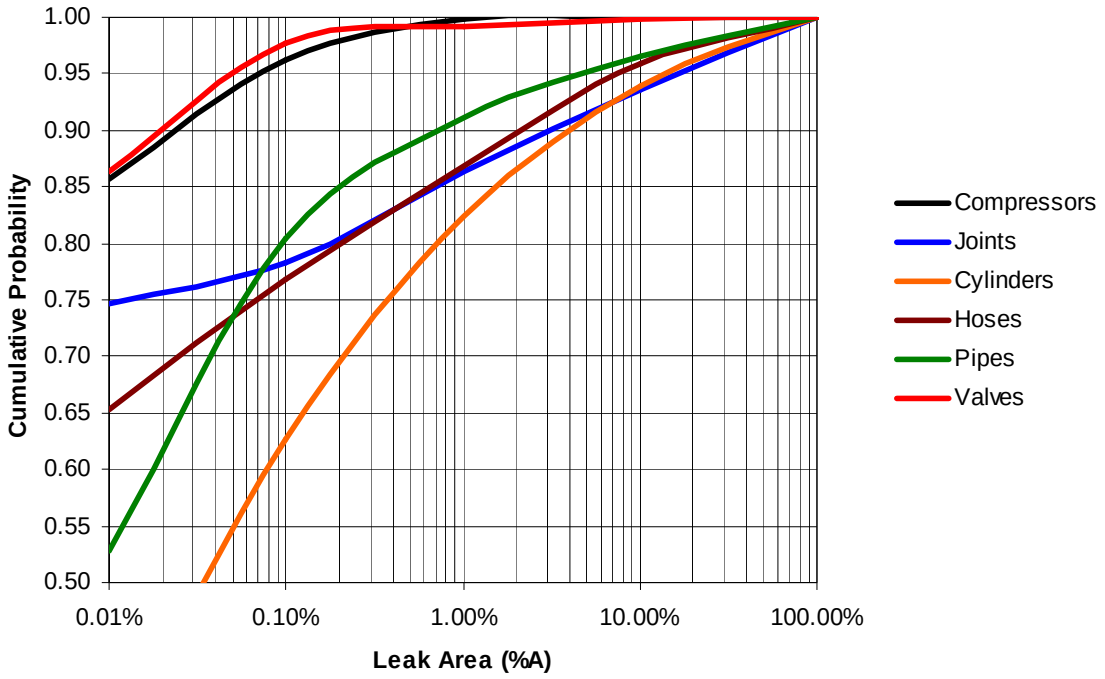

Figure 4-7. Component cumulative probability distributions for leakage sizes based on Bayesian analysis of hydrogen-specific leakage data.

Once an upper bound percentile has been selected as the value for decision making, the second consideration is deciding what cumulative distribution should be used in selecting the leak size. For example, if a 95th percentile guideline is selected, the range of leak sizes estimated in the Bayesian analysis of the six components shown in Table 4-3 range from approximately 0.05% of the component flow area to approximately 20% of the component flow area. This is a broad range. The use of the 20% value would be conservative but potentially prohibitive in that it would require large separation distances. On the other hand, use of the 0.05% value would not encompass all expected leakage events within the 95th percentile guideline. To address this dilemma, a decision maker may choose to use the arithmetic average of the values for the six components. However, the problem with this approach is that some components have high leakage rates and the use of an average value puts them on equal ground with components with low leakage rates.

A better approach is to evaluate the cumulative probability of leakage for an actual hydrogen system. The advantage of this approach is that it weights the cumulative probability by the actual number of components in a system. Figure 4-8 provides an example of a simple 20.7 MPa (3000 psig) system (generated by TG6) that was used in the evaluations performed to determine the NFPA 2 separation distances. It consists of a tube trailer, a discharge stanchion, and pressure control station. A 103.4 MPa (15000 psig) system similar to the system in Figure 4-8 was also evaluated (the 103.4 MPa system also had a compressor and 103.4 MPa storage bank). Both systems are described

in more detail in Appendix B. The total estimated leakage frequency for these two systems is shown as a function of leak size in Figure 4-9. For a 0.1% leak size, the system leakage frequency is 3 x 10^{-2}/yr and 6 x 10^{-2}/yr r for the 20.7 MPa and 103.4 MPa systems, respectively. The higher leakage frequency for the 103.4 MPa system is due to the contribution from the additional compressor and high-pressure storage modules. These values are comparative to the fire frequency in gasoline stations (7.4 x 10^{-2}/yr [21]) and suggest that a 0.1% leak would be expected during the lifetime of these facilities. To reduce the potential for significant consequences to a person at the site boundary due to expected accidents, larger and less frequent leak sizes of at least 1% should be used as the basis for separation distances.

The cumulative leakage distributions for the example 20.7 MPa and 103.4 MPa systems are shown in Figure 4-10. Nearly identical results were obtained for typical 1.7 MPa (250 psig) and 51.7 MPa (7500 psig) systems. As indicated, the system level leakage CDFs result in high percentiles for small leakage sizes. Ninety five percent of the system leakage events would be equal to or less than 0.1% of the component flow area for this system based on the use of the hydrogen-specific leakage data developed using Bayesian analysis. Use of a larger leak size was recommended to the NFPA 2 TG6 based on consideration of the actual system leakage frequencies provided in Figure 4-9 and the uncertainty in the component and system leak frequency analysis (discussed in Section 4.5).

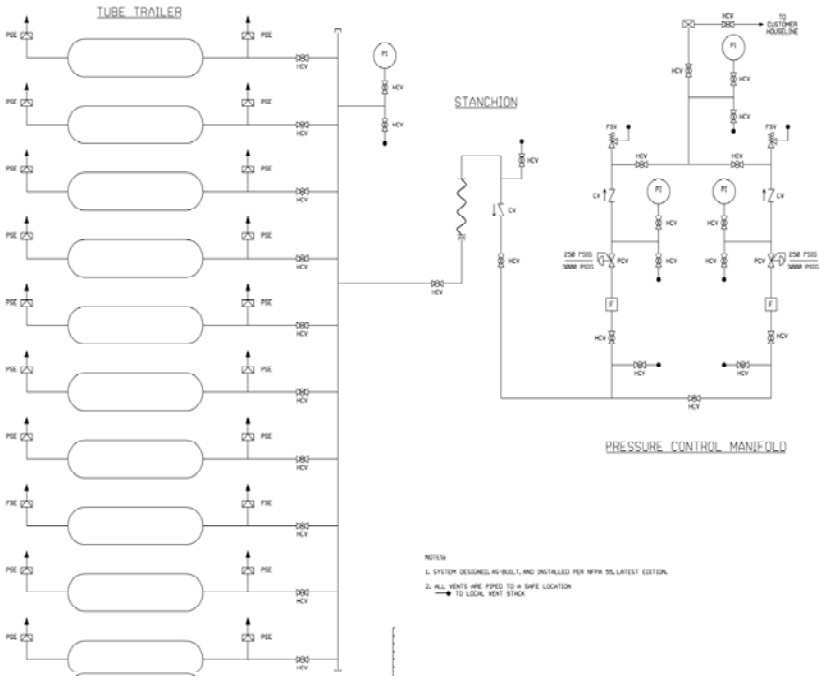

Figure 4-8. Example gas storage system modeled in NFPA analysis.

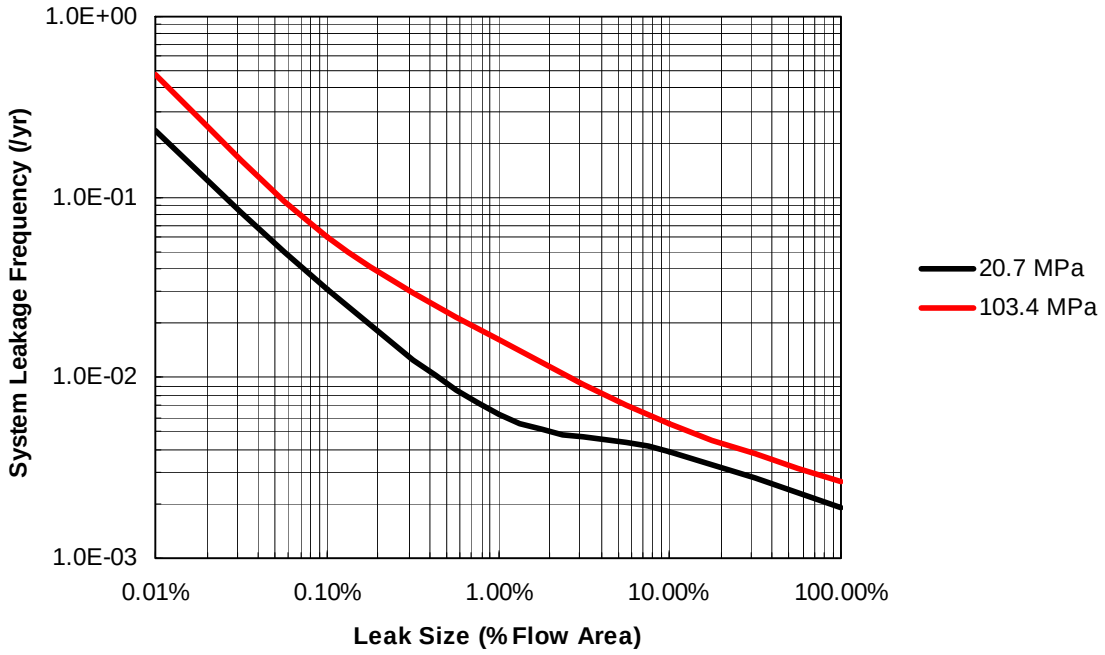

Figure 4-9. System leakage frequency for two example facilities.

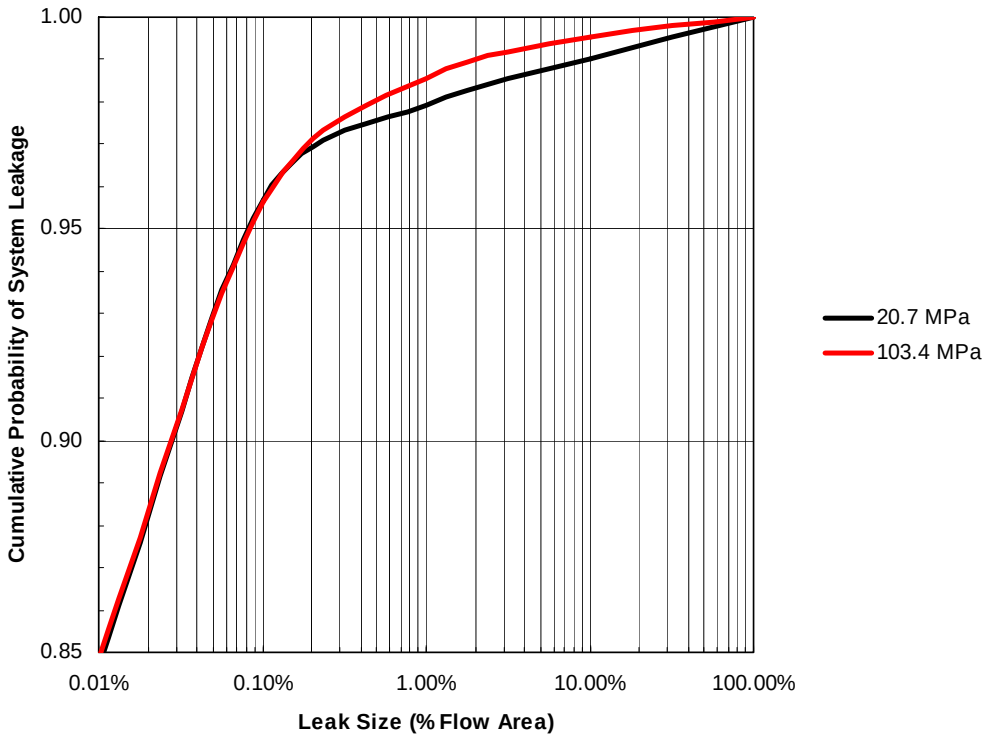

Figure 4-10. System level cumulative leakage probabilities for two example facilities.

4.5 Data Uncertainty Analyses

There are several key uncertainties associated with the data analysis that was performed, which are discussed in this section:

- Selection of the model used to describe leak frequencies as a function of leak diameters
- Selection of available leak rates for use in data analysis
- Binning of generic and hydrogen data into leak size categories
- Selection of the prior distributions used in the Bayesian process
- Typical facility configuration used in determining system leak frequency

Leak Frequency Model

As indicated in Figure 4-2, the median values predicted by the selected model fit existing pipe leak frequency estimates very well and can be used to estimate the leak frequencies for smaller leak diameters. Furthermore, the 90% uncertainty interval (shown as the brackets) generally bounded most of the available pipe leak frequency estimates used in the analysis. The same trend was true for other evaluated components. For these reasons, no other model for evaluating the component leak frequencies was pursued. However, it could be argued that the frequencies for smaller diameter leaks could be substantially higher than for larger diameter leaks (the model in Reference 17 is valid only for leaks greater than 1 mm in diameter). In fact, this trend was seen in some of the hydrogen data that was used in the analysis. Fortunately, the Bayesian updating process accounts for the trends in the hydrogen data in the calculation of hydrogen-specific leak frequencies (i.e., it adjusts for higher leak occurrences for small diameters). This is illustrated in the hydrogen-specific pipe leak frequencies shown in Figure 4-2, which reflect that there were no reported hydrogen pipe leaks of any size in the data that was provided.

Selection of Generic Leak Frequencies

Component leak frequencies were obtained from multiple sources for use in the Bayesian process. This includes estimates from different industries including chemical, oil, compressed gas, and the nuclear industry. The pedigree of the leak frequency estimates is highly variable and range from expert judgment to actual data analysis. In addition, it is questionable whether data from different industries is applicable for hydrogen systems. Unfortunately, leakage frequencies are difficult to obtain as the primary concern in most of these industries is the reliability of components to operate when required. Thus, for many components exclusion of specific data based on applicability or pedigree would significantly limit the number of data estimates that would be available for use in a hydrogen system risk assessment. Furthermore, exclusion of frequency estimates can have a variable effect on the data estimates generated in the Bayesian analysis. For example, the impact of only using leakage frequencies from compressed gas (CG) sources for pipes in the Bayesian analysis is illustrated in Figure 4-11.

Compressed gas leak frequencies may be the most appropriate for estimating hydrogen-specific estimates. Of the 60 available pipe leak frequencies used in this study, only four are from CG sources. As indicated in Figure 4-11, the CG values are on the upper end of the range of values found in the literature. Thus, when only the CG values are used, the estimated generic leak frequencies increase by a factor ranging from 2 to 10 for all leak sizes. The estimated hydrogen leak frequencies also increase for leak sizes greater than 1% of the pipe flow area because the hydrogen information (no failures) has little impact on the frequencies for these leak sizes. For smaller leak sizes, the hydrogen information has more of an impact since it reflects a lower estimate than provided by the estimated generic leak frequencies.

Figure 4-12 provides the results of the estimated valve leak frequencies when data from the nuclear industry is not included. Nuclear valve leak rates reflect leakage rates of high-pressure water or steam valves which likely would be substantially different than the leakage rates for valves in hydrogen systems. Because the nuclear valve leak rates are centered in the values from other sources, the exclusion of the nuclear leak rates does not have an impact on either the estimated generic or hydrogen leak rates.

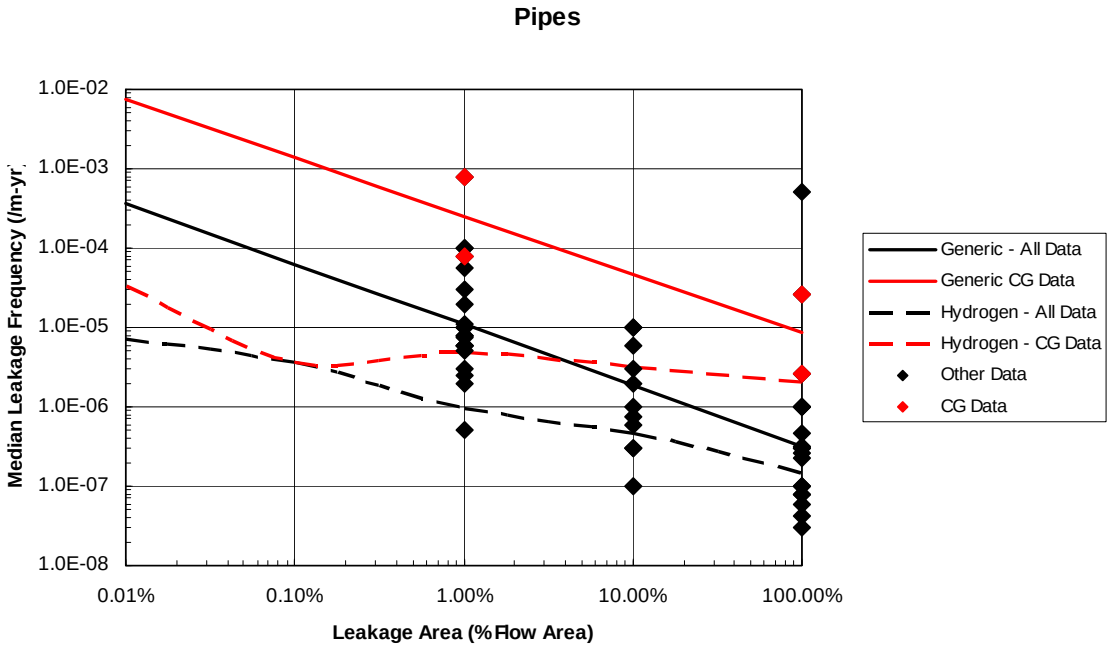

Figure 4-11. Example of impact of excluding generic frequency estimates on hydrogen-specific leak frequency estimates.

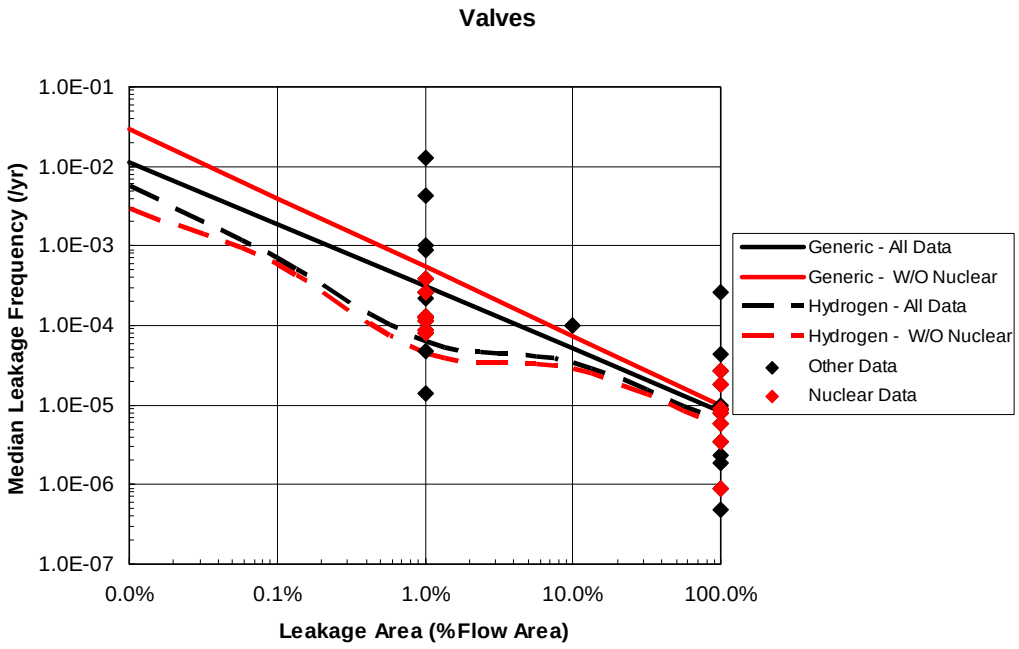

Figure 4-12. Sensitivity of estimated valve leak frequencies when nuclear data is excluded from determining the generic prior distribution.

The results of these sensitivity studies shows that the impact of using leak rates from specific types of sources can be variable. Although compressed gas sources are probably the most applicable for hydrogen components, the scarcity of such sources requires that information from other industries be utilized. Different weights can be assigned to values available from different industries in the Bayesian process utilized in the study. However, additional work is required to determine how to properly weight different sources of leak rates.

Binning of Data into Leak Size Categories

Discrete leak size categories were defined to facilitate the analysis (a risk assessment of all possible leak sizes is not practical) with each frequency range representing an order of magnitude spread in the leak area. Although the binning process is based upon limited available information, the broad leak categories generally prevent significant miss-categorization of events. For that reason, no sensitivity assessment was performed for this issue.

Selection of Prior Distribution Used in Bayesian Analysis

The results of a Bayesian analysis can be affected by the prior distribution selected in the analysis. This includes not only the distribution type but the initial values used in the Bayesian analysis. The selected prior distributions and values were non-informative. The term "non-informative" refers to the situation where very little *a priori* information about a parameter is available. This is definitely the situation with regard to both the hydrogen component leak frequencies and how they vary as a function of leak size. The hierarchal Bayes approach used in the analysis utilizes the selected distributions, Monte

Carlo sampling, and the available information to generate parameter distributions. Plausible means and wide variances for the distributions were chosen so as not to bias the results. The resulting posterior distributions are affected by the prior distributions selected for each parameter in the model. However, the results are less sensitive to the selected distribution parameters since the Monte Carlo approach converges on the most appropriate distribution parameters. The fact that the final distribution parameters are substantially different than the selected prior values indicates that the data substantially influenced the results more than the selected prior information. Thus, although the selection of the prior distributions is generally accepted as an important issue leading to uncertainty in the parameter estimates, no sensitivity studies have been performed to date.

Typical Facility Configuration

The generated hydrogen-specific component leakage rates were used to help establish a basis for determining the leak size for establishing separation distances. As discussed previously, the concept is to use the cumulative probability for different component leak sizes to identify the range of leaks that encompass the most probable leak sizes. The cumulative probability of leakage was evaluated for typical hydrogen gas storage systems, which allows the cumulative probability to be weighted by the type and number of components in the system. One uncertainty in this process was evaluated: the facility configuration used to calculate the cumulative probability of leakage.

A set of example hydrogen storage facility configurations was chosen by industry representatives for use in these separation distance evaluations. The facility descriptions specified the number of storage cylinders, valves, joints, and other components in the system. Since each component is a potential source for system leakage, the number of each of the components in the system can affect the system leakage probability. Figure 4-13 provides the system leakage frequency for the 20.7 MPa (3000 psig) tube trailer storage system presented in Figure 4-8 when the number of cylinders in the tube trailer is varied from 10 (base configuration used in analysis) to 30 cylinders. As indicated, the system leakage frequency doubles as the number of cylinders (and associated valves and joints) increases from 10 to 30 cylinders. The system leakage frequency would be expected to double again if the number of cylinders increased to 50. This result indicates the need to include some level of safety margin in selecting the leak size to account for variation in gas storage system configurations. Leak sizes of approximately 1% of the system flow area could be justified based on this analysis.

The cumulative leakage distributions for the example 20.7 MPa system as a function of the number of tube trailer cylinders are shown in Figure 4-14. As indicated, the system level cumulative probability of leakage does not substantially change. For 10 cylinders, ninety five percent of the system leakage events would be equal to or less than 0.1% of the component flow area for this system based on the use of the hydrogen-specific leakage data developed using Bayesian analysis. For 30 cylinders, the 95th percentile only increases to approximately 0.12% of the component flow area. The increase in the 95^{th} percentile would be small if the number of cylinders was increased further. For a 1% leakage size, the cumulative probability decreases from 96% to 94% when the number of

cylinders increases from 10 to 30. This difference decreases as the leak size increases since larger leaks do not contribute substantially to the cumulative leakage probability regardless of the number of cylinders present in the tube trailer.

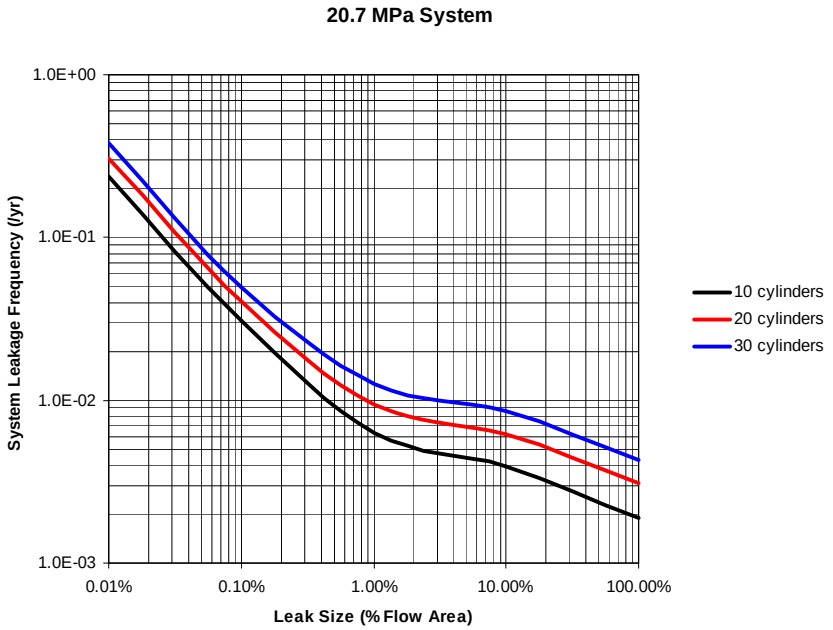

Figure 4-13. System leakage frequency as a function of the number of cylinders in a tube trailer.

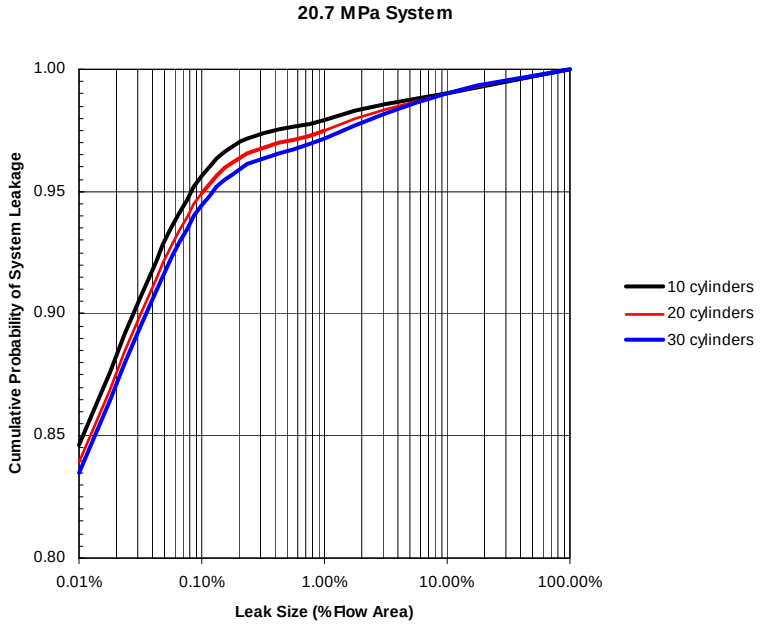

Figure 4-14. System level cumulative leakage probabilities as a function of the number of cylinders in a tube trailer.

5. Risk Analysis of Typical Hydrogen Gas Storage Configuration

Although the system level leakage frequencies for the example facilities documented in Section 4 supports the selection of a small (~1%) leak area as the basis for determining separation distances, it is important to determine if larger leaks would present significant consequences and an unacceptable level of risk to a person located at the established separation distance. This section presents a risk analysis of the typical hydrogen gas storage systems defined by the NFPA 2 TG6. The scope of the risk analysis was limited to accident sequences related to leakage events that result in ignited and un-ignited hydrogen jets.

The use of the risk-informed process described in Section 3 requires selection of risk acceptance guidelines. A survey of risk acceptance guidelines was performed and is documented in Section 5.1. Based on the survey, the NFPA 2 TG6 selected the risk guidelines for use in this study. A survey of harm criteria was also performed and is documented in Section 5.2. Based on this survey, the harm criteria used in the risk assessment was selected. The risk models developed for several gaseous storage facilities and the results of the risk analysis are presented in Section 5.3 and 5.4, respectively. An uncertainty analysis was performed, which included propagation of parameter uncertainties through the risk model and selected performance of sensitivity studies to address key assumptions. The results are documented in Section 5.5.

5.1 Risk Acceptance Guidelines

Establishing risk guidelines is a key element required to utilize the risk-informed approach discussed in Section 3. Since the primary concern is the potential for personnel injury, risk guidelines can be established for people exposed to the consequences of facility-related accidents, which could include the public located outside the boundaries of the facility (3rd party), users of the facility or customers (2nd party), and the facility workers (1st party). Public risk is generally the main focus in risk assessments and was designated by TG6 to be the focus of this risk assessment. In most QRA applications, the risk levels for the public are generally set one to two orders of magnitude less than the level for workers. Depending on the accident consequences, the selected risk guidelines could reflect acceptance levels for either injuries or fatalities. Because the frequency of fatalities is generally the concern evaluated in QRAs, the potential for fatalities was selected by TG6 as the risk measure in this evaluation.

Risk guidelines can be specified with regard to individuals or the society at large. Individual risk reflects the frequency that an average person located at a certain location is harmed. Generally, individual risk is evaluated for the most exposed individual. Characterization of the population surrounding a facility is thus not required to evaluate individual risk. Societal risk reflects the relationship between the frequency (F) and the number (N) of people harmed and is usually expressed in the form of an FN curve. The slope of the FN curve is defined by a *risk aversion factor* that is designed to reflect the

society's aversion to single accidents with multiple fatalities as opposed to several accidents with few fatalities. It is important to note that evaluation of societal risk requires determination of the population surrounding a facility. For generic QRAs used to establish code and standard requirements, the selection of a population density introduces one more uncertainty on the results. Thus, for the application of QRA to determine the separation distances specified in codes and standards, the use of individual risk measures are the most appropriate since they are site independent. Furthermore, since one cannot determine the most exposed individual for a generic site, the most exposed individual is assumed to be constantly present at the separation distance required for a member of the public.

Selection of individual risk guidelines should be based on sound arguments and reflect the consensus of all stakeholders. Ideally, the risk associated with the utilization of hydrogen should not substantially increase the injury or fatality risk of an individual. This concept is not new and in fact has been utilized in several industries. A critical question is what level of risk should be utilized in this concept? Several considerations, discussed below, were utilized by the NFPA 2 TG6 in establishing a risk guideline.

The first consideration is that the risk to individuals from hydrogen accidents should not substantially increase their existing risk from all other unintentional injuries over which they have no control. This approach has been adopted by the Nuclear Regulatory Commission (NRC) in their efforts to risk-inform the regulations for nuclear power plants. The NRC risk objective is based on the principle that the risk to an average individual in the vicinity of a nuclear power plant should be a fraction (0.1%) of the sum of the fatality risk resulting from other accidents to which members of the public are generally exposed in every day life (e.g., fatal automobile accidents). At the time the NRC established this policy in 1995, the individual fatality risk in the U.S. from all accidents was approximately 5×10^{-4}/yr.

In addition, several groups have adopted this approach for hydrogen safety applications. This includes the EIGA [15] and the European Integrated Hydrogen Project (EIHP) [19]. The fraction of the fatality rate used by these two groups to establish a risk criterion ranges from 1% (EIHP) to 17.5% (EIGA). Recent data [20] suggest that the individual fatality risk from unintentional injuries in the United States is on the order of 3.8×10^{-4}/yr (the cited rate in other countries is approximately 2×10^{-4}/yr [15]). Thus, the fatality risk criterion proposed by EIHP and EIGA are 2×10^{-6}/yr and 3.5×10^{-5}/yr, respectively. The EIHP has also established an individual fatality risk value of 1×10^{-4}/yr for refueling station workers. Finally, Spain has adopted a risk guideline of 5% of the fatality risk for children (2×10^{-4}/yr) or 1×10^{-5}/yr.

A second consideration was the concept that the risk associated with hydrogen refueling stations be equal to or less than the risk associated with gasoline or CNG stations. Unfortunately, no published risk assessments for either gasoline or CNG refueling stations that could provide those risk estimates were identified. However, there is some limited data on the frequency of fires in public gasoline stations [21] for the five-year period of 1994-1998 (no published data for CNG stations was identified) that could be

used to establish such a comparative criteria. This data indicates that the average frequency of a fire at a gasoline station is approximately 7.4 x 10^{-2}/yr. A majority of the reported fires were initiated by vehicle fires and only a small fraction (~4%) was related to spills of gasoline leading to fires or explosions. When vehicle fires are eliminated, the fire frequency is approximately 2.8 x 10^{-2}/yr and when only spills are considered, the average fire frequency is approximately 3 x 10^{-3}/yr. The reported fires resulted in, on average, 2 deaths/yr and 70 injuries/yr. Since there were approximately 100,000 public service stations in operation during this period, the average frequencies of a fatality or an injury associated with the operation of a single gasoline station are approximately 2 x 10^{-5}/yr and 7 x 10^{-5}/yr, respectively. If vehicle fires are eliminated, the average fatality and injury frequencies associated with operation of an individual gasoline station are approximately 1 x 10^{-5}/yr and 3.3 x 10^{-4}/yr, respectively. The corresponding fatality and injury frequencies attributable to gasoline spills are approximately 5 x 10^{-6}/yr and 9 x 10^{-5}/yr.

A third consideration in establishing risk guidelines was to survey countries that utilize a risk criterion in their regulations for facilities employing hazardous gases. Risk acceptance criteria for both individual and societal risk, though de facto exist everywhere, are not always obvious. In some world jurisdictions, like in most Western European countries and Australia, they are incorporated into law. In the U.S. and Canada, to the contrary, as in many other jurisdictions around the world, they are not defined in any way and are, thus, subject to interpretation. Table 5-1 presents the results of a limited survey. As indicated almost all of the countries listed utilize an upper risk criterion of 1 x 10^{-5} fatalities/yr.

Further insights are provided by examining just the individual fatality and injury risk associated with only fires. Considering that these are the major concerns associated with hydrogen facility operation, it may be better to consider available fire statistics instead of fatality statistics from all causes. The individual fatality risk due to fires in the United States is 1.2 x 10^{-5}/yr [20]. Further examination of this data indicates that the individual fatality risk from fires involving highly flammable materials such as hydrogen is approximately 2.0 x 10^{-7}/yr, the risk from structure fires is 9.5 x 10^{-6}/yr, the risk from fires outside of structures is 8 x 10^{-8}/yr, and the risk from unspecified fire sources is 1.1 x 10^{-6}/yr. Data on fire-related injuries have not been identified, but the individual injury risk from fires is expected to be approximately two orders of magnitude greater than the values cited above based on the trend exhibited in the data for other types of accidents.

Based on the review of the information provided above, a fatality risk guideline of 2 x 10^{-5}/yr for members of the public was selected for use by NFPA 2 TG6. This value is consistent with the risk at existing gasoline stations, is in general agreement with criteria being utilized in several countries, and is approximately twice the value recommended by EIGA for hydrogen facilities. Furthermore, it represents a low fraction (5%) of the risk currently experienced by the public to all causes and is roughly equal to the risk imposed by other fires. The 2 x 10^{-5}/yr value was used as a guideline rather than a hard criterion due to the uncertainty in the risk evaluations. State-of- knowledge, or epistemic,

uncertainties in modeling hydrogen accidents in a QRA preclude a definitive decision based solely on the numerical results of a QRA. Thus, in the context of risk-informed decision making, the guideline should not be interpreted as being overly prescriptive. It is intended to provide an indication, in numerical terms, of what is considered acceptable.

Table 5-1. Survey of risk criteria used in other countries.

Individual Risk Criteria	United Kingdom	The Netherlands	Hungary	Czech Republic	Australia
10^{-4}	Intolerable limit for members of the public				
10^{-5}	Risk has to be lowered to as low as reasonably possible (ALARP)	Limit for existing installations, ALARP principal applies	Upper limit	Limit for existing installations, risk reduction applied.	Limit for new installations
10^{-6}	Broadly acceptable risk level	Limit for new installations and general limit after 2010, ALARP principal applies	Lower limit	Limit for new installations	
10^{-7}	Negligible level of risk				Negligible level of risk
10^{-8}		Negligible level of risk			

5.2 Harm Criteria

The use of a risk-informed approach requires a QRA that considers all credible hazards resulting from hydrogen-related accidents. The principle hazard associated with hydrogen facilities is uncontrolled combustion of accidentally released hydrogen gas or liquid. Possible modes of gaseous hydrogen combustion include jet fires, flash fires, deflagrations (unconfined vapor cloud explosions), and detonations. For facilities with large volumes of liquid hydrogen, additional combustion concerns include the potential for pool fires and boiling liquid expanding vapor explosions (BLEVE). Other hydrogen-related hazards such as asphyxiation and cryogenic burns are also possible but are generally of secondary importance compared to hydrogen combustion. Table 5-2 summarizes the thermal characteristics of different types of hydrogen-related accidents. Since the scope of the NFPA separation distance effort currently only addresses gaseous storage facilities, the primary concerns are jet or flash fires.

The primary consequences from fire hazards are that people will be exposed to flames or high heat from jet fires, or be engulfed in a flash fire boundary (defined by the 4%

hydrogen boundary) resulting in death. Jet fires will result from immediate ignition of a hydrogen jet. Flash fires will result from delayed ignition of hydrogen.

Table 5-2. Characteristics of hydrogen accidents.*

Fire Type	Duration	Size	Intensity	Effects on People
Fireball	Very Short	Large	Very High	Radiation, little opportunity for escape
Flash Fire	Very Short	Large	Medium	Engulfment - fatalities usually within fire boundary only (4% H2), no opportunity for escape
Pool Fire (Liquid H2)	Short	Medium	Low/Medium	Radiation, engulfment, little opportunity for escape
Jet Fire	Medium/Long	Medium	High	Radiation, direct flame contact, good possibility of escape

*Adapted from HSE 129/1997[22].

Direct flame contact as a result of a jet fire is generally assumed to result in third degree burns sufficient to result in death. Although in reality, not all people will die from third degree burns, a sufficiently large fraction will die. For this assessment, a 100% probability of fatality was assumed for people engulfed in a hydrogen jet flame. Direct flame contact as a result of a flash fire will also occur if a person is within the 4% hydrogen envelope when hydrogen ignition occurs. For accidents involving delayed hydrogen ignition, a person located within the 4% envelope was assumed to be a fatality.

For people not in the flame, there is still a potential for exposure to high radiation heat fluxes for a sufficient time to result in third degree burns and death. A variety of radiant heat flux levels and associated injury or damage levels are quoted in the literature. In addition, harm from radiation heat fluxes is also expressed in terms of a thermal dose. The thermal dose is evaluated by the following equation:

$$\text{Thermal Dose} = I^{4/3}t \qquad (5.1)$$

where I is the radiation heat flux in kW/m^2 and t is the exposure time in seconds

Table 5-3 presents a range of thermal doses presented in the literature that can result in first, second, or third degree burns. As indicated in the table, the thermal dose levels are

a function of whether the radiation spectrum is in the ultraviolet or infrared range. The radiation heat flux in the infrared spectrum is of most concern for generating burns. Thermal dose levels have also been used to define "Dangerous Dose" levels, which are usually defined as dose resulting in death to 1% of the exposed population. In addition, "LD50" values have also been specified. An LD50 is the lethal dose (LD) where 50% of exposed population would die. Table 5-4 presents "Dangerous Dose" and LD50 values cited in the literature for infrared radiation. Either parameter could be used as a harm criterion. The Health and Safety Executive (HSE) of Great Britain has proposed the use of an LD50 of 2000 $(kW/m^2)^{4/3}s$ for offshore oil and gas facilities [22].

Table 5-3. Radiation burn data.

Burn Severity	**Threshold Dose $(kW/m^2)^{4/3}s$***	
	Ultraviolet	**Infrared (mean)**
First Degree	260-440	80-130 (105)
Second Degree	670-1100	240-730 (290)
Third Degree	1220-3100	870-2640 (1000)

*From HSE CRR 129/1997 [22] - Many factors account for range of values including the type of heat source and type of animal skin used in experiments (some values are based on nuclear blast data).

Table 5-4. Dangerous dose and LD50 thermal dose levels.

Source	**Thermal Dose $(kW/m^2)^{4/3}s$ for infrared radiation**	
	Dangerous Dose	**LD50**
Eisenberg	960	2380
Tsao & Perry	420	1050
TNO	520	3600[1]
Lees	1655	3600[2]
HSE	1000	2000

[1] Maximum probability of fatality =14%, but ignition of clothing at 3600 $(kW/m^2)^{4/3}s$ gives 50-100% fatality
[2] Based on ignition of clothing at 3600 $(kW/m^2)^{4/3}s$

Another method to express the consequences from a thermal dose is to use a probit function which translates the dose level to a probability of a fatality. Several probit functions are available to evaluate probability of fatality or injury as a function of thermal dose. Additional probit functions are available for first and second degree burns. Table 5-5 lists four available probit functions that can be used to determine the probability of a fatality from a radiation heat flux. Figure 5-1 shows a comparison of the four probit functions. The HSE recommended values for "Dangerous Dose" and LD50 are also shown on the figure for comparison.

Table 5-5. Thermal dose probit functions.

Probit	Probit Equation	Comment
Eisenberg [23]	$Y = -14.9 + 2.56 \ln V$[1]	Based on nuclear data from Hiroshima and Nagasaki (ultraviolet)
Tsao &Perry [24]	$Y = -12.8 + 2.56 \ln V$	Eisenberg model modified to account for infrared (2.23 factor)
Opschoor, van Loo, and Pasman [25]	$Y= -13.65 + 2.56 \ln V$	No information available
Lees [26]	$Y = -10.7 + 1.99 \ln V'$[2]	Accounts for clothing, based on porcine skin experiments using ultraviolet source

[1] $V = I^{4/3}t$ = thermal dose in $(kW/m^2)^{4/3}s$ or
[2] $V' = F*I^{4/3}t$ = thermal dose in $(kW/m^2)^{4/3}s$ where F=0.5 for normally clothed population and 1.0 when clothing ignition occurs

The probability of a fatality is evaluated using the following equation:

$$P(\text{fatality}) = 50*(1+(Y-5)/ABS(Y-5)+ERF(ABS(Y-5)/SQRT(2))) \quad (5.2)$$

where Y= probit function from Table 5-5.

It is important to consider the following points in selecting the most appropriate probit function:

1. The probit functions shown in Figure 5-1 provide the probability of fatality given a thermal dose. The Tsao and Perry probit include the infrared spectrum where the Eisenberg and Lee probits only include ultraviolet (the spectrum covered by the Opschoor probit is unknown). The major contributor to radiation heat flux is from the infrared spectrum. This is true whether the source is hydrocarbon fires or hydrogen fires. Thus, a probit that does not include the infrared spectrum would considerably under

predict the consequences from any fire. Thus, the Lee probit is likely the least appropriate for hydrogen fires.

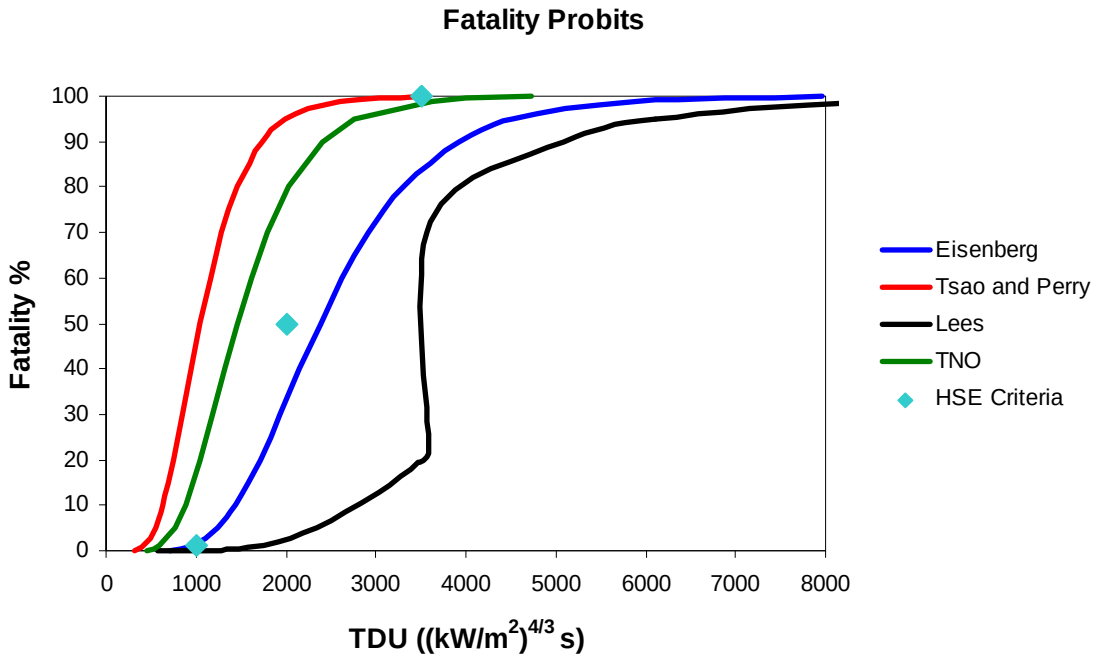

Figure 5-1. Comparison of thermal radiation probit functions.

2. The Eisenberg and Tsao and Perry probits are both highly uncertain. The Eisenberg probit was developed from analyzing data from Hiroshima (nuclear radiation is in the ultraviolet spectrum). The uncertainty associated with back-calculating the probability of fatality based on peoples location versus the blast is unknown. The Tsao and Perry probit is a modified version of the Eisenberg probit that accounts for the infrared spectrum by increasing the thermal dose by a factor of 2.27, which was determined based on measurements of both ultraviolet and infrared heat fluxes from hydrocarbon fires. Its validity is thus even more questionable than the Eisenberg probit.

3. Hydrogen fires emit less intensive infrared radiation than hydrocarbon fires (especially hydrocarbon fires with a lot of soot). That is why you can get closer to a hydrogen fire. It should be noted that the combustion products from hydrocarbon fires (water and carbon dioxide) emit in the infrared range where as hydrogen combustion only results in water. As indicated in Figure 5-2, the radiant fraction from hydrogen fires is roughly a factor of two less than non-sooting hydrocarbon fires (methane). Thus, the Tsao and Perry probit is probably conservative for hydrogen fires by perhaps a factor of two.

4. If you look at all of the suggested heat flux levels and durations that are quoted in the literature as resulting in a fatality (both experimental and suggested values) and map them on the same curve as the two probit functions you can get an indication which

probit is more in line with those estimates. HSE has done that to a limited extent and selected values for 1% and 50% fatalities which lies between the two probits (see Figure 5-1) but are closer to the values predicted by the Eisenberg probit function.

5. Neither the Eisenberg nor Tsao and Perry probits account for the affects of clothing. With clothing, the thermal doses required for a fatality would be expected to be greater than predicted by the probits for small thermal doses that are not sufficient to ignite clothing.

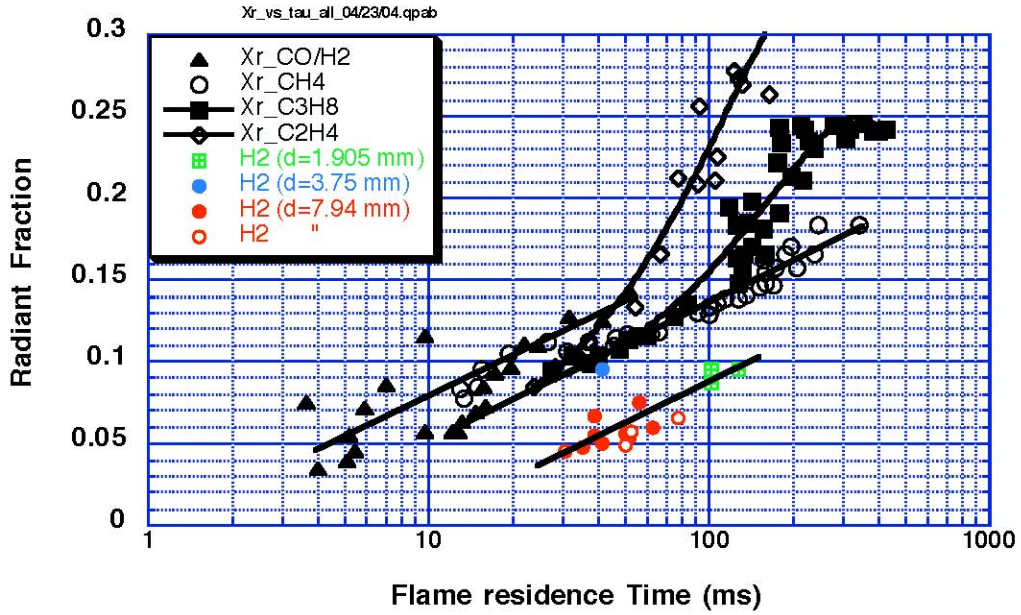

Figure 5-2. Radiant fraction as a function of flame residence time from hydrocarbons and hydrogen flames [7].

Based on the above points, it appears that the use of the Tsao and Perry probit would result in conservative results for exposure to hydrogen fires. Because the Eisenberg probit does not include the infrared spectrum, it should provide lower estimates of fatalities. However, it may provide better estimates of the probability of a fatality for exposure to hydrogen flames than the Tsao and Perry probit. This is due to the radiant fraction in the infrared spectrum from hydrogen flames being significantly less than for hydrocarbon fires. Although the Tsao & Perry probit appears to be applicable for hydrocarbon fuels, the reality is that the Eisenberg function is being applied to hydrocarbon fires. It is believed the true results may lie somewhere between the two probit predictions, perhaps close to the prediction by the Opschoor probit. Thus, rather than selecting one as the preferred probit, it is desirable to use both to bound the results.

5.3 Risk Analysis Model and Data

The evaluation of risk for the example gas storage facilities presented in Appendix B requires generation of models that delineate the potential accident sequences for

hydrogen leakage events, the component leakage frequencies, additional data for phenomenological events such as hydrogen ignition, and an assessment of the consequences of the different accident sequences. The model is determined by the scope of the analysis, which was established by the NFPA 2 TG6. Only random component failures leading to hydrogen leakage were included in the current QRA scope. Leakages initiated by human errors, or natural events, or by other mechanisms such as automobile accidents were not included. However, leakage contributions from valves, piping, gas cylinders, connections, and instrument lines were included in the analysis. Only accidents leading to exposure to ignited and un-ignited hydrogen jets were included. Overpressure events were excluded since the facilities were stipulated to be located outdoors.

Figure 5-3 illustrates the accident event tree that was used for evaluating the hydrogen release scenarios from the example gas storage facilities. The accident sequence modeling is relatively simple since the modeled facilities do not include the capability to automatically isolate leaks. Manual isolation of leaks was also not credited due to the uncertainty in leak detection. The accident event tree includes several phenomenological events that influence the accident sequence and resulting consequences. Included in these phenomenological events is the size of the leak, the potential for immediate ignition, and delayed ignition. The event tree illustrates the resulting consequences for each sequence which includes jet fires, flash fires following delayed ignition of hydrogen and un-ignited gas releases.

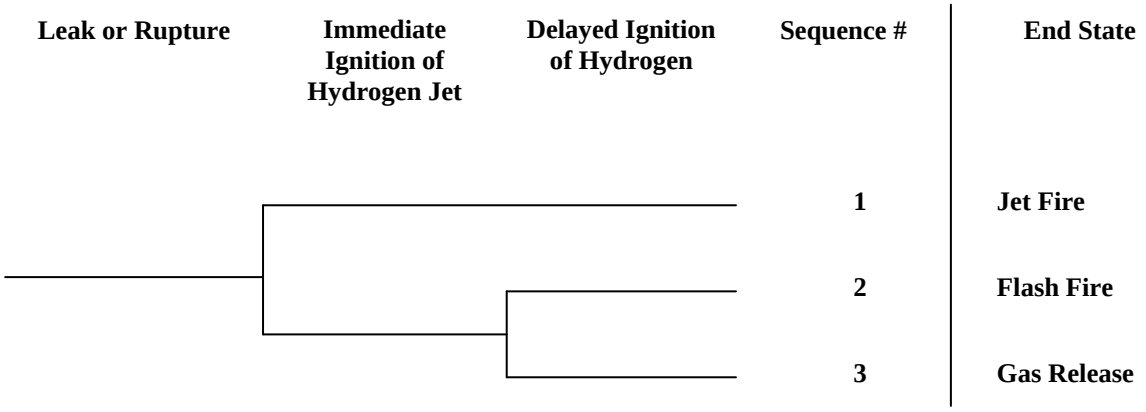

Figure 5-3. Hydrogen gas storage leakage/rupture event tree.

Supporting analyses and data are required to quantify the event tree shown in Figure 5-3. Specifically, failure data is required to quantify the accident scenarios. The data required includes component leakage frequencies and hydrogen ignition probabilities. The hydrogen-specific component leakage data generated using Bayesian analysis was used to quantify the model. The leakage rates are presented in Table 4-2.

A review of hydrogen ignition probabilities was performed to help select appropriate values. A summary of existing ignition models used in hydrogen risk assessments was generated for the HYSAFE program [27]. Values are presented for both immediate and

delayed ignition and are in some cases expressed as a function of the hydrogen release rate. Immediate ignition probabilities range from 0.0001 to 0.9. Delayed ignition probabilities range from 0.004 to 0.5. Hydrogen-specific ignition probabilities suggested by two sources are shown in Table 5-6. As indicated, the ignition probabilities are a function of the hydrogen release rate. The Tchouvelev values [28] were adapted for hydrogen from values suggested in Cox, Lee, & Ang [18]. The HYSAFE probabilities are for self-ignition only and thus are not totally appropriate for use in this study. The results of this survey were presented to NGPA TG6, which subsequently decided that the Tchouvelev value were reasonable and should be used in the bas- line risk analysis. However, a sensitivity analysis was performed to determine the impact of this parameter.

Table 5-6. Hydrogen ignition probabilities.

Tchouvelev			**HYSAFE**	
Hydrogen Release Rate (kg/s)	Immediate Ignition Probability	Delayed Ignition Probability	Hydrogen Release Rate (kg/s)	Immediate Ignition Probability
<0.125	0.008	0.004	0.01- 0.1	0.001
0.125 – 6.25	0.053	0.027	0.01-1	0.001 + 0,001 when P>100 bar
>6.25	0.23	0.12	1-10	0.01 + 0.01 when P>100 bar
			>10	0.1 + 0.01 or 0.02

The QRA analysis also required the evaluation of the consequences for each hydrogen release scenario. As indicated previously, the consequences considered in the QRA were limited to exposure to radiant heat fluxes and flash fires. The Houf and Schefer model [7] was used to determine the resulting consequences for the hydrogen leakage events. The leak orientation was assumed to be directly at the target which results in the largest required separation distances.

5.4 Risk Analysis Results

The risk evaluation was performed for the four gaseous storage facilities presented in Appendix B. Because different modules or portions of these systems have different diameter components and operating pressures which impact the consequences from leaks, it was necessary to evaluate the risk for each module and to aggregate the results to get the complete facility risk. The risk analysis was also performed for different size leaks in order to help select a leak size for determining separation distances.

The framework for calculating and presenting the risk results is illustrated in Figure 2-7. This framework requires evaluation of the cumulative frequencies of different leak diameters resulting in a specified consequence and plotting the frequencies against the separation distances required to protect people from a specified level of harm. The use of cumulative probabilities is critical in this method as it allows identification of the risk associated with leaks greater than a specified size. The results for the 20.7 MPa and 103.4 MPA systems are presented below. The results for the 1.7 MPa and 50.7 MPa systems are similar and are not presented in this report.

5.4.1 Risk Results for 20.7 MPa System

The risk results are presented by accident type (jet fire or flash fire) and module. The 20.7 MPa system was separated into four modules: tube trailer, stanchion (product transfer module), pressure control module, and instrument module. The instrument module is actually part of the pressure control module, but was modeled separately because the tubing diameter is different than the pressure control piping. The jet fire scenarios involve immediate ignition of a hydrogen jet and uses the hydrogen flame length to determine the harm distance for the scenarios. The flash fire scenarios involve delayed ignition of a hydrogen jet. The harm distance associated with these scenarios was determined by the extent of the 4% hydrogen envelope. For both scenarios, direct contact with the flame was assumed to result in a 100% probability of a fatality. Thus, the frequency of each type of scenario was equated to the frequency of a fatality (i.e., the associated risk).

Figure 5-4 provides the results for the jet fire scenarios. The results for the flash fire sequences are provided in Figure 5-5. The results for 0.1%, 1%, 10%, and 100% leak areas are shown as points on the figure (0.1% on the far left and 100% on the far right). For both scenarios, the dominant contributor involves leaks from the tube trailer module. The risk from the other modules combined is approximately a factor of 3 less than the risk from the tube trailer. The risk contribution from each component in the modules is presented in Appendix D. A review of that information reveals that the majority of the leakage frequency for the tube trailer comes from leakage of the tube trailer isolation valves and the flexible hose connections (pigtails). The valves in the other modules are also important contributors. Leakage from joints, pipes, and cylinders were not major contributors because of the low leakage rates provided by the Bayesian analysis.

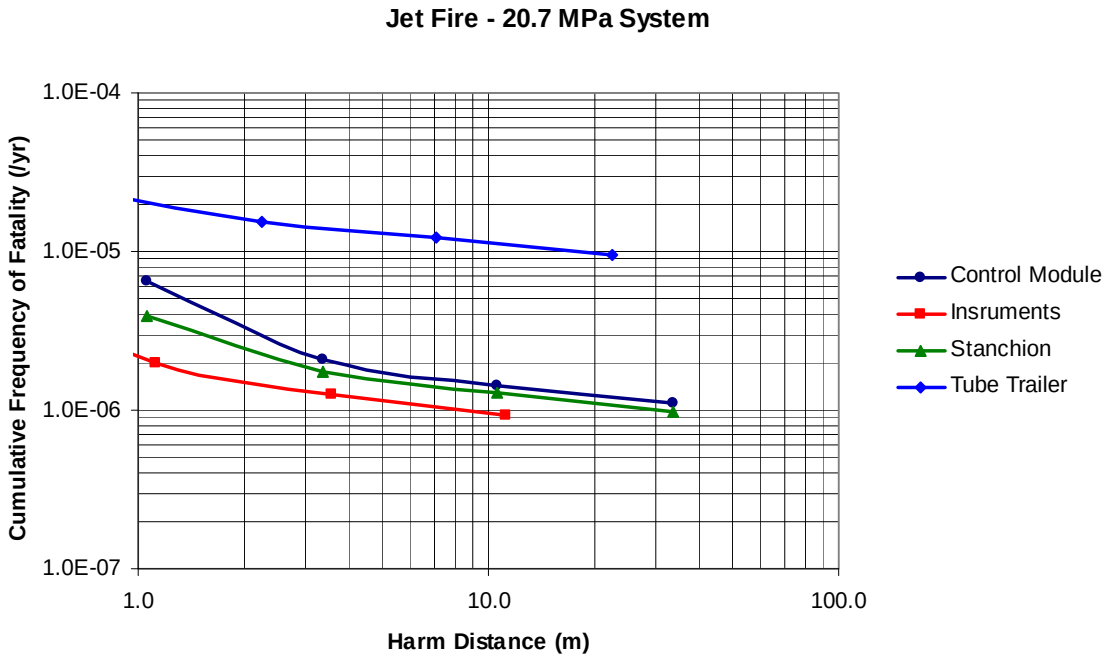

Figure 5-4. Risk results for jet fire scenarios for the example 20.7 MPa system.

The total risk for the 20.7 MPa system is shown in Figure 5-6. The figure shows the total risk to an individual standing at different distances from the storage facility (variation in the module locations are conservatively ignored). As indicated in the figure, the cumulative risk to an individual decreases as the distance of the person increases and becomes nearly constant at distances greater than 10 m. The total risk is close to the $2x10^{-5}$/yr risk guideline at these distances. The risk to a person at these harm distances is primarily due to leaks greater than 1% of the component flow area. Little risk is presented from smaller, more frequent leaks since the hydrogen flames from these leaks would not reach the person (there is some risk from the radiation heat flux). The risk to a person located at less than 5 m from the system increases dramatically since the person would be engulfed in flames from both small and large leaks. As indicated in Figure 4-9, the system leakage frequency increases dramatically for leaks less than 1%.

Superimposed on Figure 5-6 are the harm distances based on a 4% hydrogen envelope for leaks equal to 0.1%, 1%, and 10% of the component flow area. As indicated on the figure, the use of 0.1% of the component flow area as the basis for determining separation distances results in risk estimates that significantly exceed the 2×10^{-5} /yr risk guideline selected by the NFPA separation distance working group. On the other hand, use of a leak size equal to between 1% and 10% of the component flow area results in risk estimates that are reasonably close to the risk guideline.

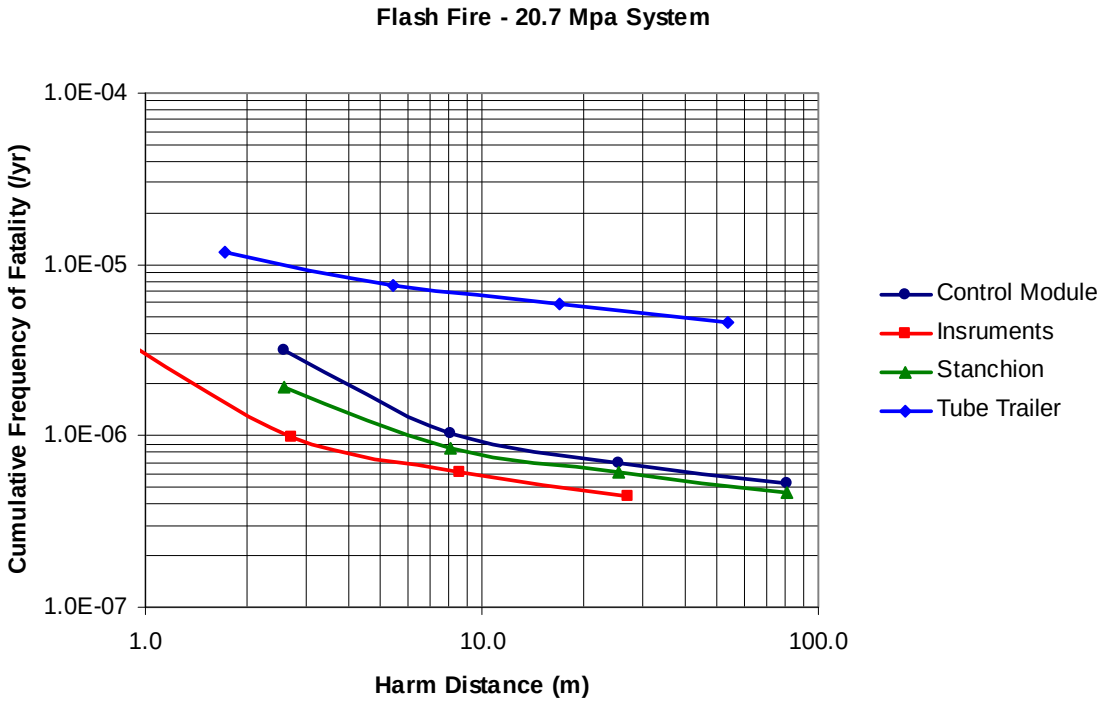

Figure 5-5. Risk results for flash fire scenarios for the example 20.7 MPa system.

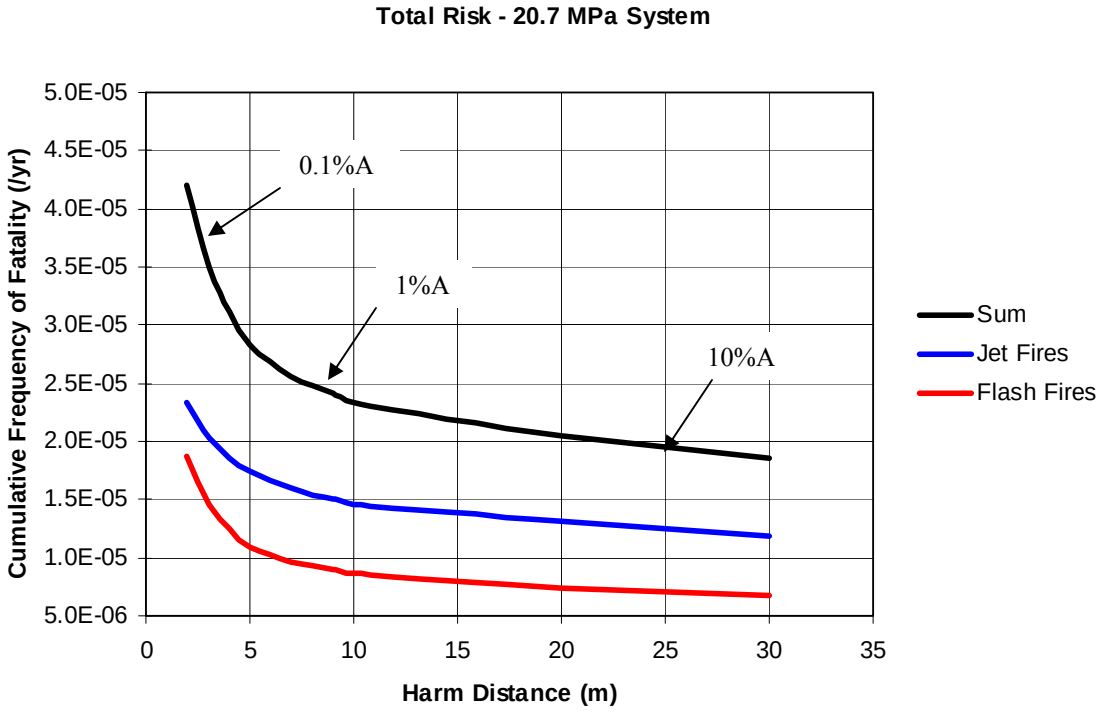

Figure 5-6. Total risk for the example 20.7 MPa system.

5.4.2 Risk Results for 103.4 MPa System

The 103.4 MPa system was separated into four modules: tube trailer, stanchion (product transfer module), pressure control module, and a high-pressure storage module that includes the compressor. Figure 5-7 provides the results for the jet fire scenarios for the 103.4 MPa system.. The results for the flash fire sequences are provided in Figure 5-8. The results for 0.1%, 1%, 10%, and 100% leak areas are shown as points on the figure (0.1% on the far left and 100% on the far right). For both scenarios, the dominant contributor involves leaks from the tube trailer and high-pressure storage modules. The risk from the other two modules combined is approximately a factor of 10 less than the combined risk from the tube trailer and storage modules. The storage module is the dominant contributor for small leak sizes. This is because hydrogen-specific data for compressors indicated a significant number of small leaks but not many large leaks. When this data was inserted into the Bayesian model, a high leakage frequency estimate for small leaks and a low frequency estimate for large leaks were obtained (see Figure 4-5).

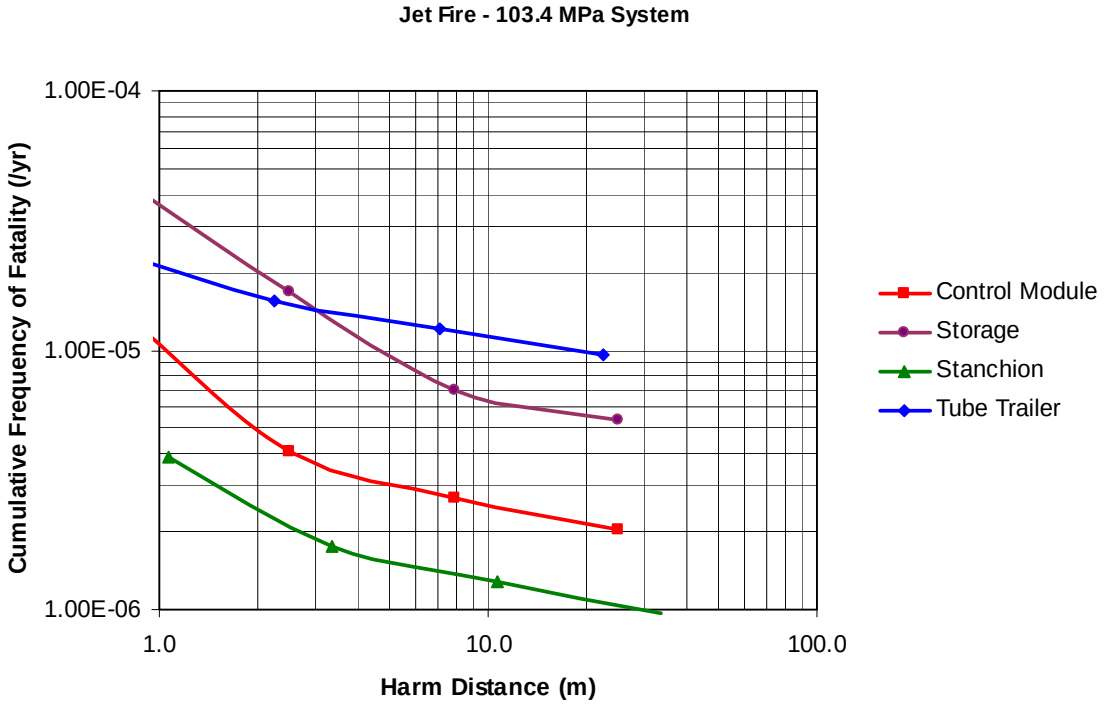

Figure 5-7. Risk results for jet fire scenarios for the example 103.4 MPa system.

The risk contribution from each component in the modules is presented in Appendix D. A review of that information reveals that the majority of the leakage frequency for the tube trailer comes from leakage of the tube trailer isolation valves and the flexible hose connections (pigtails). The contribution from the high-pressure storage module is dominated by the compressor. The valves in the other modules are also important contributors.

Figure 5-8. Risk results for flash fire scenarios for the example 103.4 MPa system.

The total risk for the 103.4 MPa system is shown in Figure 5-9. The figure shows the total risk to an individual standing at different distances from the storage facility (variation in the module locations are conservatively ignored). The total risk results follow the same trend as for the 20.7 MPa system with the exception that the increase in risk for small distances is much greater due to the contribution of small leaks from the compressor (see Figure 5-10 for a comparison). Thus, as with 20.7 MPa system, the use of 0.1% of the component flow area as the basis for determining separation distances results in risk estimates that significantly exceed the 2×10^{-5} /yr risk guideline selected by the NFPA separation distance working group. On the other hand, use of a leak size equal to between 1% and 10% of the component flow area results in risk estimates that are reasonably close to the risk guideline.

5.5 Separation Distance Uncertainty Analysis

The use of a risk-informed process should include an assessment of the uncertainties and assumptions used in the analysis. In addition, parameter uncertainties should be propagated through the models to determine the distribution of the results. The risk assessment results should be weighed in light of the uncertainties in the QRA models, most of which result in conservative risk estimates. These uncertainties include factors that impact both the frequency and consequences of hydrogen releases. The uncertainties and associated insights and results of sensitivity studies are discussed below.

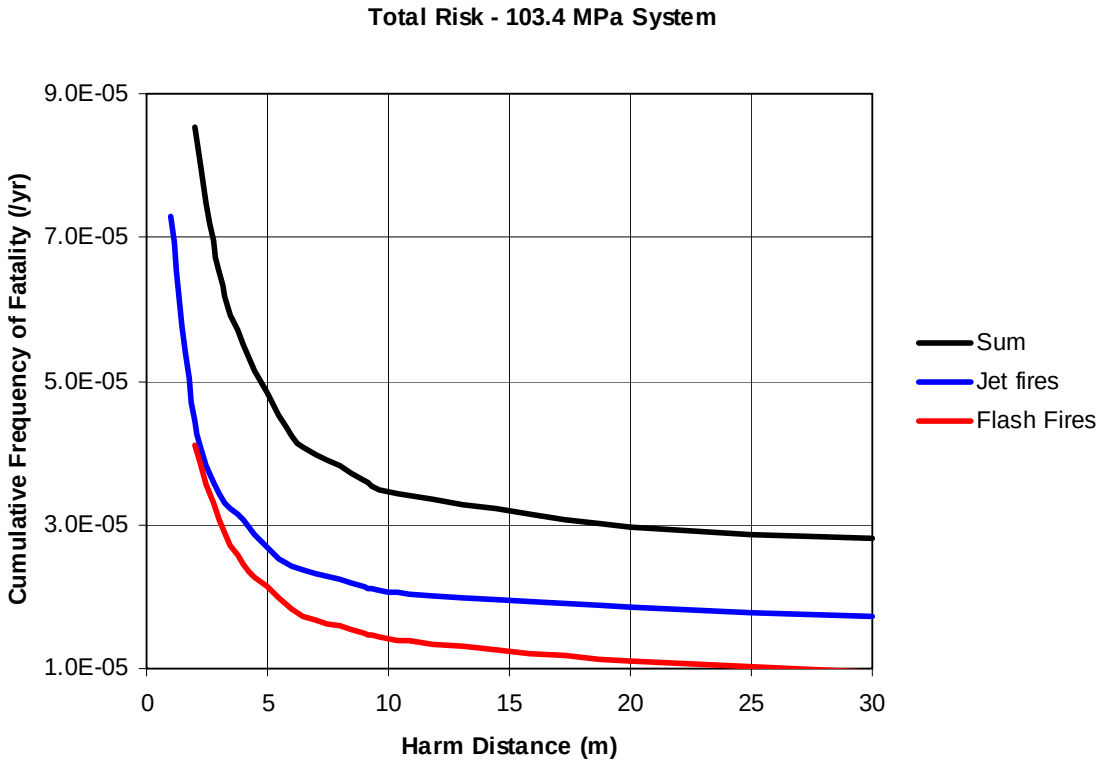

Figure 5-9. Total risk for the example 103.4 MPa system.

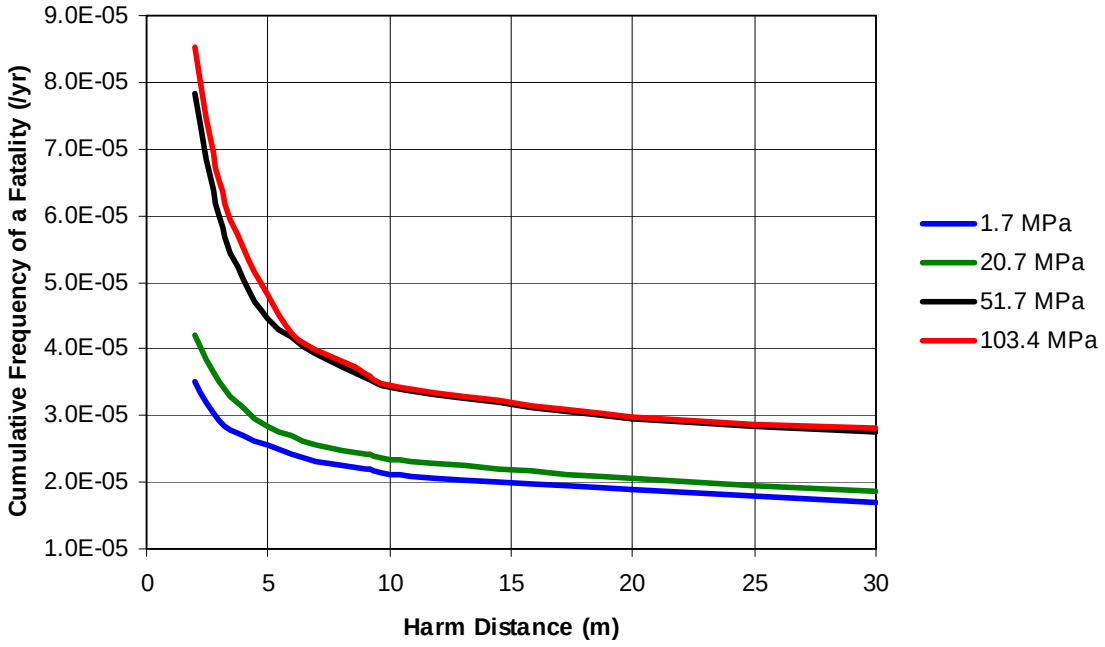

Figure 5-10. Comparison of risk results for 1.7 MPa, 20.7 MPa, 51.7 MPa, and 103.4 MPa facilities.

Ignition probability – The probability of hydrogen ignition listed in the literature varies widely. For some situations, the ignition probabilities vary by three orders of magnitude. For the base case assessment reflected in Figure 5-10, an immediate ignition probability of 0.008 and a delayed ignition probability of 0.004 were used for most leak sizes (higher values were used for large leaks). Increasing these ignition probabilities by one or two orders of magnitude obviously would increase the risk results significantly. These results indicate the need for experimental work to establish ignition probabilities.

Harm criteria – The harm criteria used in the risk evaluation can potentially impact the risk assessment. For example, when one uses the radiation heat flux as a harm criterion, probit functions are used to convert the heat flux level and exposure time to a probability of fatality or injury. There are several probit functions available that could be used which provide substantially different results. However, this issue was avoided by basing the risk estimate for jet fires on direct flame contact (resulting in third degree burns and assumed fatality) – not radiation heat flux. Assuming exposure to a flame for a small period of time results in death may be conservative. However, ignition of clothing by the flame is highly probable and once clothing ignites, data indicates that the probability of fatality ranges from 30% to 70%.

A sensitivity study was performed to evaluate the impact of radiation heat flux on the risk estimate. The risk for a 4.7 kW/m^2 heat flux exposure for 3 minutes (equivalent to a thermal dose of 1400 $(kW/m^2)^{4/3}s$) was evaluated for the 20.7 MPa system using the Tsao and Perry probit function (the most conservative probit described in Section 5.2). The calculated probability of fatality is 0.8. The risk results for this level of heat flux exposure are compared in Figure 5-11 to the risk results for the direct flame contact calculation shown in Figure 5-4. The risk from an exposure to a 4.7 kW/m^2 heat flux for 3 minutes is a factor of two less than the risk from direct flame contact. Use of the Eisenberg probit would reduce the probability of fatality for this thermal dose to 0.1 resulting in a significantly smaller risk (approximately an order of magnitude) than when direct flame contact is used.

Escalation of fire scenarios – The escalation of events is not explicitly included in the risk analysis. However, it is indirectly addressed by establishing separation distances for other combustibles. In the case of other gases or liquids in metal containers, the exposure time for direct flame contact or high radiation heat fluxes is an important factor. Obviously, the exposure times for combustibles such as cellulose and wood are much less. A survey of referenced material suggests that 10 minute exposures to high heat fluxes (20 to 30 kW/m^2) for 10 minutes is required to ignite paper and wood. It is unlikely that these levels of heat flux would be present for that period of time in most leakage scenarios. However, direct flame contact could ignite these materials more quickly.

The additional heat from the additional burning material could increase the risk to people. However, it is likely that the ignition of secondary material would be less of an immediate threat to people than the hydrogen since they will have time to react to the fire. The reaction time would mitigate this additional risk. A risk estimate on the

importance of escalation should be made, but it is not believed to be important due to the factors cited above.

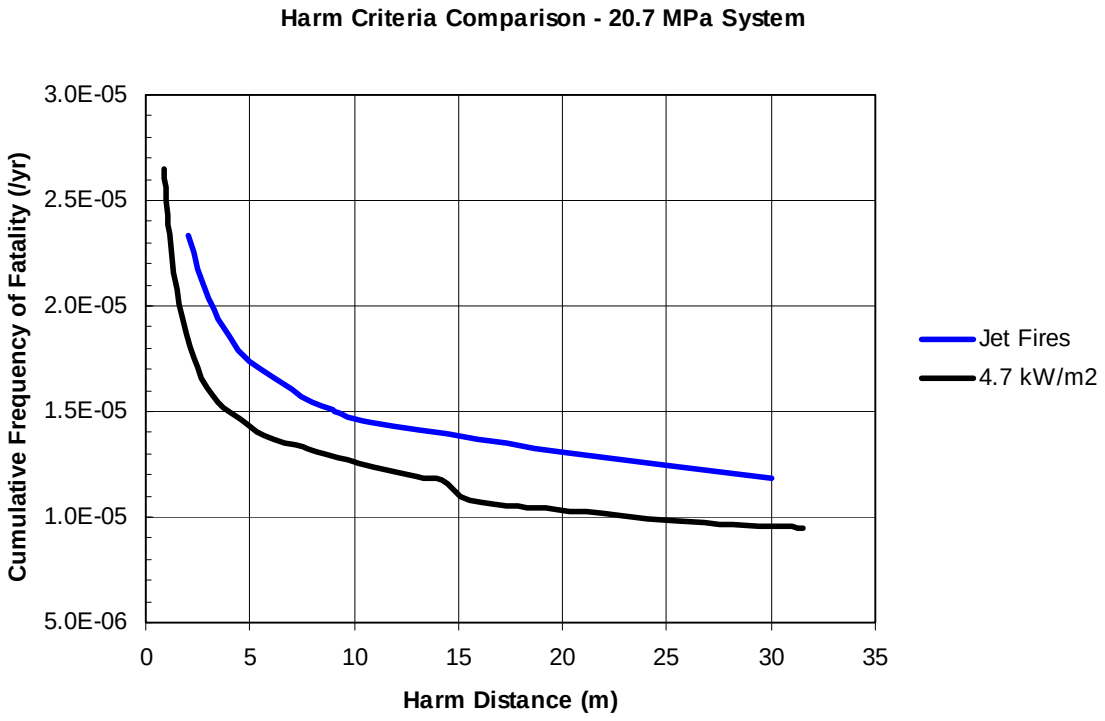

Figure 5-11. Risk from 4.7 kW/m^2 radiation heat flux for the 20.7 MPA system.

Treatment of the leak as a circular orifice – This assumption is used in the evaluation of the consequences from a leak and is believed to result in conservative consequences. Leak geometries are more likely to be slot leaks or consist of more irregular geometries. Unfortunately, there currently is no model for evaluating the consequences from irregular hydrogen leaks.

Pressure drop between the gas storage and leak location – Ignoring the pressure drop is also conservative since it provides consequence estimates based on the gas storage pressure.

Gas storage pressure decrease over time – A decrease in gas storage pressure as the leak depressurizes the system has been ignored in the consequence assessment. A sensitivity study was performed that indicated the thermal dose to a person from a jet fire does not substantially decrease as the hydrogen volume decreases. Most of the thermal dose is obtained early when the pressure is high and thus the risk reduction calculated was only a factor of two. However, because direct flame contact was used as the consequence measure for jet fires in our risk evaluation, the thermal dose reduction was not important. The duration of the flame contact does not have to be long in order to cause third degree burns suggesting that volume impacts for this consequence measure are not significant. The one scenario where it could be important is in a delayed hydrogen ignition that

results in flash fires. Since these scenarios contribute approximately 33% of the risk in our evaluation, volume impacts would be expected to reduce the risk. In summary, accounting for smaller volumes of hydrogen would only serve to reduce that risk estimate.

Surface effects on jet flame lengths – Preliminary experimental work and code analysis by Canadian colleagues[1] suggest that the presence of jet flames relatively close to a surface can increase the length of the jet flames. The impact of this phenomenon on the risk results will need to be determined once the Canadian work is finalized and understood.

Finally, parameter uncertainty was propagated through the risk models to generate estimates of the uncertainty in the risk results. The predicted mean, median, 5%ile and 95%ile risk values for the four example facilities are shown in Table 5-7. The results show that there is approximately an order of magnitude spread between the 5%ile and 95%ile values. Figure 5-12 illustrates the uncertainty in the risk results and associated harm distances for the 20.7 MPa system.

Table 5-7. Results of parameter uncertainty analysis for four example facilities.

Leak Size	Frequency of Fatalities (/yr)			
	Mean	5%ile	Median	95%ile
1.7 MPa System				
Very small leak (0.001A)	7.21E-05	1.97E-05	5.83E-05	1.63E-04
Small leak (0.01A)	4.31E-05	1.21E-05	3.54E-05	1.01E-04
Large leak (0.1A)	3.32E-05	8.03E-06	2.56E-05	8.23E-05
Rupture (A)	2.64E-05	5.16E-06	1.87E-05	7.29E-05
20.7 MPa System				
Very small leak (0.001A)	8.69E-05	2.29E-05	6.96E-05	2.03E-04
Small leak (0.01A)	4.87E-05	1.39E-05	4.03E-05	1.13E-04
Large leak (0.1A)	3.72E-05	9.09E-06	2.91E-05	9.16E-05
Rupture (A)	2.96E-05	5.74E-06	2.10E-05	8.05E-05
50.7 MPa System				
Very small leak (0.001A)	9.14E-05	2.34E-05	7.33E-05	2.19E-04
Small leak (0.01A)	4.94E-05	1.40E-05	4.04E-05	1.11E-04
Large leak (0.1A)	3.86E-05	9.44E-06	3.03E-05	9.42E-05
Rupture (A)	3.04E-05	5.81E-06	2.15E-05	8.34E-05
103.4 MPa System				
Very small leak (0.001A)	9.14E-05	2.34E-05	7.33E-05	2.19E-04
Small leak (0.01A)	4.94E-05	1.40E-05	4.04E-05	1.11E-04
Large leak (0.1A)	3.86E-05	9.44E-06	3.03E-05	9.42E-05
Rupture (A)	3.04E-05	5.81E-06	2.15E-05	8.34E-05

[1] Andrei Tchouvelev, "Surface Jets – Modeling Results," Presentation at International Energy Agency Task 19 Hydrogen Safety meeting in Sacacombie, Quebec, Canada, March 1-5, 2008.

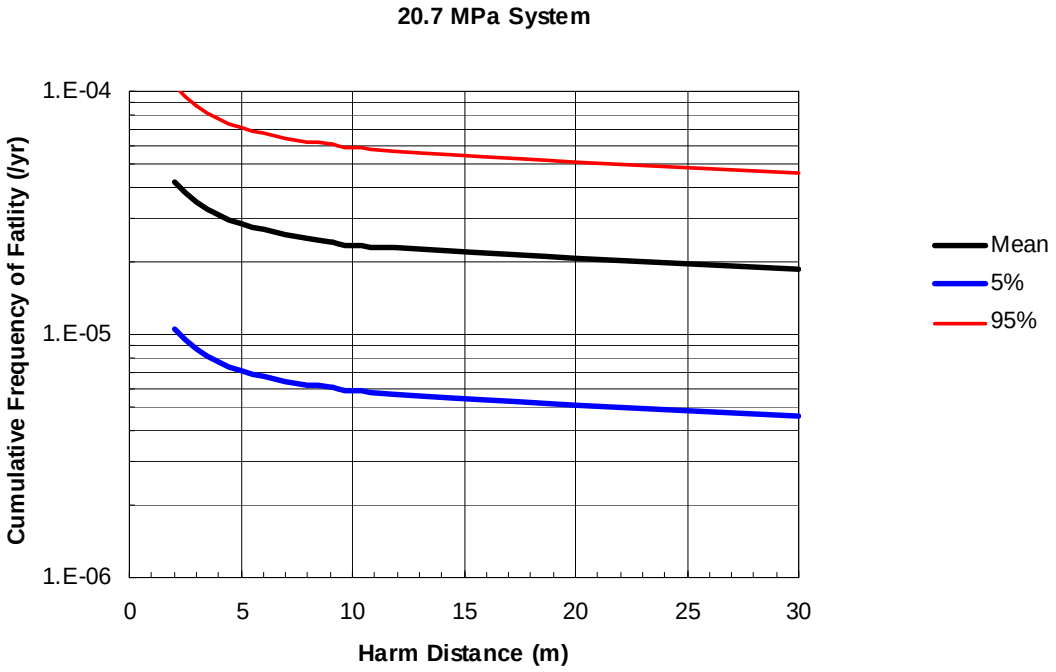

Figure 5-12. Parameter uncertainty impacts on the harm distances for 20.7 MPa system.

6. Summary and Conclusions

A risk-informed approach for selecting the leak diameters was utilized to establish the separation distances in NFPA 2 and NFPA 55. The risk-informed approach included three considerations: the frequency of leakage for typical hydrogen facilities, the cumulative frequency of system leakage, and the risk from leakage events for the example facilities. All three are dependent upon the establishment of example facilities and the generation of hydrogen-specific component leakage frequencies. Facility descriptions were provided by members of NFPA 2 TG6 for four typical facilities operating at different pressures.

Hydrogen-specific component leak frequencies were generated as a function of leak size for several hydrogen components using Bayesian analysis. Hydrogen leakage data was provided by members of NFPA 2 TG6 for use in this analysis. The hydrogen-specific data was utilized to generate system leakage estimates for a 20.7 MPa and 103.4 MPa facility. For a 0.1% leak size, the system leakage frequency is 3×10^{-2}/yr and 6×10^{-2}/yr for the 20.7 MPa and 103.4 MPa systems, respectively. The higher leakage frequency for the 103.4 MPa system is due to the contribution from the additional compressor and high-pressure storage modules. These values are comparative to the fire frequency in gasoline stations (7.4×10^{-2}/yr [21]) and suggest that a 0.1% leak would be expected during the lifetime of these facilities. To reduce the potential for significant consequences to a person at the site boundary due to expected accidents, larger and less frequent leak sizes of at least 1% should be used as the basis for separation distances.

The cumulative probability for different leak sizes was then calculated to determine what range of leaks represents the most likely leak sizes. When evaluated on a cumulative distribution basis, leaks equal or less than 0.1% of the component flow area was estimated to represent 95% of the system leakage frequency. Basing separation distances on this size of leak would ensure that they cover the majority of possible leakage events. However, the use of a larger leak size was recommended to the NFPA 2 TG6 based on consideration of the actual system leakage frequencies discussed above and uncertainty in the component and system leak frequency analysis.

The risk resulting from different size leaks was also evaluated for four standard gas storage configurations. The risk evaluation indicates that the use of 0.1% of the component flow area as the basis for determining separation distances results in risk estimates that significantly exceed the 2×10^{-5} /yr risk guideline selected by the NFPA 2 TG6 for both the 20.7 MPa (3000 psig) and 103.4 MPa (15000 psig) example systems. On the other hand, use of a leak size equal to 1% to 10% of the component flow area results in risk estimates that are slightly above, but reasonably close to the risk guideline.

Based on this input, the NFPA 2 TG6 decided that the separation distances specified in NFPA2 and NGPA 55 would be based on a leak size equal to 3% of the largest flow area downstream of a gaseous storage system greater than 11.3 m^3 (400 scf).

References

1. NFPA 55, "Standard for the Storage, Use, and Handling of Compressed Gases, and Cryogenic Fluids in Portable and Stationary Containers, Cylinders, and Tanks," 2005 Edition, National Fire Protection Association.
2. S.E Rose, S. Flamberg, and F. Leverenz, "Guidance Document for Incorporating Risk Concepts into NFPA Codes and Standards," Fire Protection Research Foundation, March 2007.
3. "2003 International Fire Code," International Code Council, ISBN # 892395-60-6.
4. NFPA 52, "Vehicular Fuel Systems Code", 2006 Edition, National Fire Protections Association. 29 CFR Occupational Safety and Health Administration, ¶1920.103 Hydrogen.
5. 29 CFR Occupational Safety and Health Administration, ¶1920.103 Hydrogen.
6. ISO/TS 20100:2008(E), "Gaseous hydrogen – Fuelling stations," ISO TC 197, International Organization for Standardization, March 14, 2008.
7. W.G. Houf and R.W. Schefer, "Predicting Radiative Heat Fluxes and Flammability Envelopes from Unintended Releases of Hydrogen," *International Journal of Hydrogen Energy*, Vol. 32, pp. 136-151, January 2007.
8. "Determination of Safety Distances," European Industrial Gases Association, IGC Doc 75/07/E, 2007.
9. F.P Lees, "Loss Prevention in the Process Industries," Third Addition, Elsevier Butterworth-Heineman, Burlington, MA, 2005.
10. Thomas F. Barry, "Fire Exposure Profile Modeling: some Threshold Damage (TDL) Data," www.fireriskforum.com.
11. API 521
12. W. S. Winters, "TOPAZ – A Computer Code for Modeling Heat Transfer and Fluid Flow in Arbitrary Networks of Pipes, Flow Branches, and Vessels," SAND83-8253, Sandia National Laboratories, Albuquerque, NM, January 1984.
13. "Risk Management Plan Guidance Document for Bulk Liquid Hydrogen Systems," CGA P28, Compressed Gas Association, Second Edition, 2003.
14. http://www.h2incidents.org/
15. EIGA, "Determination of Safety Distances," IGC Doc 75/01/E/rev, 2001.
16. C.L. Atwood, J.L. LaChance, H.F. Martz, D.J. Anderson, M. Englehardt, D. Whitehead, T. Wheeler, "Handbook of Parameter Estimation for Probabilistic Risk Assessment," NUREG/CR-6823, U.S. Nuclear Regulatory Commission, Washington, D.C. (2003).
17. John Spouge, "New Generic Leak Frequencies for Process Equipment," *Process Safety Progress* (Vol. 24, No. 4), December 2005.
18. A.W. Cox, F.P. Lees, and M.L. Ang, "Classification of Hazardous Locations," Institution of Chemical Engineers, May 2003.
19. "Risk Acceptance Criteria for Hydrogen Refueling Stations," European Integrated Hydrogen Project, February 2003.
20. "Injury Facts," 2007 Edition, National Safety Council
21. "Fires in or at Service Stations and Motor Vehicle Repair and Paint Shops," National Fire Protection Association, April 2002.

22. HSE 129/1997, “LD50 Equivalent for the Effect of Thermal Radiation on Humans”
23. N.A. Eisenberg, et al., “Vulnerability Model. A Simulation System for Assessing Damage Resulting from Marine Spills,” ADA-0150245, U.S. Coast Guard, Report CG-D-137-75.,
24. C.K. Tsao and W.W. Perry, “Modifications to the Vulnerability Model” a Simulation System for Assessing Damage Resulting from Marine Spills,” ADA 075 231, U.S. Coast Guard, Report CG-D-38-79, March 1979.
25. G. Opschoor, R. O. M. van Loo, and H.J. Pasman, “Methods for Calculation of Damage Resulting from Physical Effects of the Accidental Release of Dangerous Materials,” International Conference on Hazard Identification and Risk analysis, Human Factors, and Human Reliability in Process Safety, Orlando, Florida, January 15-17, 1992.
26. F.P. Lees, “The Assessment of Major Hazards: A Model for Fatal Injury from Burns,” Transactions of the Institution of Chemical Engineers, Vol. 72, Part B, pp. 127-134, 1994.
27. L.K. Rodsaetre and K. Ottestad Holmefjord, “An Ignition Probability Model for Hydrogen Risk Analysis,” HYSAFE Deliverable No.71, January 6, 2007.
28. Canadian Hydrogen Safety Program, “Quantitative Risk Comparison of Hydrogen and CNG Refueling Options,” Presentation, IEA Task 19 Meeting, 2006.
29. Canadian Hydrogen Installation Code, Bureau de Normalisation du Quebec, CAN/BNQ 1784-000.
30. http://www.mrc-bsu.cam.ac.uk/bugs/winbugs/contents.shtml

Appendix A
Description of Hazard Models used in the Development of Separation Distance Tables for NFPA 55 and NPFA 2

A.1 Description of Engineering Hazard Models

The development of an infrastructure for hydrogen utilization requires codes and standards that establish guidelines for building the components of this infrastructure. Based on a workshop on unintended hydrogen releases, one release case of interest involves leaks from pressurized hydrogen-handling equipment [1]. These leaks range from small-diameter, slow-release leaks originating from holes in delivery pipes to larger, high-volume releases resulting from accidental breaks in the tubing from high-pressure storage tanks. In all cases, the resulting hydrogen jet represents a potential fire hazard, and the buildup of a combustible cloud poses a hazard if ignited downstream of the leak.

A case in which a high-pressure leak of hydrogen is ignited at the source is best described as a classic turbulent-jet flame, shown schematically in Figure A-1. The distances of importance are the radial distance from the geometrical flame centerline, r, and the distance downstream of the jet exit, x. Other variables of interest are the jet exit diameter, d_j, and the jet exit velocity and density, u_j and ρ_j, respectively. Schefer *et al.* [2, 4] reported experimental measurements of large-scale hydrogen jet flames and verified that measurements of flame length, flame width, radiative heat flux, and radiant fraction are in agreement with non-dimensional flame correlations reported in the literature. This work verifies that such correlations can be used to predict the radiative heat flux from a wide variety of hydrogen flames. The present analysis builds upon this work by incorporating the experimentally verified correlations into an engineering model that predicts flame length, flame width, and the radiative heat flux at an axial position, x, and radial distance, r. The engineering model is then used to predict radiative heat fluxes for hydrogen flames.

For cases where the high-pressure leak of hydrogen is un-ignited, a classic high-momentum turbulent jet is formed that can be described using the same coordinate system shown in Figure A-1. The hydrogen concentration within the jet varies with axial and radial position due to entrainment and turbulent mixing with the ambient air. The concentration contour beyond which the hydrogen-air mixture is no longer ignitable is of importance to hydrogen ignition studies. The present study develops an engineering model for the concentration decay of a high-momentum turbulent jet based on experimentally-measured entrainment rates and similarity scaling laws for turbulent jets. The model is then verified by comparing simulations for high-pressure natural gas leaks with the experimental data of Birch [4] for the concentration decay of high-pressure natural gas jets. The engineering model is then applied to hydrogen and used to predict un-ignited jet mean (time-averaged over turbulent fluctuations) concentration contours for high-pressure hydrogen leaks.

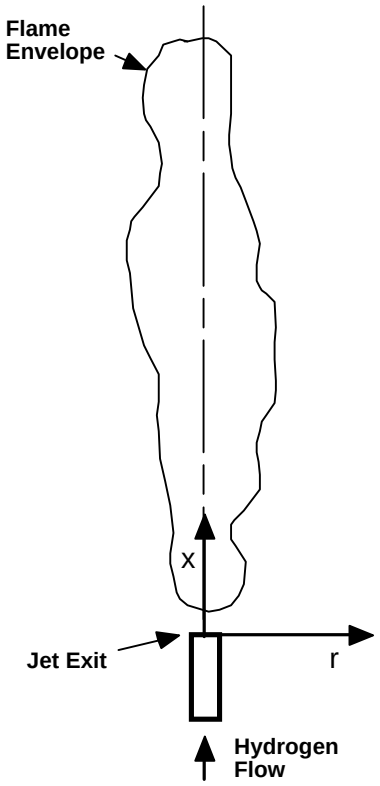

Figure A-1. Coordinate system for turbulent jet flame and un-ignited jet.

A.1.1 Flame Radiation Heat Flux and Flame Length Model

Gaseous flame radiation is the primary heat transfer mechanism from hydrogen flames. The flame radiation heat flux model follows the approach of Sivathanu and Gore [5] where the flame properties of importance are the visible flame length, L_{vis}, total radiative power emitted from the flame, S_{rad}, and total heat released due to chemical reaction, $m_{fuel}\Delta H_c$ where m_{fuel} and ΔH_c are the total fuel mass flow rate and the heat of combustion, respectively. The radiant fraction, X_{rad}, is defined as the fraction of the total chemical heat release that is radiated to the surroundings and is given by an expression of the form

$$X_{rad} = S_{rad} / m_{fuel}\Delta H_c \, . \qquad (A.1)$$

For turbulent-jet flames, the radiative heat flux at an axial position x and radial position r can be expressed in terms of the non-dimensional radiant power, C*, and, S_{rad}, the total emitted radiative power. The radiative heat flux is given by an expression of the form [5]

$$q_{rad}(x, r) = C^*(x/L_{vis}) \, S_{rad} / 4 \, \pi \, r^{\,2} \qquad (A.2)$$

where $q_{rad}(x, r)$ is the radiant heat flux measured at a particular axial location, x, and radial location, r. Experimental data further show that C* may be expressed in non-

dimensionalized form as a function of burner diameter, flow rate and fuel type and, for turbulent-jet flames, is dependent only on the normalized axial distance. Figure A-2 shows typical profiles of C* measured in six different turbulent-jet flames using CH_4, C_2H_2 and C_2H_4 as the fuel [5] as well as the measurements of Schefer *et al.* [2, 3] for large-scale H_2 jet flames.

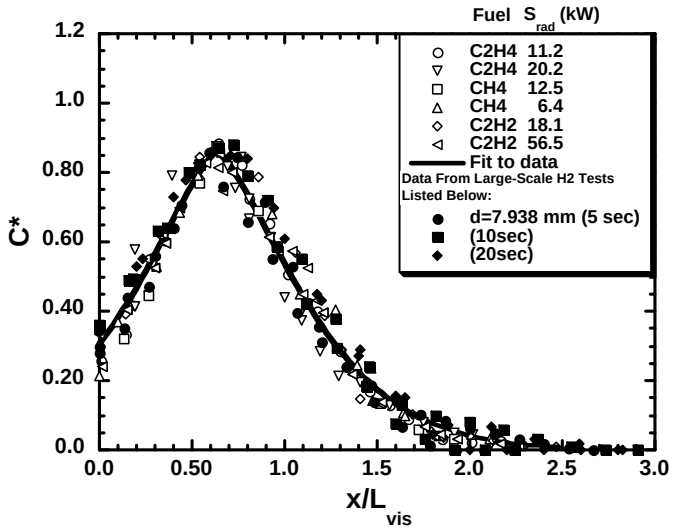

Figure A-2. Axial variation of normalized radiative heat flux.

The use of Eq. (A.2) to calculate flame radiation heat flux levels requires knowledge of the flame radiant fraction. Turns and Myhr [6] measured the radiant fraction from turbulent jet flames using four hydrocarbon fuels with a wide variety of sooting tendencies. These fuels included methane, ethylene, propane, and a 57% CO/43% H_2 mixture. A plot of the radiant fraction data from Turns and Myhr along with the radiant fraction data for large-scale H_2 flames is shown in Figure A-3. The radiant fraction data, X_{rad}, is plotted versus the global flame residence time where the residence time is given by an expression of the form

$$\tau_f = (\rho_f W_f^2 L_{vis} f_s) / (3 \rho_j d_j^2 u_j) \qquad (A.3)$$

where ρ_f, W_f, and L_{vis} are the flame density, width, and length, and f_s is the mass fraction of hydrogen in a stoichiometric mixture of hydrogen and air. For turbulent-jet flames, the flame width, W_f, is approximately equal to 0.17 L_{vis} [2]. This definition of residence time takes into account the actual flame density and models the flame as a cone. The flame density, ρ_f, is calculated from the expression $\rho_f = p_\infty W_{mix}/(R_u T_{ad})$, where p_∞ is the ambient pressure, W_{mix} is the mean molecular weight of the stoichiometric products of hydrogen combustion in air, R_u is the universal gas constant, and T_{ad} is the adiabatic flame temperature for hydrogen. The figure suggests that for flames with a lower sooting tendency, there is a well-defined relationship between radiant fraction and global flame residence time. Both methane and the CO/H_2 mixture show a well-behaved dependence on residence time and nearly collapse onto the same curve over the range of

conditions studied. Values for the large-scale hydrogen jet flames are approximately a factor of two lower than the hydrocarbon flames for the same flame residence time.

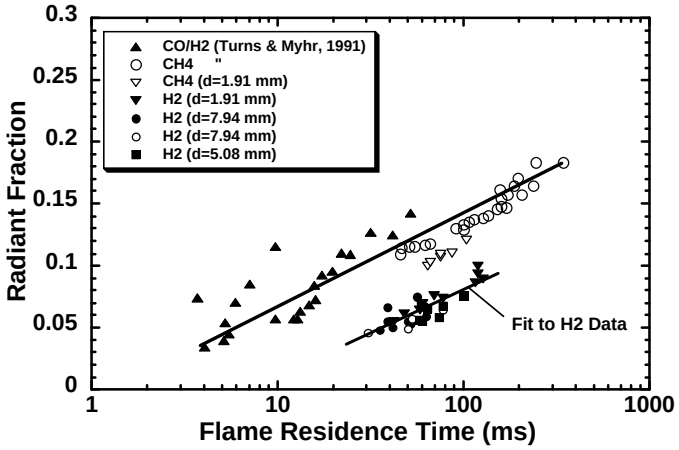

Figure A-3. Radiant fraction as a function of flame residence time (lab H2 flame data for diameters of 1.905 and 3.75 mm, large-scale H2 flame test data at diameter of 7.94 mm).

The visible flame length, L_{vis}, is required for computing the global flame residence time, τ_f, to determine the flame radiant fraction. Based on an analysis of the transition from momentum-controlled to buoyancy-controlled turbulent jet flame dynamics, Delichatsios [7] developed a useful correlation for turbulent flame lengths. The correlation is based on a non-dimensional Froude number that measures the ratio of buoyancy to momentum forces in jet flames. Using the nomenclature of Turns [8] the Froude number is defined as:

$$Fr_f = \frac{u_j f_s^{3/2}}{(\rho_j / \rho_\infty)^{1/4} [\frac{\Delta T_f}{T_\infty} g d_j]^{1/2}} \qquad \text{(A.4)}$$

where u_j is the jet exit velocity, f_s is the mass fraction of fuel at stoichiometric conditions, (ρ_j/ρ_∞) is the ratio of jet gas density to ambient gas density, d_j is the jet exit diameter, and ΔT_f is the peak flame temperature rise due to combustion heat release. Small values of Fr_f correspond to buoyancy-dominated flames while large values of Fr_f correspond to momentum-dominated flames. Note that the parameters known to control turbulent flame length such as jet diameter, flow rate, stoichiometry, and (ρ_j/ρ_∞) are included in Fr_f. Further, a non-dimensional flame length, L*, can be defined as

$$L^* = \frac{L_{vis} f_s}{d_j (\rho_j / \rho_\infty)^{1/2}} = \frac{L_{vis} f_s}{d^*} \qquad \text{(A.5)}$$

where L_{vis} is the visible flame length and d* is the jet momentum diameter. Figure A-4 shows the resulting correlation of flame length data for a range of fuels (H_2, C_3H_8 and CH_4) and inlet flow conditions. In the buoyancy-dominated regime, L* is correlated by the expression

$$L^* = \frac{13.5 Fr_f^{2/5}}{(1 + 0.07 Fr_f^2)^{1/5}} \quad \text{for} \quad Fr_f < 5 \tag{A.6a}$$

and in the momentum-dominated regime by the expression

$$L^* = 23 \quad \text{for} \quad Fr_f > 5 \quad . \tag{A.6b}$$

The flame length data of Schefer *et al*. [2, 3] for large-scale hydrogen flames is shown on the plot and is found to be in good agreement with the L* correlations given by Eqs. (6a) and (6b). For choked flow conditions the concept of a notional expansion and effective source diameter (see next section) was used to reduce the hydrogen flame length measurements for plotting in terms of L* in Figure A-4. The simulation also uses this same effective diameter approach to recover the visible flame length, L_{vis}, from the values of L* computed from Eqs. (6a) and (6b).

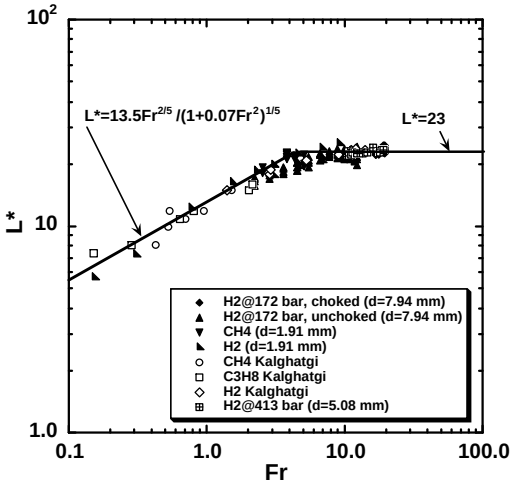

Figure A-4. Variation of dimensionless visible flame length with flame Froude number.

If the jet exit velocity and density of a hydrogen flame are known, then Eq. (A.4) can be used to calculate the flame Froude number and Eqs. (A.5) and (A.6) can then be used to compute the visible length of the flame, L_{vis}. The flame width, W_f, can be computed from the expression $W_f = 0.17 L_{vis}$ and used in Eq. (A.3) to compute the global flame residence time, τ_f. Knowing the flame residence time, a curve-fit to the hydrogen radiant fraction data in Figure A-3 can be used to determine the radiant fraction of the hydrogen flame. Knowing the radiant fraction and using a curve-fit to the C* curve shown in Figure A-2, Eq. (A.2) can be used to compute the radiant heat flux from the hydrogen flame at any axial position, x, and radial position r.

A.1.2 Un-ignited Jet Concentration Decay Model

For cases where the high-pressure leak of hydrogen is un-ignited, a classic high-momentum turbulent jet is formed that can be described using the same coordinate system shown in Figure A-1. The hydrogen concentration within the jet varies with axial position, x, and radial position, r, due to entrainment and turbulent mixing with the ambient air.

The nature of the concentration field of subsonic, momentum-dominated incompressible turbulent free jets is well documented in the literature [9]. The decay of the mean volume fraction, $\overline{\eta}_{cl}$, (or mean mole fraction) along the centerline of the jet is given by an expression of the form

$$\overline{\eta}_{cl}(x) = \frac{K d_j}{x + x_o}\left(\frac{\rho_\infty}{\rho_{gas}}\right)^{1/2} \tag{A.7}$$

where K is the entrainment constant, ρ_∞ is the density of the ambient fluid, ρ_{gas}, is the density of the exiting gas evaluated at ambient temperature and pressure, and x_o is the virtual origin of the jet [9].

For high-pressure leaks of hydrogen, the exit flow chokes at the sonic velocity if the pressure ratio across the leak is greater than the critical pressure ratio (approximately 1.9 for hydrogen). At pressure ratios higher than the critical value, the exit velocity remains locally sonic. For these supercritical releases, the flow leaves the exit to form an under expanded jet that quickly expands to ambient pressure through a complex flow structure involving one or more shocks. As a result, the concentration field behaves as if it were produced by a larger source than the actual exit diameter and the diameter of this effective source is referred to as the effective diameter, d_{eff}. The work of Birch [4, 10] for natural gas jets indicates that the classical laws for concentration decay for turbulent jets in pressure equilibrium (i.e., Eq. (A.7)) can be applied to under expanded jets resulting from supercritical releases provided that the jet exit diameter, d_j, is replaced by the effective diameter d_{eff}. The reports of Britter [11, 12] discuss various approaches for computing effective diameter source models for under expanded jets.

The effective source diameter model used in this work is formulated by considering a notional expansion [10] that conserves both mass and momentum while retaining the assumption that the pressure is reduced to ambient pressure at the end of the expansion. Based on the work of Birch [10], the equation for the effective source diameter is

$$d_{eff} = \left(\frac{\rho_j u_j}{\rho_{gas} u_{eff}}\right)^{1/2} d_j \tag{A.8}$$

where ρ_j is the jet exit density, u_j is the jet exit velocity, ρ_{gas} is the density of the exiting gas evaluated at ambient pressure and temperature, d_j is the jet exit diameter, and

u_{eff} is the velocity at the end of the expansion. The effective velocity at the end of the expansion is given by an expression of the form

$$u_{eff} = u_j + (p_j - p_\infty)/(\rho_j u_j) \tag{A.9}$$

where p_j is the jet exit pressure and p_∞ is the ambient pressure. Equations (8) and (9) can be used to compute the effective source diameter for supercritical releases and are valid for real gas as well as ideal gas models as long as the jet exit conditions are computed properly. For hydrogen at 200 bar and 300K the compressibility factor Z (where $Z = p/(\rho RT)$) is approximately 1.12; at a pressure of 800 bar and the same temperature the compressibility factor is approximately 1.51. For an ideal gas, Z is equal to unity.

For supercritical releases the effective source diameter replaces the jet diameter in Eq. (A.7) and centerline concentration decay equation becomes

$$\overline{\eta}_{cl}(x) = \frac{Kd_{eff}}{x + x_o}\left(\frac{\rho_\infty}{\rho_{gas}}\right)^{1/2} \tag{A.10}$$

At each axial position, x, the radial variation of the concentration is computed from the expression

$$\overline{\eta}(x,r) = \eta_{cl}(x)e^{-K_c(r/x+x_o)^2} \tag{A.11}$$

where the value of $K_c = 57$ for a round jet [9]. Equations (A.8), (A.9), (A.10), and (A.11) can be used to compute the concentration field from a high-momentum turbulent jet resulting from the supercritical release of hydrogen. For the studies performed in this paper, a value of the entrainment coefficient equal to K=5.40 [10] was used for the simulations. The value of the virtual origin, x_o, is typically a small multiple (less than 5) of the jet exit diameter and was set to zero for these studies in accordance with the work of Birch [10].

A.2 Comparison of Models with Experimental Data

A.2.1 Flame Radiation Heat Flux and Flame Length Model

The hydrogen flame radiation and flame length models were compared against the large-scale hydrogen jet flame experiments of Schefer *et al.* [2, 3]. In these experiments, hydrogen gas was released from a "six-pack" of high-pressure cylinders, each connected to a central manifold with a common outlet. Typical pressure in the full cylinders was 137.9 bar (2000 psia) to 172.3 bar (2500 psia).

To obtain jet exit conditions, a network flow model of the piping and high-pressure cylinders used in the experiment was developed using the Sandia developed Topaz code [13]. The network flow model considers the non-ideal gas behavior of hydrogen through an Abel-Nobel equation of state [14] of the form

$$p = \frac{\rho R_{H_2} T}{(1 - b\rho)} \tag{A.12}$$

where the values of R_{H_2} = 4,124.18 J/kg-K and b = 7.691x10^{-3} m^3/kg were used for hydrogen. The model can also be used with an ideal-gas equation of state by setting the value b equal to zero.

The tank blow-down and network flow model was used to predict the flow and pressure drop through the piping leading to the jet exit. These jet exit conditions were then used with the flame length and radiant fraction correlations described in the previous section to predict the hydrogen jet flame characteristics. Comparisons of the measured and predicted pressure history curves in the high-pressure cylinders were used to validate the tank blow-down network flow model [2]. Simulations with the network flow model indicated that significant pressure drop occurred in the piping of the experiment with the total pressure at the jet exit being approximately 16.4 bar (226 psig) or a static pressure of approximately 13.6 bar (182 psig) at 0.1 second into the blow-down.

Figure A-5 shows a comparison of the flame length predictions from the model with the large-scale hydrogen jet flame length data. Because an approximate ±10% scatter occurs in the data around the L* correlation (see Figure A-4) used in the model, an uncertainty analysis was performed where the L* correlation was increased and then decreased by 10% from its nominal value. Calculations are shown in Figure A-5 for the nominal L* correlation, and an increase in L* of 10% and a decrease in L* of –10%. Predictions from the model are found to be in good agreement with the measured hydrogen flame lengths.

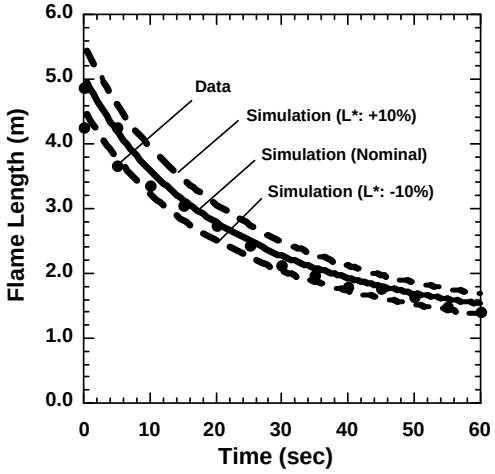

Figure A-5. Comparison of simulation of hydrogen visible flame length with the hydrogen jet flame data of Schefer et al. [2].

Figure A-6 shows a comparison of simulations and measured radiation heat flux data along the axis of a hydrogen jet flame at a radial distance of 1.82m (6 ft) from the flame centerline at a time 5 seconds into the blow-down of the high-pressure hydrogen cylinders. An approximate ±10% scatter occurs in the data around the L* correlation (see Figure A-4), the C* correlation (see Figure A-2), and the radiant fraction correlation (see Figure A-3), X_{rad}. Hence, an uncertainty analysis was performed where model calculations were performed with the nominal values of these correlations, and an increase of 10% to each of the 3 correlations (upper bound on radiative heat flux), and a decrease of –10% to each of the correlations (lower bound on radiative heat flux). The results of these calculations are shown in Figure A-6. An additional comparison with data using the same approach is shown in Figure A-7 at a time of 10 seconds into the blow-down. The range of the calculations with either an increase of 10% or decrease of 10% in each of the correlations for L*, C*, and X_{rad} are able to bound the range of experimental data adequately at both times.

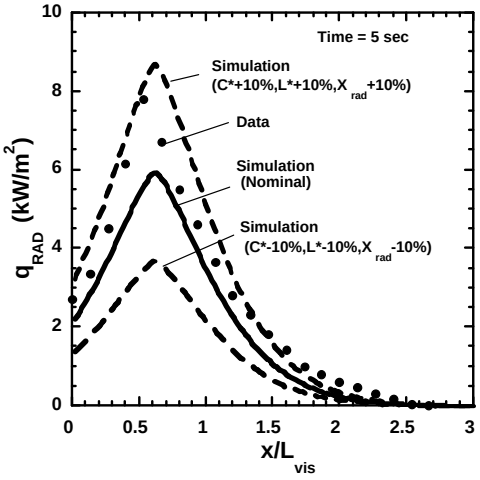

Figure A-6. Comparison of simulation of radiative heat flux from a hydrogen flame at a radial position of r=1.83 m with the data at 5 seconds into the blow-down.

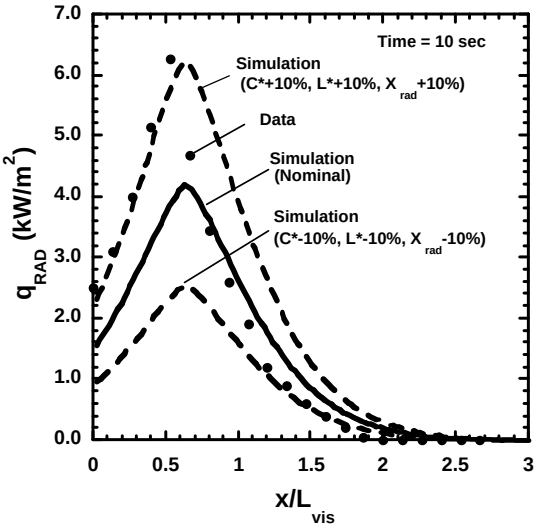

Figure A-7. Comparison of simulation of radiative heat flux from a hydrogen flame at a radial position of r=1.83 m with the data at 10 seconds into the blow-down.

A.2.2 Un-ignited Jet Concentration Decay Model

There appears to be a lack of data in the literature for the concentration decay of momentum-dominated, choked flow, un-ignited turbulent hydrogen jets resulting from supercritical releases. Hence the un-ignited jet model was compared with the jet concentration decay data of Birch [4] for supercritical releases of natural gas. Birch measured the concentration decay of natural gas into air for a 2.7 mm diameter round nozzle connected to a regulated high-pressure natural gas supply. The method of concentration measurement in the experiment integrated the turbulent concentration fluctuations in the flow and resulted in a time-averaged concentration measurement at each axial location. Measurements of the mean concentration level at different axial positions along the jet centerline were made for supply pressures ranging from 3.5 to 71 bar. Birch found if the mean concentration decay along centerline was plotted in terms of the non-dimensional coordinate $x/(d_j(p_{supply}/p_\infty)^{0.5})$, then the data collapsed onto a single curve.

Calculations with the un-ignited jet model discussed in the previous section were performed using natural gas properties and generating jet exit conditions for a large high-pressure supply attached to a short round nozzle. The Topaz network flow code with an ideal gas equation of state for natural gas was used to generate jet exit conditions for this geometry. Calculations were performed at pressures of 18.25 bar (250 psig) and 207.85 bar (3000 psig) for jet exit diameters of 0.794 mm and 1.158 mm. The axial variation of the reciprocal of the mean concentration ($1/\overline{\eta}_{cl}$) on jet centerline was plotted in terms of the non-dimensional axial coordinate, $x/(d_j(p_{supply}/p_\infty)^{0.5})$, where d_j is the jet exit diameter, p_{supply} is the pressure in high-pressure supply, p_∞ is the ambient pressure. Comparison of the calculations from the model with the data of Birch [4] using the nominal value of the

turbulent entrainment constant (K = 5.40) is shown in Figure A-8. Based on data reported by Birch [4, 10] there appears to be approximately ±10% variation in the value of the turbulent entrainment constant, K. Hence, in addition to using the nominal value of K, calculations were performed for the 207.85 bar 1.158 diameter nozzle by varying K ±10% from the nominal value. Results of the calculations using the nominal value of K are in excellent agreement with the data of Birch. Moreover the calculations at 207.8 bar, which are well beyond the maximum pressure of 71 bar used in Birch's experiments, are found to be in excellent agreement with the collapsed data curve plotted in terms of $x/(d_j(p_{supply}/p_\infty)^{0.5})$. The work of Ruffin *et al*. [15] also appears to confirm the notional expansion concentration decay model of Birch for supercritical jets of methane and hydrogen at a pressure of 40 bar.

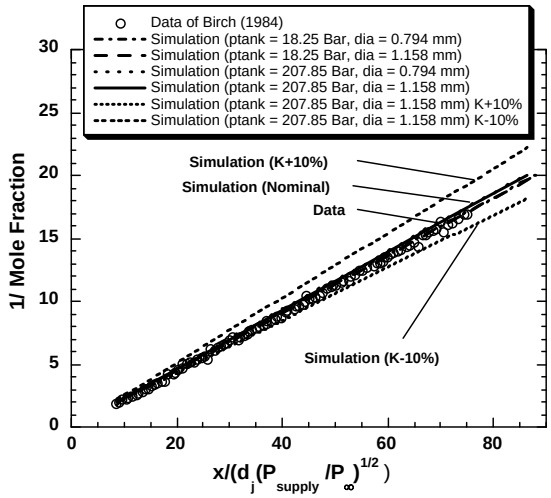

Figure A-8. Comparison of simulation of centerline concentration decay for natural gas un-ignited jets with the data of Birch [4].

A.3 Simulation of Unintended Releases

A.3.1 Hydrogen Jet Flame Radiation and Un-ignited Jet Concentration Decay

Simulations for unintended releases of hydrogen were performed by considering a break in the tubing directly connected to a large hydrogen storage container. Based on a survey of a panel of experts [16] familiar with current and intended uses of hydrogen, pressures in the range from 18.25 bar (250 psig) to 1,035.21 bar (15,000 psig) and leak diameters in the range from 9.525 mm (3/8 inch) to 0.25 mm were suggested for analysis.

For the simulations reported in this section a storage tank volume of 29.7 m^3 was used based on the recommendation of the expert panel. Calculations are reported for pressures of 18.25 bar (250 psig), 207.85 bar (3000 psig), 518.11 bar (7500 psig), and 1,035.21 bar (15,000 psig) and leak diameters ranging between 1.587 mm (1/16 inch) and 6.35 mm (1/4 inch). Jet exit conditions were computed using the Topaz network flow code with an Abel-Noble equation of state for hydrogen to simulate a large tank of hydrogen

connected to a short length of tubing (3.175 mm) with a diameter equal to the diameter of the leak under consideration. The tank temperature was assumed to be initially at ambient temperature (294K) with the end of the tubing exiting to the ambient environment (1.0133 bar, 294K). Calculations were performed for hydrogen jet flames and un-ignited jets with the results for radiative heat flux and concentration decay being reported at 1 second into the tank blow-down for each case. At 1 second, the tank pressure has not changed significantly from its initial value and the radiative and concentration length scales are at their largest values.

For the hydrogen jet flames, radiative heat flux contours were recorded for heat flux levels of 1577 W/m^2 (500 Btu/hr-ft^2), 4732 W/m^2 (1500 Btu/hr-ft^2), and 25237 W/m^2 (8000 Btu/hr-ft^2). These heat flux levels corresponding to values listed in the 2003 International Fire Code [17] for exposure at property line, exposure for employees for a maximum of 3 minutes, and exposure for noncombustible equipment, respectively. Figure A-9 shows results for the radiative heat flux from a hydrogen jet flame with a tank pressure of 207.85 bar (3000 psig) and a leak diameter of 3.175 mm (1/8 inch). Important safety related information recorded from the simulations includes the maximum radial position from the flame centerline for the given heat flux level, R_{max}, the axial location at which the maximum occurs, $X(R_{max})$, the combination of these two distances, $D_{rad}= (R_{max}+X(R_{max}))$, and the visible flame length, L_{vis}. Figure A-10 shows a plot of D_{rad} and the visible flame length for various leak diameters for a tank pressure of 207.85 bar. Also included on the plot are the upper and lower bounds for D_{rad} and L_{vis} assuming an uncertainty of ±10% in each of the values of C*, L*, and X_{rad}. Figure A-11 shows a plot of R_{max} and $X(R_{max})$ for various leak diameters for a tank pressure of 207.85 bar, including the upper and lower bounds for R_{max} and $X(R_{max})$ assuming ±10% uncertainty in each of the values of C*, L*, and X_{rad}. At this pressure the value of D_{rad} can be computed to approximately ±14% to ±18% depending on the jet diameter, while the flame length can be computed to approximately ±10%.

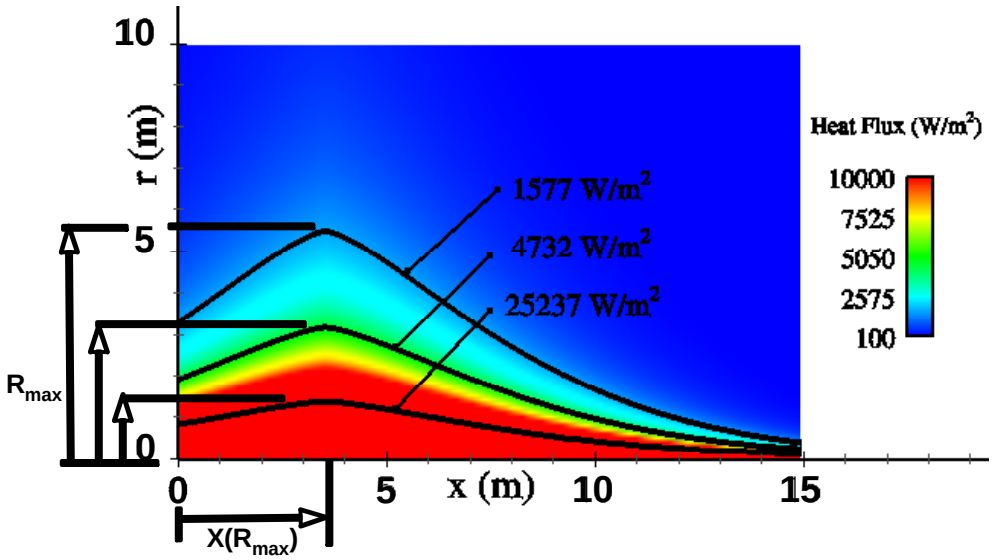

Figure A-9. Simulation of radiation heat flux from a hydrogen jet flame with a leak diameter of 3.175 mm and a tank pressure of 207.85 bar (3000 psig).

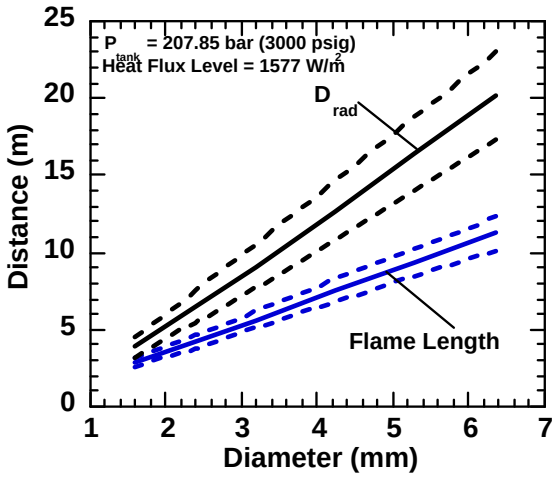

Figure A-10. Simulations of hydrogen jet flame radiation from a tank at pressure 207.85 bar (3000 psig) for various diameter leaks. Results showing radiation distance, Drad = (X(Rmax) + Rmax), for a heat flux level of 1577 W/m2 and the visible flame length. Solid lines show distances using nominal values of C*, L*, and Xrad. Dashed lines show upper and lower bounds for Drad and visible flame length with ±10% uncertainty in each of the values of C*, L*, and Xrad.

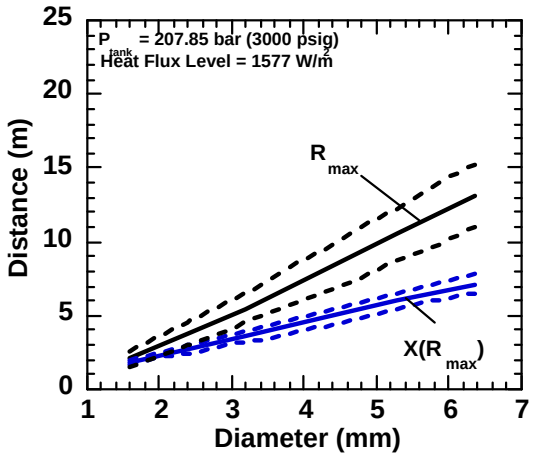

Figure A-11. Simulations of hydrogen jet flame radiation from a tank at pressure 207.85 bar (3000 psig) for various diameter leaks. Results showing maximum radial distance from the flame centerline, Rmax, for a heat flux level of 1577 W/m2 and the axial location on centerline, X(Rmax), where the maximum occurs. Solid lines show distances using nominal values of C*, L*, and Xrad. Dashed lines show upper and lower bounds for Rmax and X(Rmax) with ±10% uncertainty in each of the values of C*, L*, and Xrad.

Figure A-12 shows mole fraction contours for the simulation of the concentration decay of an un-ignited jet of hydrogen for a tank pressure of 207.85 bar (3000 psig) and a leak diameter of 3.175 mm (1/8 inch). Important safety information recorded from the simulations is the distance from the jet exit to where the mean concentration decays to a given concentration level on the jet centerline. Although the generally accepted value for the upward-propagating lower flammability limit of hydrogen in air is 0.04 mole fraction,

experimental data in the literature indicate that the limit may be as high as 0.072 mole fraction for horizontal-propagating flames and 0.095 mole fraction for downward-propagating flames [18, 19]. For the un-ignited hydrogen jet simulations, distances from the origin to jet centerline concentration levels of 0.08, 0.06, 0.04, and 0.02 mole fraction were recorded, and these distances are referred to as x8%, x6%, x4%, and x2% respectively. Figure A-13 shows a plot of un-ignited jet concentration decay distances for a tank pressure of 207.85 bar (3000 psig) for various leak diameters. Upper and lower bounds for the concentration decay distances are also shown on the plot assuming a ±10% uncertainty in the turbulent jet entrainment constant K.

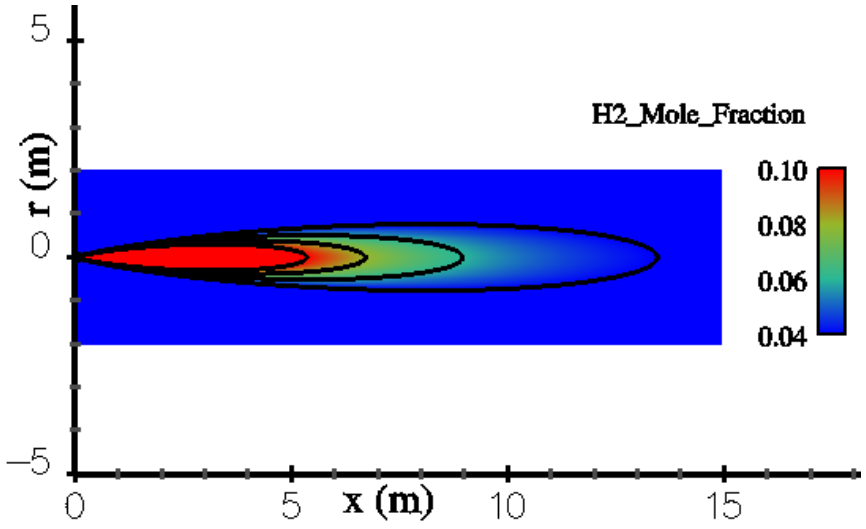

Figure A-12. Simulations of concentration decay of an un-ignited hydrogen jet with a diameter of 3.175 mm (1/8 inch) and a tank pressure of 207.85 bar (3000 psig). Contour lines correspond to mole fraction levels shown in the color legend.

Table A-1 shows a summary of radiation distances recorded from hydrogen jet flame simulations for tank pressures of 18.25 bar (250 psig), 207.85 bar (3000 psig), 518.11 bar (7500 psig), and 1035.21 bar (15,000 psig) for selected leak diameters using the nominal values of C*, L*, and X_{rad}. Table A-2 shows a summary of concentration decay distances for un-ignited hydrogen jets for the same tank pressures and selected leak diameters using the nominal value of the entrainment constant K.

Figure A-14 shows a comparison of hydrogen jet flame radiation hazard distances with un-ignited jet concentration decay distances for a range of tank pressures and leak diameters. Results are shown for the visible flame length and the radiation hazard distance, D_{rad}, for heat flux levels of 1577 W/m^2 and 4732 W/m^2. These radiation hazard distances are compared with un-ignited jet concentration decay distances from origin to jet centerline mean concentration levels of 0.08, 0.06, 0.04 mole fractions. For the range of pressures studied, the un-ignited jet concentration decay distance to the generally accepted lower flammability limit of hydrogen in air (0.04 mole fraction) is greater than the radiation jet flame hazard distance (D_{rad}) for exposure at property line (1577 W/m^2).

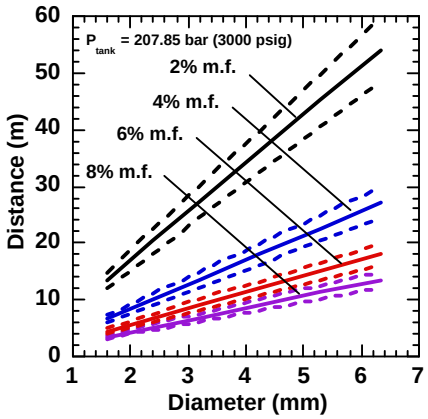

Figure A-13. Simulations of concentration decay for a turbulent high-momentum supercritical un-ignited hydrogen jet from a tank at pressure 207.85 bar (3000 psig) for various diameter leaks. Results showing axial distance from jet origin to the point where jet concentration reaches 2.0%, 4.0%, 6.0%, and 8.0% mole fraction on jet centerline. Solid lines show distances using the nominal value of the turbulent jet entrainment constant, K = 5.40. Dashed lines show upper and lower bounds for distances with ±10% uncertainty in the value of K.

Figures A-15 through A-19 give detailed plots of the hydrogen jet flame radiation hazard distances (D_{rad}, $X(R_{max})$, R_{max}) and un-ignited jet concentration decay distances (including upper and lower bounds) for tank pressures of 18.25 bar (250 psig), 207.85 bar (3000 psig), 518.11 bar (7500 psig), and 1035.21 bar (15,000 psig) over a range of leak diameters from 0.25 mm to 6.35 mm. Figure A-15 shows simulation results of un-ignited hydrogen jet concentration decay distances and their uncertainty for the range of leak diameters and tank pressures studied while Figures A-16 through A-19 show simulation results of hydrogen jet flame radiation distances and their uncertainty for the range of leak diameters and tank pressures studied.

A.4 Summary and Conclusions

The previous sections presented methods by which the radiant heat flux from hydrogen jet flames and the concentration decay of supercritical high-momentum un-ignited hydrogen jets may be computed. If the jet exit conditions can be computed at the leak [20], then these methods can be used to compute hydrogen jet flame radiation and un-ignited jet concentration decay based on the models.

An uncertainty analysis of the hydrogen jet flame radiation model (207.85 bar case) using an uncertainty of ±10% in each of the three experimentally measured correlations (C*, L*, X_{rad}), indicates that the radiation distance, D_{rad}, can be computed to approximately ±14% to ±18% for the jet diameters studied. The flame length can be computed to approximately ±10%. Assuming a ±10% uncertainty in the experimentally measured turbulent jet entrainment constant, K, an uncertainty analysis of the un-ignited jet

concentration decay model indicates that concentration decay distances can be computed to ±10%.

Table A-1. Hydrogen jet flame radiation distances for selected leak diameters and tank pressures. (Note: Assuming worst case of no pressure loss in tubing).

P_{tank} (bar)	d_j (mm)	$X(R_{max})$ (m)	R_{max} (m)	D_{rad} (m)	L_{vis} (m)	Heat Flux (W/m^2)
18.25	1.00	0.35	0.10	0.45	0.55	1577
18.25	1.00	0.35	0.059	0.41	0.55	4732
18.25	1.00	0.35	0.026	0.38	0.55	25237
18.25	2.3810	0.84	0.52	1.36	1.32	1577
18.25	2.3810	0.84	0.30	1.14	1.32	4732
18.25	2.3810	0.84	0.13	0.97	1.32	25237
18.25	4.2333	1.49	1.59	3.09	2.35	1577
18.25	4.2333	1.49	0.92	2.41	2.35	4732
18.25	4.2333	1.49	0.39	1.89	2.35	25237
18.25	6.35	2.24	2.90	5.14	3.52	1577
18.25	6.35	2.24	1.67	3.91	3.52	4732
18.25	6.35	2.24	0.72	2.96	3.52	25237
207.85	1.00	1.13	0.96	2.08	1.77	1577
207.85	1.00	1.13	0.55	1.68	1.77	4732
207.85	1.00	1.13	0.24	1.36	1.77	25237
207.85	2.3810	2.68	3.75	6.43	4.22	1577
207.85	2.3810	2.68	2.16	4.84	4.22	4732
207.85	2.3810	2.68	0.93	3.61	4.22	25237
207.85	4.2333	4.76	7.94	12.71	7.50	1577
207.85	4.2333	4.76	4.58	9.35	7.50	4732
207.85	4.2333	4.76	1.98	6.75	7.50	25237
207.85	6.35	7.14	13.09	20.23	11.25	1577
207.85	6.35	7.14	7.55	14.70	11.25	4732
207.85	6.35	7.14	3.27	10.42	11.25	25237
518.11	1.00	1.68	1.91	3.60	2.65	1577
518.11	1.00	1.68	1.10	2.79	2.65	4732
518.11	1.00	1.68	0.48	2.16	2.65	25237
518.11	2.3810	4.01	6.46	10.47	6.31	1577
518.11	2.3810	4.01	3.73	7.74	6.31	4732
518.11	2.3810	4.01	1.61	5.62	6.31	25237
518.11	4.2333	7.13	13.27	20.40	11.23	1577
518.11	4.2333	7.13	7.66	14.79	11.23	4732
518.11	4.2333	7.13	3.31	10.45	11.23	25237
518.11	6.35	10.69	21.58	32.28	16.84	1577
518.11	6.35	10.69	12.46	23.16	16.84	4732
518.11	6.35	10.69	5.39	16.09	16.84	25237
1035.21	1.00	2.21	2.89	5.10	3.48	1577
1035.21	1.00	2.21	1.67	3.88	3.48	4732
1035.21	1.00	2.21	0.72	2.93	3.48	25237
1035.21	2.3810	5.26	9.30	14.56	8.29	1577
1035.21	2.3810	5.26	5.37	10.63	8.29	4732
1035.21	2.3810	5.26	2.32	7.59	8.29	25237

Table A-2. Un-ignited hydrogen jet concentration decay distances on jet centerline for selected leak diameters, tank pressures, and mole fractions. (i.e. X2% indicates the distance from jet origin to the point where the centerline concentration has decayed to a mean concentration of 2% mole fraction).

P_{tank} (bar)	d_j (mm)	X 2% (m)	X 4% (m)	X 6% (m)	X 8% (m)
18.25	0.25	0.67	0.33	0.22	0.16
18.25	0.50	1.34	0.67	0.44	0.33
18.25	1.00	2.67	1.34	0.89	0.67
18.25	2.3810	6.36	3.18	2.12	1.59
18.25	4.2333	11.31	5.65	3.77	2.82
18.25	6.35	16.97	8.48	5.65	4.24
207.85	0.25	2.13	1.07	0.71	0.53
207.85	0.50	4.26	2.13	1.42	1.07
207.85	1.00	8.53	4.26	2.84	2.13
207.85	2.3810	20.30	10.15	6.76	5.07
207.85	4.2333	36.10	18.05	12.03	9.02
207.85	6.35	54.13	27.06	18.04	13.53
518.11	0.25	3.19	1.59	1.06	0.80
518.11	0.50	6.38	3.19	2.13	1.60
518.11	1.00	12.77	6.38	4.25	3.19
518.11	2.3810	30.39	15.19	10.13	7.598
518.11	4.2333	54.03	27.01	18.01	13.50
518.11	6.35	81.03	40.51	27.01	20.25
1035.21	0.25	4.18	2.09	1.39	1.05
1035.21	0.50	8.37	4.18	2.79	2.09
1035.21	1.00	16.74	8.37	5.58	4.18
1035.21	2.3810	39.86	19.93	13.29	9.96
1035.21	4.2333	70.85	35.42	23.62	17.71
1035.21	6.35	106.24	53.12	35.41	26.56

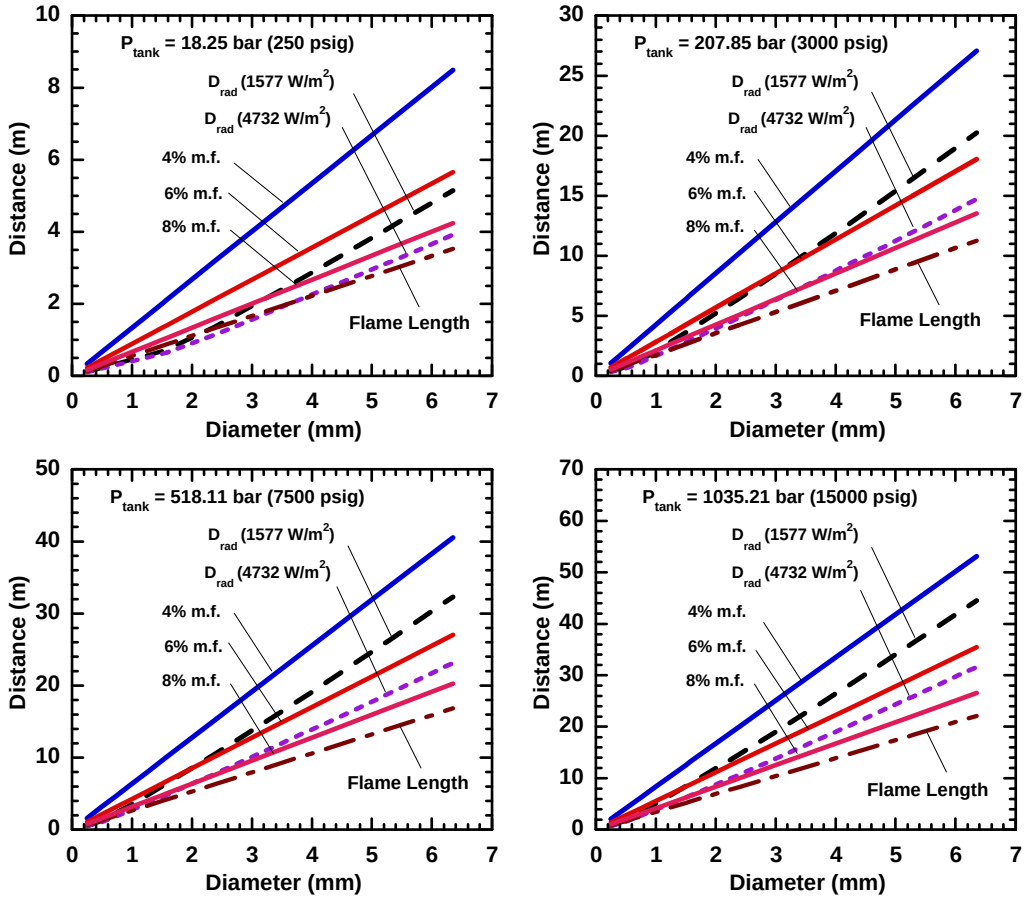

Figure A-14. Comparison of simulations of hydrogen jet flame radiation hazard distances with un-ignited hydrogen jet centerline concentration decay distances for various tank pressures (18.25 bar (250 psig), 207.85 bar (3000 psig), 518.11 bar (7500 psig), 1035.21 bar (15000 psig)) and leak diameters. Dashed lines show the radiation hazard distance, Drad = (X(Rmax) + Rmax), for radiation heat flux levels of 1577 W/m2 and 4732 W/m2 and the visible flame length. Solid lines show un-ignited jet concentration decay distances along jet centerline for concentration levels of 4%, 6%, and 8% mole fraction.

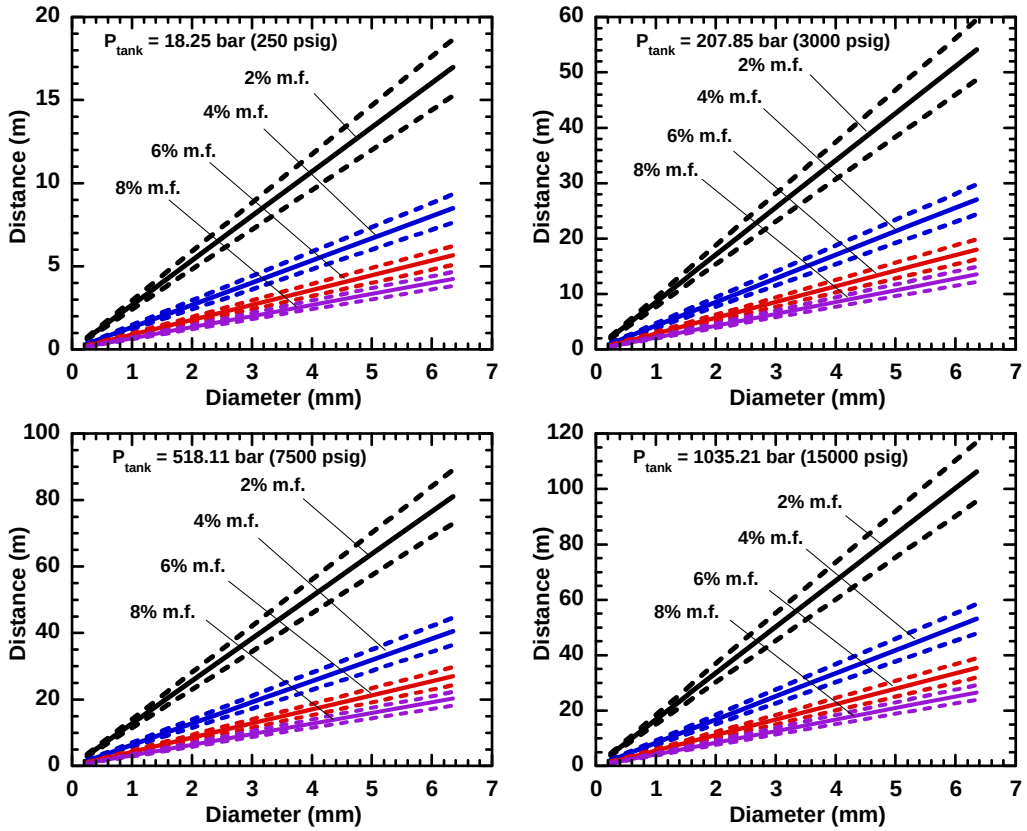

Figure A-15. Simulations of concentration decay for turbulent high-momentum supercritical un-ignited hydrogen jets from tanks at pressures from 18.25 bar (250 psig) to 1035.21 bar (15000 psig) for various diameter leaks. Results showing axial distance from jet origin to the point where jet concentration reaches 2.0%, 4.0%, 6.0%, and 8.0% mole fraction on jet centerline. Solid lines show distances using the nominal value of the turbulent jet entrainment constant, K = 5.40. Dashed lines show upper and lower bounds for distances with ±10% uncertainty in the value of K.

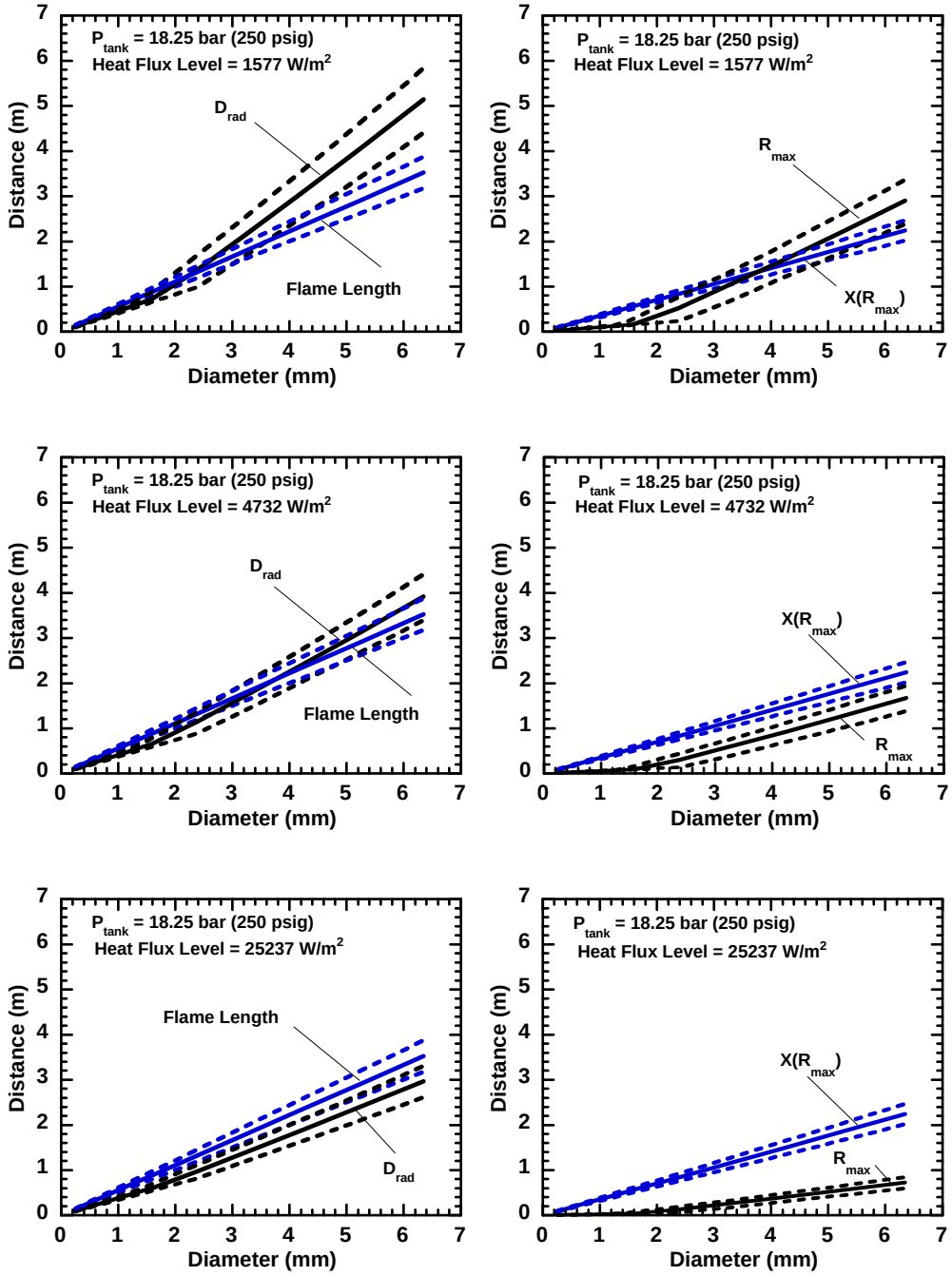

Figure A-16. Simulations of hydrogen jet flame radiation from a tank at pressure 18.25 bar (250 psig) for various diameter leaks. Results showing maximum radial distance from the flame centerline, Rmax, for a heat flux levels of 1577, 4732, and 25237 W/m2 and the axial location on centerline, X(Rmax), where the maximum occurs. Solid lines show distances using nominal values of C*, L*, and Xrad. Dashed lines show upper and lower bounds for Rmax and X(Rmax) with ±10% uncertainty in each of the values of C*, L*, and Xrad.

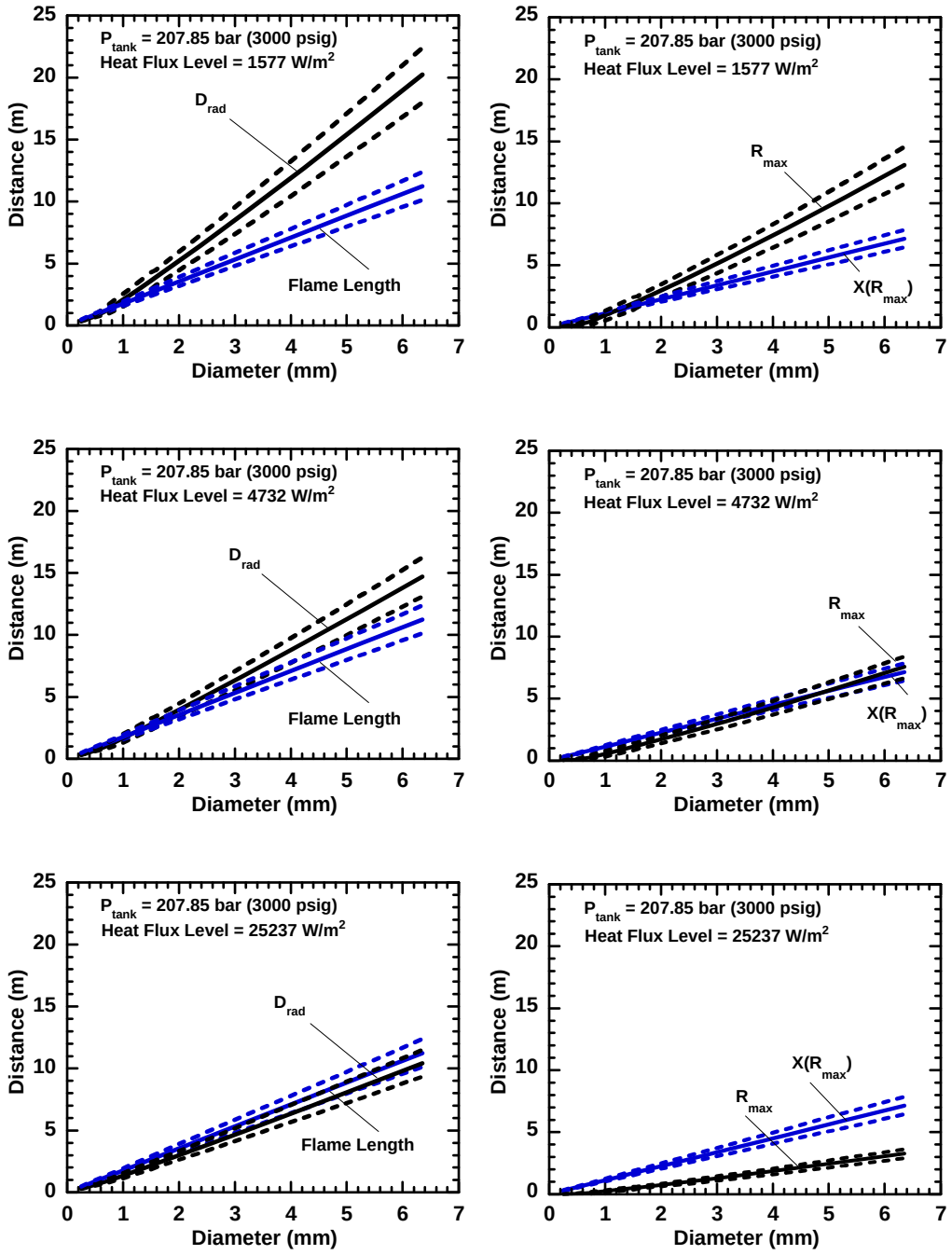

Figure A-17. Simulations of hydrogen jet flame radiation from a tank at pressure 207.85 bar (3000 psig) for various diameter leaks. Results showing maximum radial distance from the flame centerline, Rmax, for a heat flux levels of 1577, 4732, and 25237 W/m2 and the axial location on centerline, X(Rmax), where the maximum occurs. Solid lines show distances using nominal values of C*, L*, and Xrad. Dashed lines show upper and lower bounds for Rmax and X(Rmax) with ±10% uncertainty in each of the values of C*, L*, and Xrad.

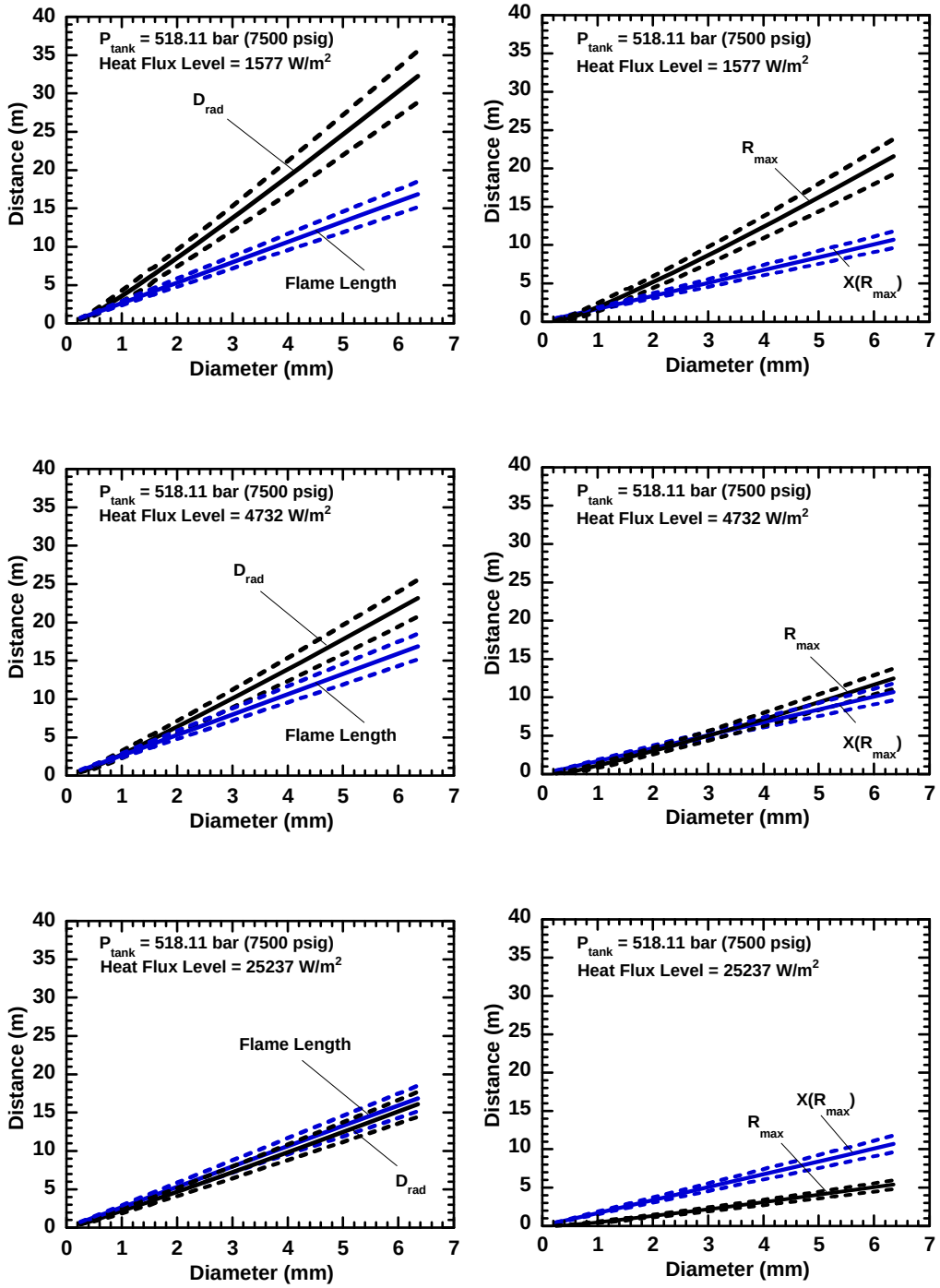

Figure A-18. Simulations of hydrogen jet flame radiation from a tank at pressure 518.11 bar (7500 psig) for various diameter leaks. Results showing maximum radial distance from the flame centerline, Rmax, for a heat flux levels of 1577, 4732, and 25237 W/m2 and the axial location on centerline, X(Rmax), where the maximum occurs. Solid lines show distances using nominal values of C*, L*, and Xrad. Dashed lines show upper and lower bounds for Rmax and X(Rmax) with ±10% uncertainty in each of the values of C*, L*, and Xrad.

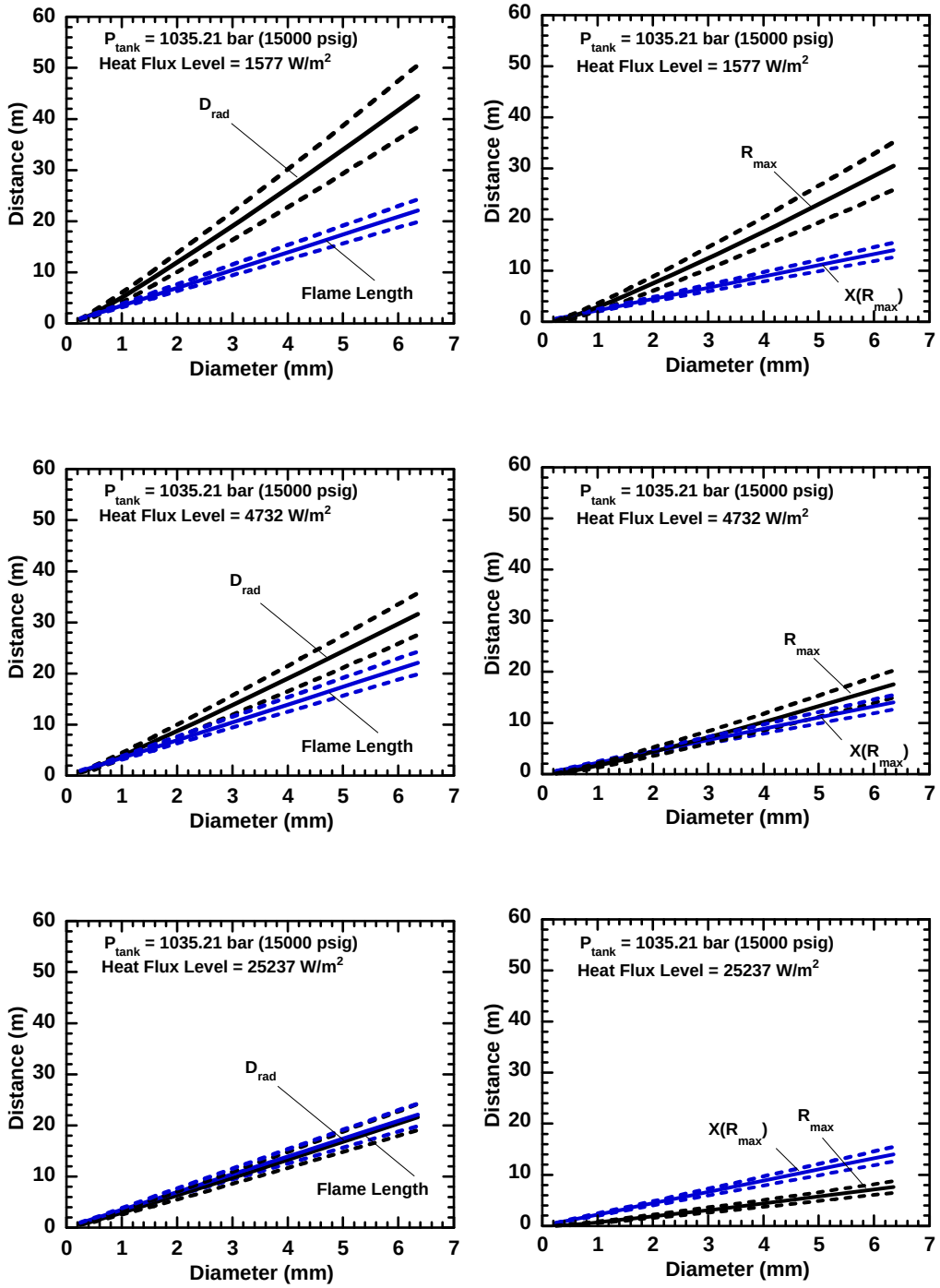

Figure A-19. Simulations of hydrogen jet flame radiation from a tank at pressure 1035.21 bar (15000 psig) for various diameter leaks. Results showing maximum radial distance from the flame centerline, Rmax, for a heat flux levels of 1577, 4732, and 25237 W/m2 and the axial location on centerline, X(Rmax), where the maximum occurs. Solid lines show distances using nominal values of C*, L*, and Xrad. Dashed lines show upper and lower bounds for Rmax and X(Rmax) with ±10% uncertainty in each of the values of C*, L*, and Xrad.

A.5 Appendix A References

1. Schefer, R. W., Houf, W. G., Moen, C. D., Chan, J. P., Maness, M. A., Keller, J. O., Leon, M. V., Tam, R., "Hydrogen Codes and Standards Unintended Release Workshop: Workshop Analysis," Workshop held December 12, 2003 at Sandia National Laboratories, Livermore CA, 2004b.
2. Schefer, R., Houf, W., Bourne, B., and Colton, J., "Spatial and Radiative Properties of an Open-Flame Hydrogen Plume," Inter. Jour. of Hydrogen Energy **31**: 1332-1340, 2006.
3. Schefer, R., Houf, W., Williams, T.C., Bourne, B., and Colton, J., "Characterization of High-Pressure, Underexpanded Hydrogen-Jet Flames," Inter. Jour. of Hydrogen Energy **32**: 2081-2093, 2007.
4. Birch, A.D., Brown, D.R., Dodson, M.G., and Swaffield, F., "The Structure and Concentration Decay of High Pressure Jets of Natural Gas," Combustion Science and Technology **36**: 249-261, 1984.
5. Sivathanu, Y. R. and Gore, J. P., *Combust. Flame* **94**: 265-270, 1993.
6. Turns, S. R. and Myhr, F. H., *Combust. Flame* **87**: 319-335, 1991.
7. Delichatsios, M. A., *Combust. Flame* **92**: 349-364, 1993.
8. Turns, S. R., "An Introduction to Combustion," 2nd edition, McGraw-Hill, 2000.
9. Chen, C. and Rodi, W., "Vertical Turbulent Buoyant Jets – A Review of Experimental Data," Pergamon Press, 1980.
10. Birch, A.D., Hughes, D.J., Waffield, F., "Velocity Decay of High Pressure Jets," Combustion Science and Technology **52**: 161-171, 1987.
11. Britter, R.E., "Dispersion of Two Phase Flashing Releases – FLADIS Field Experiment, The modelling of a pseudo-source for complex releases," Report FM89/2, Cambridge Environmental Research Consultants Ltd., December, 1994.
12. Britter, R.E., "Dispersion of Two Phase Flashing Releases – FLADIS Field Experiment, A further note on modelling flashing releases," Report FM89/3, Cambridge Environmental Research Consultants Ltd., November, 1995.
13. Winters, W. S., "TOPAZ - A Computer Code for Modeling Heat Transfer and Fluid flow in Arbitrary Networks of Pipes, Flow Branches, and Vessels," SAND83-8253, Sandia National Laboratories, Livermore, CA, January, 1984.
14. Chenoweth, D.R., "Gas-Transfer Analysis Section H – Real Gas Results via the van der Waals Equation of State and Virial Expansion Extensions of its Limiting Abel-Noble Form," Sandia Report SAND83-8229, June, 1983.
15. Ruffin, E., Mouilleau, Y., Chaineaux, J. "Large Scale Characterization of the Concentration Field of Supercritical Jets of Hydrogen and Methane," J. Loss Prev. Process Ind., Vol. 9, No. 4, pp. 279-284, 1996.
16. International Code Council (ICC) Ad-Hoc Committee for Hydrogen Gas, October 2003.
17. 2003 International Fire Code, International Code Council, Inc., 2002.
18. Zebetakis, M.G., U.S. Bureau of Mines, Bulletin 627, 1965.
19. Coward, H.F, and Jones, G.W., "Limits of Flammability of Gases and Vapors," Bureau of Mines Bulletin 503, 1952.
20. Chernicoff, W., Engblom, L. Schefer, W. Houf, W., and San Marchi, C., "Characterization of Leaks from Compressed Hydrogen Dispensing Systems and

Related Components," 16th Annual Hydrogen Conference and Hydrogen Expo USA, March 28 – April 1, Washington, D.C., 2005.

Appendix B
Representative Facility Descriptions

This appendix provides a description of the four hydrogen gas storage systems used in both the system frequency assessment and QRA to determine the NFPA 2 and NFPA 55 separation distances. The four facilities were defined by industrial members of the NFPA 2 TG6 based on their knowledge of existing gas storage systems. As indicated in Figure B-1, two lower pressure systems consisted of three modules: a mobile tube trailer assumed to be at 20.7 MPa, a stanchion or product transfer module that connects the tube trailer to the facility, and a pressure control station for reducing (1.7MPa system only) or controlling the gas pressure. The storage facility ends at the source valve that separates the storage from the associated process equipment. The two higher pressure systems include additional modules: a compressor for raising the gas pressure from 20.7 MPa to the facility operating pressure and a high-pressure storage module.

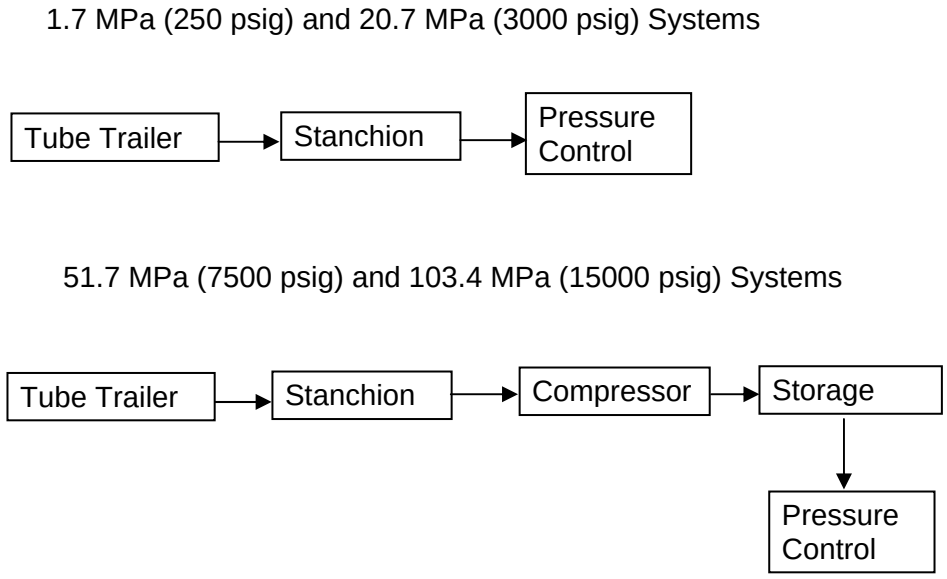

Figure B-1. Simplified schematic of example gas storage modules.

A detailed piping and instrumentation diagram (P&ID) for the 1.7 MPa and 20.7 MPa systems is provided in Figure B-2. The major components in the tube trailer, stanchion, and pressure control modules are illustrated in this figure. For the 1.7MPa system, the pressure control station reduces the gas pressure from 20.7 MPa down to 1.7MPa. Thus, the pressure control module includes components at both pressures. For the 20.7MPa system, all of the components are at that pressure. The P&IDs for the compressor and high-pressure storage modules used in the 51.7 MPa and 103.4 MPa systems are provided in Figures B-3 and B-4, respectively. The compressor, high-pressure storage, and pressure control modules are all at these high pressures while the tube trailer and stanchion are at 20.7MPa.

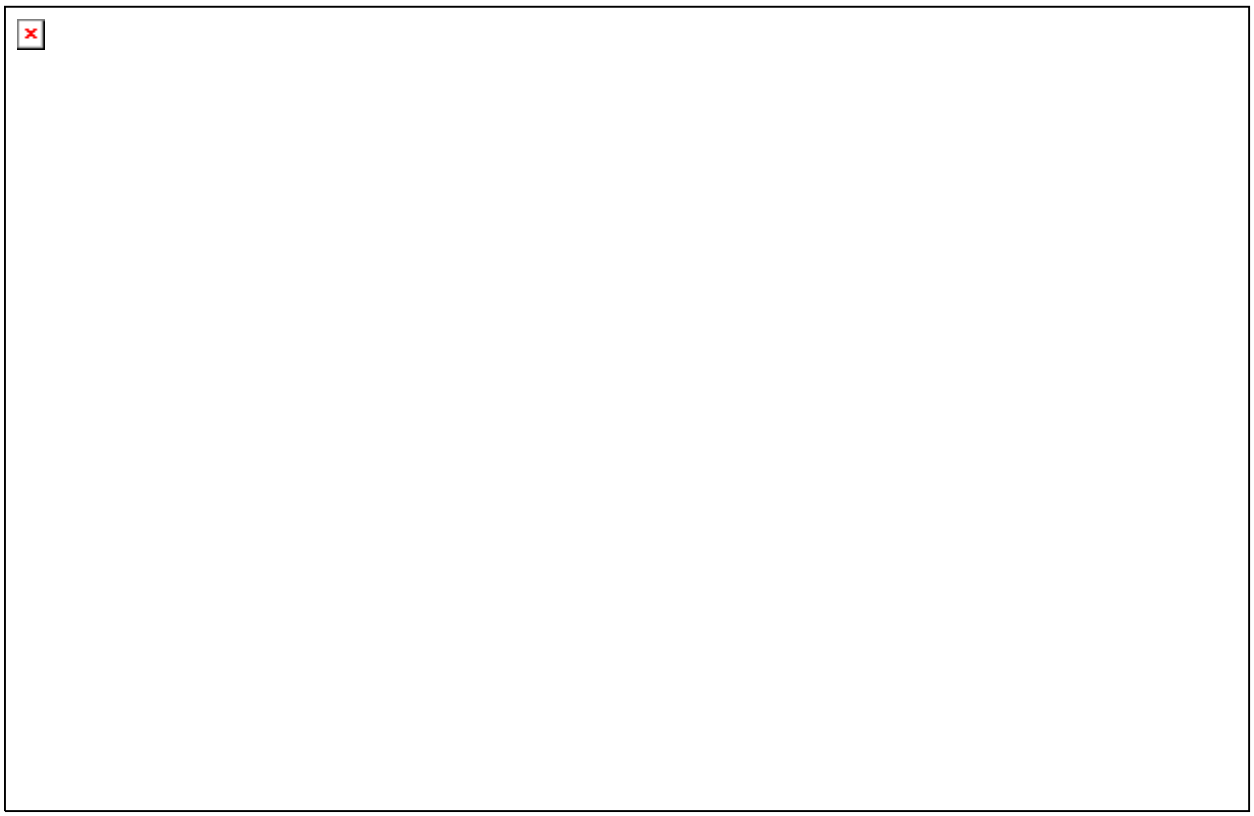

Figure B-2. Tube trailer, stanchion, and pressure control modules P&ID.

A description of the components in each module is provided in Table B-1. The primary purpose of the table is to identify the type and number of joints in the systems. The information for the pressure control module is provided for the 1.7 MPa system and differentiates the components that are at the 1.7 MPa and 20.7 MPa operating pressures. The number of components in each module is summarized in Table B-4. This data is necessary to generate the total system leakage frequency used in this analysis. The number of cylinders in a tube trailer can range from 8 to 60. Ten cylinders were assumed in the example systems. Similarly, the number of high-pressure storage cylinders can range from 3 to 12 and 6 were assumed in the high pressure system configuration.

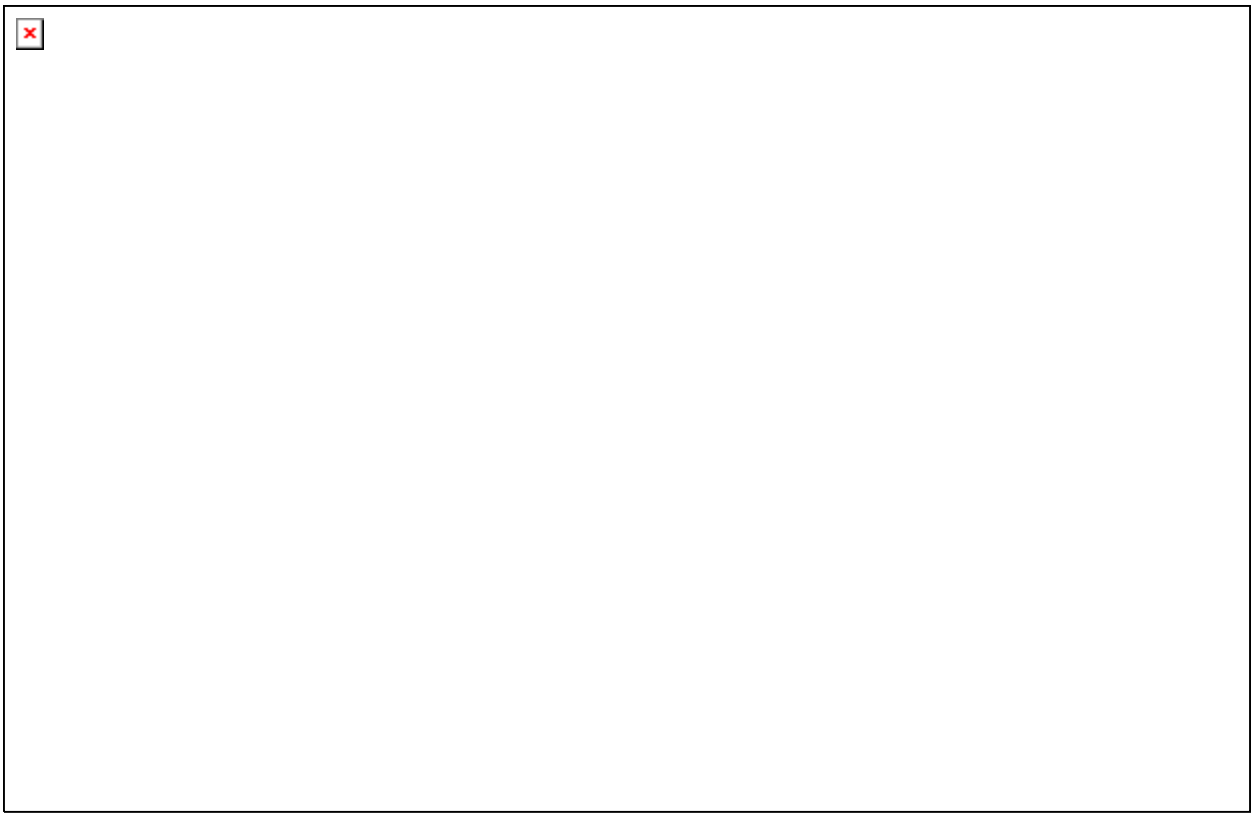

Figure B-3. Compressor module P&ID.

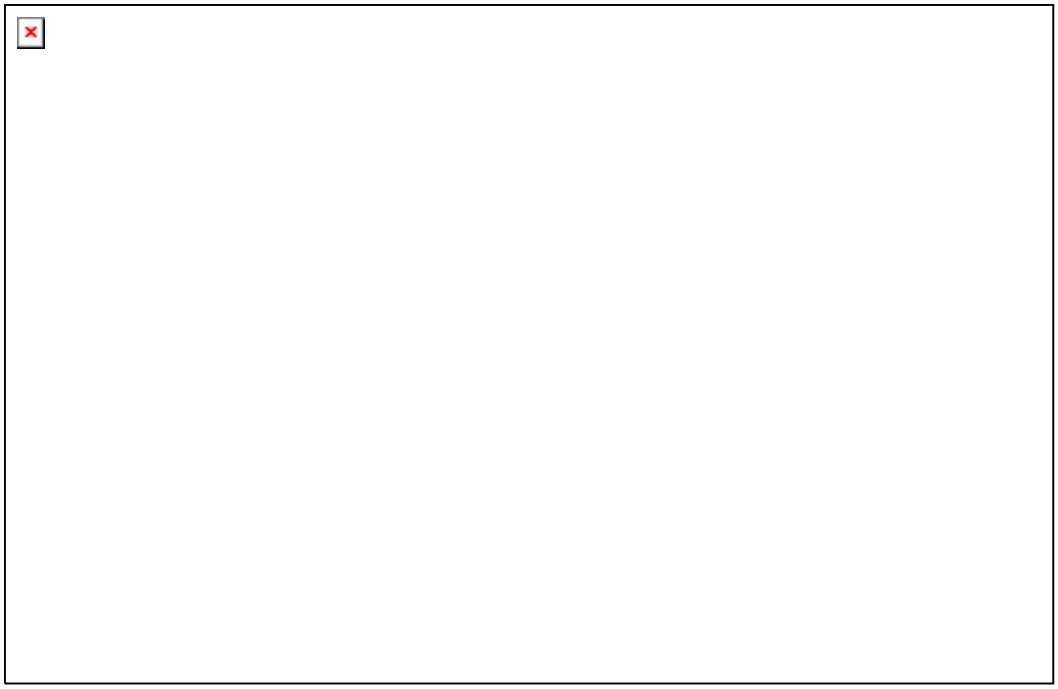

Figure B-4. High-pressure storage module P&ID.

Table B-1. Component list in modules of example systems.

Item or component	Joint Type	Method of joining	Number of joints	Component Material of construction
Pressure Control Module				
Components Rated With 20.7MPa (3000 psig) Design Pressure				
Inlet connection	M	T	1	B
Y300H	M	T	2	B
X304H	M	T	T2;P1	B
Tee	M	T	3	B
X310H	M	T	2	B
Tee	M	T	3	B
X300H	M	T	T2;P1	B
Tee	M	T	3	B
V300H	M	T	T1;P1	B
El (90 degree)	M	T	2	B
STR300H	M	T	2	SS
Tee	M	T	3	B
P305H	M	C	T2;P1	B
Tee	M	T	3	B
PI305	M	T	1	SS
V305H	M	C	T1;P1	B
PCV301H	M	T	T2;1G	BR
X302H	M	T	T2;P1	B
Tee	M	T	3	B
V302H	M	T	T1;P1	B
El (90 degree)	M	T	2	B
STR302H	M	T	2	SS
Tee	M	T	3	B
P306H	M	C	T2;P1	B
Tee	M	T	3	B
PI306	M	T	1	SS
V306H	M	C	T1;P1	B
PCV303H	M	T	T2;1G	BR
Components Rated With 1.7MPa (250 psig) Design Pressure				
El (90 degree)	M	T	2	B
Tee	M	T	3	B
V301H	M	T	T1;P1	B
Relief Valve	M	T	1	B
Tee	M	T	3	B
X301H	M	T	T2;P1	B
El (90 degree)	M	T	2	B
Tee	M	T	3	B

Table B-1. Component list in modules of example systems.

Item or component	Joint Type	Method of joining	Number of joints	Component Material of construction
V303H	M	T	T1;P1	B
Relief Valve	M	T	1	B
Tee	M	T	3	B
X303H	M	T	T2;P1	B
Tee	M	T	3	B
P304H	M	C	C2;P1	B
Tee	M	T	3	B
Tee	M	T	3	B
PI304	M	T	1	SS
V304H	M	C	C1;P1	B
Source Valve	M	T	3	B
Piping Schedule 80 Red Brass				
Length	5 feet	-	-	B
Piping Schedule 40 Red Brass				
Length	5 feet	-	-	B
Stanchion (Product Transfer Module)				
Components Rated With 20.7MPa (3000 psig) Design Pressure				
Valves (3)	M	T	T5, P3	B
Tees (2)	M	6	6	B
Els (3)	M	T	6	B
Pressure Gauges (1)	M	T	1	SS
Pressure Relief (0)	M	T	0	B
Union (1)	M	G	2T, 1G	B
Cylinder Valve (0)	M	P	0	B
Check Valve (1)	M	T	3T	B
Hose (1)	M	T	2	Polymer
Tube Trailer				
Components Rated With 20.7MPa (3000 psig) Design Pressure				
Control Valves (2)	M	T	4T, 2P	B
Tees (13)	M	T	39	B
Els (2)	M	T	4	B
Pressure Gauges (1)	M	T	1	SS
Sample Port Valve (1)	M	T	1T, 1P	B
Union (0)	M	G	0	B

Table B-1. Component list in modules of example systems.

Item or component	Joint Type	Method of joining	Number of joints	Component Material of construction
Cylinder Valve (10)	M	P	10T, 10P	B
Bull Plug (20)	M	T	20*	Steel
Rupture disk (20)	M	G	20	B
Caps (3)	M	T	3	B
Pigtail	M	T	10	B
High-Pressure Storage Module				
Components Rated at Either 51.7MPa (7500 psig) or 103.4 MPa (15000 psig) Pressure				
Control Valves (2)	M	T	4T, 2P	B
Tees (6)	M	T	18	B
Els (2)	M	T	4	B
Pressure Gauges (1)	M	T	1	SS
Pressure Relief (1)	M	T	1T, 1G	B
Union (1)	M	G	2T, 1G	B
Cylinder Valve	M	P	12T, 6G	B
Rupture disk (0)	M	G	0	B
Pigtails (6)	M	T	6	SS
Bull Plugs (12)	M	T	12	Steel

Legend

Type of joint:

M – Mechanical joint (as opposed to welded)
T- Threaded connection
C- Compression fitting connection
P – Packed (or fitted with packing)
G – Gasketed or fitted with gasket

Number of joints:

Where indicated with letters and numbers, e.g., C1;P1 the annotation indicates "compression 1 joint; Packed 1 joint, etc.

Material of Construction:

B – red brass
SS – Stainless Steel
BR – Bronze alloy

Table B-2. Number of components used in risk model.

Components	Number of Components in Model	
51.7 MPa and 103.4 MPa Modules	**Pressure Control Module**	**High Pressure Storage & Compressor**
Joints	28	3 + 3* number of cylinders[1]
Pipes	10 feet	20 feet[1]
Valves	20	3 + number of cylinders[1]
Filters	2	0
Compressor	0	1[1]
Cylinders	0	number of cylinders (6) [1]
Pigtails	0	number of cylinders (6) [1]
20.7 MPa Modules[2]	**Stanchion (Product Transfer Module)**	**Tube Trailer**
Joints	6	8 + 3* number of cylinders
Hoses	1	0
Pipe	5 feet	40 feet
Valves	4	3 + number of cylinders
Cylinders	0	number of cylinders (10)
Pigtails	0	number of cylinders (10)
Rupture Disks	0	2*number of cylinders

[1] For the 1.7 MPa and 20.7 MPa (250 and 3000 psig) systems, the number of storage cylinders and compressors is 0. There are no pipes, joints or valves because there is no storage module.

[2] This number account for all of the components applies to all four pressure ranges

Appendix C
Generic Component Leakage Frequencies

The identification of component failure rates from other industries is an appropriate initial phase to the Bayesian process described in Section 4.0. Component leakage frequencies have been identified from sources related to the chemical processing, compressed gas, nuclear power, and offshore petroleum industries. Sources used in the data analysis were obtained from a narrow range of available studies listed below. They varied in nomenclature, component specifics, component classification, and data reliability. The identified component leakage frequencies are provided in Table C-1.

Because of the scarcity of component leakage data, the data for specific component types were binned together into one component category. For example, leakage data for both reciprocating and centrifugal compressors were combined together in the Bayesian analysis to generate generic compressor leakage rates.

Most of the identified data sources provided leakage frequencies as a coarse function of leak size. In general, the leakage frequencies were binned into one of the following leak sizes:

- Small Leak
- Large Leak
- Rupture

The definition of each of these leak sizes varied between sources. Thus, based on the leakage size description presented in the available data sources, some judgment was needed in order to bin the available data consistently into one of these three groups. Furthermore, these definitions are different than the definitions used in this study. The relationship between the generic leak size definitions and the definitions used in this study are shown below. Note that no leakage frequencies were identified in the literature for "very small" and "minor" leaks that are less than 0.1% of the total flow area.

- Very Small- Leak area is 0.01 % of total flow area (no generic data was available for this size leak)
- Minor – Leak area is 0.1% of total flow area (no generic data was available for this size leak)
- Small Leak = Medium – Leak area is 1% of total flow area
- Large Leak = Major – Leak area is 10% of total flow area
- Rupture – Leak area is 100% of total flow area (the same definition is used in the referenced sources and this study)

References

1. A.W Cox, F.P. Lees, M.L Ang, “Classifications of Hazardous Locations,” Institution of Chemical Engineers, 2003.
2. CPR 18E ed. 1, “Guidelines for Quantitative Risk Assessment: The Purple Book,” 1999.
3. Center for Chemical Process Safety of the American Institute of Chemical Engineers, “Guidelines for Process Equipment Reliability Data with Data Tables,” 1989.
4. S.A Eide, S.T.,Khericha. M.B. Calley, D.A. Johnson, M.L. Marteeny, “Component External Leakage and Rupture Frequency Estimates,” EGG-SSRE-9639, Nov 1991.
5. NUREG/CR-6928, “Industry-Average Performance for Components and Initiating Events at U.S. Commercial Nuclear Power Plants,” February 2007.
6. NUREG-75/014, “Reactor Safety Study: An Assessment of Accident Risks in U.S. Commercial Nuclear Power Plants,” WASH-1400, Oct 1975.
7. Rijnmond, Openbaar Lichaam; “Risk Analysis of Six Potentially Hazardous Industrial Objects in the Rijnmond Area, A Pilot Study,” COVO, 1982.
8. Savannah River Site, “Generic Data Base Development,” WSRC-TR-93-263, June 1993.
9. Canadian Hydrogen Safety Program, “Quantitative Risk Comparison of Hydrogen and CNG Refueling Options,” Presentation, IEA Task 19 Meeting, 2006.
10. A.J.C.M. Matthijsen, E.S. Kooi, "Safety Distances for Hydrogen Filling Stations," Journal of Loss Prevention in the Process Industries 19, pp. 719 - 723, 2006.
11. R. E. Melchers, W. R Feutrill, "Risk Assessment of LPG Automotive Refueling Facilities," Reliability Engineering and System Safety, 74, 2001.
12. Rosyid, Oo Abdul, "System-Analytic Safety Evaluation of the Hydrogen Cycle for Energetic Utilization," Dissertation, 2006.
13. J. Spouge, “New Generic Leak Frequencies for Process Equipment,” *Process Safety Progress*, Vol. 4, No. 24, 2005

Table C- 1. Generic component leakage frequencies.

Component	Specific Component Type	Severity	Frequency	Units	Leak Size Description	Source Type	Source
Compressor							
Compressor	Centrifugal	Small Leak	2.00E-03	Per Year	>1 mm	Hydrocarbon Process	Spouge, John, "New Generic Leak Frequencies for Process Equipment, “Process Safety Progress, Vol. 24, No. 4, 2005
Compressor	Motor Driven	Small Leak	2.63E-03	Per Year	No definition of leak size was provided	Compressed Gas	Savannah River Site, "Generic Data Base Development," WSRC-TR-93-263, June 1993.
Compressor	Reciprocating	Small Leak	2.70E-02	Per Year	>1 mm	Hydrocarbon Process	Spouge, John, "New Generic Leak Frequencies for Process Equipment, “Process Safety Progress, Vol. 24, No. 4, 2005
Compressor	Centrifugal	Rupture	2.00E-06	Per Year	> 50 mm	Hydrocarbon Process	Spouge, John, "New Generic Leak Frequencies for Process Equipment, “Process Safety Progress, Vol. 24, No. 4, 2005
Compressor	Reciprocating	Rupture	1.10E-05	Per Year	> 50 mm	Hydrocarbon Process	Spouge, John, "New Generic Leak Frequencies for Process Equipment, “Process Safety Progress, Vol. 24, No. 4, 2005
Compressor	Motor Driven	Rupture	8.76E-05	Per Year	No definition of leak size was provided	Compressed Gas	Savannah River Site, "Generic Data Base Development," WSRC-TR-93-263, June 1993.
Cylinder							
Cylinder	Pressure	Small Leak	8.76E-04	Per Year	No definition of leak size was provided	Compressed Gas	Savannah River Site, "Generic Data Base Development," WSRC-TR-93-263, June 1993.
Vessel	Pressure	Large Leak	1.00E-05	Per Year	10 mm diameter	General	Guidelines for quantitative risk assessment. "Purple Book" CPR 18E, ed. 1, 1999
Tube Trailer	Transportation	Rupture	5.00E-07	Per Year	Instantaneous release	General	Guidelines for quantitative risk assessment. "Purple Book" CPR 18E, ed. 1, 1999
Cylinder	Gas	Rupture	1.00E-06	Per Year	Instantaneous Release	General	Guidelines for quantitative risk assessment. "Purple Book" CPR 18E, ed. 1, 1999
Filter							
Filter	No Additional Information	Small Leak	8.90E-04	Per Year	>1 mm	Hydrocarbon Process	Spouge, John, "New Generic Leak Frequencies for Process Equipment, “Process Safety Progress, Vol. 24, No. 4, 2005
Filter	No Additional Information	Small Leak	2.63E-02	Per Year	No definition of leak size was provided	Compressed Gas	Savannah River Site, "Generic Data Base Development," WSRC-TR-93-263, June 1993.

Table C- 1. Generic component leakage frequencies.

Component	Specific Component Type	Severity	Frequency	Units	Leak Size Description	Source Type	Source
Filter	No Additional Information	Rupture	4.38E-03	Per Year	No definition of leak size was provided	Compressed Gas	Savannah River Site, "Generic Data Base Development," WSRC-TR-93-263, June 1993.
Flange							
Flange	No Additional Information	Small Leak	4.70E-06	Per Year	Hole diameter from original source was not stated; EIGA assumed 2% flow area	Compressed Gas	EIGA, "Determination of Safety Distances," IGC Doc 75/01/E/rev, 2001
Flanged Joints	Flanged, 2 inch diameter	Small Leak	3.20E-05	Per Year	> 1 mm	Hydrocarbon Process	Spouge, John, "New Generic Leak Frequencies for Process Equipment, “Process Safety Progress, Vol. 24, No. 4, 2005
Flanged Joints	Flanged, 6 inch diameter	Small Leak	4.30E-05	Per Year	> 1 mm	Hydrocarbon Process	Spouge, John, "New Generic Leak Frequencies for Process Equipment, “Process Safety Progress, Vol. 24, No. 4, 2005
Flange	No Additional Information	Small Leak	8.76E-05	Per Year	50 gpm (water) or less	Nuclear	Eide, S.A, Khericha, S.T., Calley, M.B., Johnson, D.A., Marteeny, M.L., "Component External Leakage and Rupture Frequency Estimates," EGG-SSRE-9639, Nov 1991.
Flanged Joints	Flanged, 18 inch diameter	Small Leak	1.20E-04	Per Year	> 1 mm	Hydrocarbon Process	Spouge, John, "New Generic Leak Frequencies for Process Equipment, “Process Safety Progress, Vol. 24, No. 4, 2005
Flange	No Additional Information	Small Leak	1.70E-04	Per Year	Hole diameter from original source was not stated; EIGA assumed 2% flow area	Chemical Process	EIGA, "Determination of Safety Distances," IGC Doc 75/01/E/rev, 2001
Flange	No Additional Information	Small Leak	8.76E-04	Per Year	No definition of leak size was provided	Compressed Gas	Savannah River Site, "Generic Data Base Development," WSRC-TR-93-263, June 1993.
Flange	All Sizes	Small Leak	1.00E-03	Per Year	10% of flange area	Chemical Process	Cox, A.W., Lees, F.P., Ang, M.L., "Classifications of Hazardous Locations," Institution of Chemical Engineers, 2003
Flange	No Additional Information	Small Leak	2.60E-03	Per Year	Hole diameter from original source was not stated; EIGA assumed 2% flow area	Hydrogen Fueling Process	EIGA, "Determination of Safety Distances," IGC Doc 75/01/E/rev, 2001

Table C- 1. Generic component leakage frequencies.

Component	Specific Component Type	Severity	Frequency	Units	Leak Size Description	Source Type	Source
Flange	Gasket	Small Leak	2.63E-02	Per Year	No definition of leak size was provided	Nuclear	NUREG-75/014, "Reactor Safety Study: An Assessment of Accident Risks in U.S. Commercial Nuclear Power Plants," WASH-1400, Oct 1975
Flanged Joints	Flanged, 6 inch diameter	Rupture	3.60E-07	Per Year	> 50 mm	Hydrocarbon Process	Spouge, John, "New Generic Leak Frequencies for Process Equipment, "Process Safety Progress, Vol. 24, No. 4, 2005
Flanged Joints	Flanged, 18 inch diameter	Rupture	1.10E-06	Per Year	> 50 mm	Hydrocarbon Process	Spouge, John, "New Generic Leak Frequencies for Process Equipment, "Process Safety Progress, Vol. 24, No. 4, 2005
Flange	No Additional Information	Rupture	3.50E-07	Per Year	Hole diameter from original source was not stated; EIGA assumed 100% flow area	Compressed Gas	EIGA, "Determination of Safety Distances," IGC Doc 75/01/E/rev, 2001
Flange	No Additional Information	Rupture	8.76E-07	Per Year	>50 gpm (water) or complete failure	Nuclear	Eide, S.A, Khericha, S.T., Calley, M.B., Johnson, D.A., Marteeny, M.L., "Component External Leakage and Rupture Frequency Estimates," EGG-SSRE-9639, Nov 1991.
Flange	No Additional Information	Rupture	8.76E-06	Per Year	No definition of leak size was provided	Compressed Gas	Savannah River Site, "Generic Data Base Development," WSRC-TR-93-263, June 1993.
Flange	No Additional Information	Rupture	1.70E-05	Per Year	Hole diameter from original source was not stated; EIGA assumed 100% flow area	Chemical Process	EIGA, "Determination of Safety Distances," IGC Doc 75/01/E/rev, 2001
Flange	All Sizes	Rupture	1.00E-04	Per Year	100% of flange area	Chemical Process	Cox, A.W., Lees, F.P., Ang, M.L., "Classifications of Hazardous Locations," Institution of Chemical Engineers, 2003
Hose							
Hose	No Additional Information	Small Leak	1.00E-01	Per Year	Hole diameter from original source was not stated; EIGA assumed 2% flow area	Hydrogen Fueling Process	EIGA, "Determination of Safety Distances," IGC Doc 75/01/E/rev, 2001
Hose	Transportation, Tube Trailer	Small Leak	3.50E-01	Per Year	10% of hose diameter (1% of area)	General	Guidelines for quantitative risk assessment. "Purple Book" CPR 18E, ed. 1, 1999

Table C- 1. Generic component leakage frequencies.

Component	Specific Component Type	Severity	Frequency	Units	Leak Size Description	Source Type	Source
Hose	No Additional Information	Large Leak	1.00E-02	Per Year	Hole diameter from original source was not stated; EIGA assumed 20% flow area	Hydrogen Fueling Process	EIGA, "Determination of Safety Distances," IGC Doc 75/01/E/rev, 2001
Hose	No Additional Information	Rupture	3.40E-04	Per Year	Hole diameter from original source was not stated; EIGA assumed 100% flow area	Hydrogen Fueling Process	EIGA, "Determination of Safety Distances," IGC Doc 75/01/E/rev, 2001
Hose	No Additional Information	Rupture	1.00E-03	Per Year	Hole diameter from original source was not stated; EIGA assumed 100% flow area	Hydrogen Fueling Process	EIGA, "Determination of Safety Distances," IGC Doc 75/01/E/rev, 2001
Hose	No Additional Information	Rupture	4.99E-03	Per Year	Hole diameter was not stated	Process Equipment Data	Guidelines for Process Equipment Reliability Data with Data Tables, Center for Chemical Process Safety of the American Institute of Chemical Engineers, 1989.
Hose	Transportation, Tube Trailer	Rupture	3.50E-02	Per Year	100% of hose flow area	General	Guidelines for quantitative risk assessment. "Purple Book" CPR 18E, ed. 1, 1999
Instrument							
Instrument	0.5 inch	Small Leak	2.30E-04	Per Year	>1 mm	Hydrocarbon Process	Spouge, John, "New Generic Leak Frequencies for Process Equipment, “Process Safety Progress, Vol. 24, No. 4, 2005
Joints							
Joints	No Additional Information	Small Leak	3.60E-03	Per Year	Hole diameter from original source was not stated; EIGA assumed 2% flow area	Hydrogen Fueling Process	EIGA, "Determination of Safety Distances," IGC Doc 75/01/E/rev, 2001
Joints	No Additional Information	Small Leak	3.30E-02	Per Year	Hole diameter from original source was not stated; EIGA assumed 2% flow area	Hydrogen Fueling Process	EIGA, "Determination of Safety Distances," IGC Doc 75/01/E/rev, 2001

Table C- 1. Generic component leakage frequencies.

Component	Specific Component Type	Severity	Frequency	Units	Leak Size Description	Source Type	Source
Joints	No Additional Information	Large Leak	4.00E-03	Per Year	Hole diameter from original source was not stated; EIGA assumed 20% flow area	Hydrogen Fueling Process	EIGA, "Determination of Safety Distances," IGC Doc 75/01/E/rev, 2001
Joints	No Additional Information	Large Leak	4.99E-03	Per Year	10% cross sectional area or more	Process Equipment Data	Guidelines for Process Equipment Reliability Data with Data Tables, Center for Chemical Process Safety of the American Institute of Chemical Engineers, 1989.
Joints	No Additional Information	Large Leak	5.00E-03	Per Year	Hole diameter from original source was not stated; EIGA assumed 20% flow area	Hydrogen Fueling Process	EIGA, "Determination of Safety Distances," IGC Doc 75/01/E/rev, 2001
Joints	No Additional Information	Rupture	5.00E-04	Per Year	Hole diameter from original source was not stated; EIGA assumed 100% flow area	Hydrogen Fueling Process	EIGA, "Determination of Safety Distances," IGC Doc 75/01/E/rev, 2001
Joints	No Additional Information	Rupture	5.00E-04	Per Year	Hole diameter from original source was not stated; EIGA assumed 100% flow area	Hydrogen Fueling Process	EIGA, "Determination of Safety Distances," IGC Doc 75/01/E/rev, 2001
Pipe							
Pipe	Pipe Diameter is Greater than or Equal to 150 mm	Small Leak	5.00E-07	Per Meter Year	10% of pipe diameter (1% of area)	General	Guidelines for quantitative risk assessment. "Purple Book" CPR 18E, ed. 1, 1999
Pipe	Pipe Diameter is between 75 mm to 150 mm	Small Leak	2.00E-06	Per Meter Year	10% of pipe diameter (1% of area)	General	Guidelines for quantitative risk assessment. "Purple Book" CPR 18E, ed. 1, 1999
Pipe	Pipe Diameter Equals 100 mm	Small Leak	2.50E-06	Per Meter Year	Hole diameter from original source was not stated; EIGA assumed 2% flow area	Hydrogen Fueling Process	EIGA, "Determination of Safety Distances," IGC Doc 75/01/E/rev, 2001
Pipe	Pipe Diameter is Greater than 150 mm	Small Leak	3.00E-06	Per Meter Year	5% of flow area	Chemical Process	Rjinmond, Openbaar Lichaam; Risk Analysis of Six Potentially Hazardous Industrial Objects in the Rijnmond Area, A Pilot Study; COVO; 1982

Table C- 1. Generic component leakage frequencies.

Component	Specific Component Type	Severity	Frequency	Units	Leak Size Description	Source Type	Source
Pipe	Pipe Diameter is Less than 75 mm	Small Leak	5.00E-06	Per Meter Year	10% of pipe diameter (1% of area)	General	Guidelines for quantitative risk assessment. "Purple Book" CPR 18E, ed. 1, 1999
Pipe	Pipe Diameter Equals 100 mm	Small Leak	6.00E-06	Per Meter Year	Hole diameter from original source was not stated; EIGA assumed 2% flow area	Hydrogen Fueling Process	EIGA, "Determination of Safety Distances," IGC Doc 75/01/E/rev, 2001
Pipe	Pipe Diameter Equals 100 mm	Small Leak	6.00E-06	Per Meter Year	Hole diameter from original source was not stated; EIGA assumed 2% flow area	Hydrogen Fueling Process	EIGA, "Determination of Safety Distances," IGC Doc 75/01/E/rev, 2001
Pipe	Pipe Diameter is between 50 mm and 150 mm	Small Leak	6.00E-06	Per Meter Year	5% of flow area	Chemical Process	Rjinmond, Openbaar Lichaam; Risk Analysis of Six Potentially Hazardous Industrial Objects in the Rijnmond Area, A Pilot Study; COVO; 1982
Pipe	Pipe Diameter Equals 25 mm	Small Leak	7.50E-06	Per Meter Year	Hole diameter from original source was not stated; EIGA assumed 2% flow area	Hydrogen Fueling Process	EIGA, "Determination of Safety Distances," IGC Doc 75/01/E/rev, 2001
Pipe	No Additional Information	Small Leak	8.01E-06	Per Meter Year	50 gpm (water) or less	Nuclear	Eide, S.A, Khericha, S.T., Calley, M.B., Johnson, D.A., Marteeny, M.L., "Component External Leakage and Rupture Frequency Estimates," EGG-SSRE-9639, Nov 1991.
Pipe	No Additional Information	Small Leak	8.01E-06	Per Meter Year	No definition of leak size was provided	Chemical Process	Savannah River Site, "Generic Data Base Development," WSRC-TR-93-263, June 1993.
Pipe	Pipe Diameter Equals 300 mm	Small Leak	1.00E-05	Per Meter Year	1% cross sectional area	Chemical Process	Cox, A.W., Lees, F.P., Ang, M.L., "Classifications of Hazardous Locations," Institution of Chemical Engineers, 2003
Pipe	Pipe Diameter is Less than or Equal to 50 mm	Small Leak	1.00E-05	Per Meter Year	5% of flow area	Chemical Process	Rjinmond, Openbaar Lichaam; Risk Analysis of Six Potentially Hazardous Industrial Objects in the Rijnmond Area, A Pilot Study; COVO; 1982
Pipe	Pipe Diameter Equals 450 mm	Small Leak	1.10E-05	Per Meter Year	>1 mm	Hydrocarbon Process	Spouge, John, "New Generic Leak Frequencies for Process Equipment, “Process Safety Progress, Vol. 24, No. 4, 2005

Table C- 1. Generic component leakage frequencies.

Component	Specific Component Type	Severity	Frequency	Units	Leak Size Description	Source Type	Source
Pipe	Pipe Diameter Equals 150 mm	Small Leak	2.00E-05	Per Meter Year	>1 mm	Hydrocarbon Process	Spouge, John, "New Generic Leak Frequencies for Process Equipment, “Process Safety Progress, Vol. 24, No. 4, 2005
Pipe	Pipe Diameter Equals 100 mm	Small Leak	3.00E-05	Per Meter Year	1% cross sectional area	Chemical Process	Cox, A.W., Lees, F.P., Ang, M.L., "Classifications of Hazardous Locations," Institution of Chemical Engineers, 2003
Pipe	Pipe Diameter Equals 50 mm	Small Leak	5.70E-05	Per Meter Year	>1 mm	Hydrocarbon Process	Spouge, John, "New Generic Leak Frequencies for Process Equipment, “Process Safety Progress, Vol. 24, No. 4, 2005
Pipe	No Additional Information	Small Leak	8.01E-05	Per Meter Year	No definition of leak size was provided	Compressed Gas	Savannah River Site, "Generic Data Base Development," WSRC-TR-93-263, June 1993.
Pipe	Pipe Diameter Equals 25 mm	Small Leak	1.00E-04	Per Meter Year	1% cross sectional area	Chemical Process	Cox, A.W., Lees, F.P., Ang, M.L., "Classifications of Hazardous Locations," Institution of Chemical Engineers, 2003
Pipe	Pipe Diameter Equals 50 mm	Small Leak	1.00E-04	Per Meter Year	1% cross sectional area	Chemical Process	Cox, A.W., Lees, F.P., Ang, M.L., "Classifications of Hazardous Locations," Institution of Chemical Engineers, 2003
Tubing	No Additional Information	Small Leak	8.01E-04	Per Meter Year	No definition of leak size was provided	Compressed Gas	Savannah River Site, "Generic Data Base Development," WSRC-TR-93-263, June 1993.
Pipe	Pipe Diameter is Greater than 150 mm	Large Leak	1.00E-07	Per Meter Year	20% of flow area	Chemical Process	Rjinmond, Openbaar Lichaam; Risk Analysis of Six Potentially Hazardous Industrial Objects in the Rijnmond Area, A Pilot Study; COVO; 1982
Pipe	Pipe Diameter Equals 100 mm	Large Leak	3.00E-07	Per Meter Year	Hole diameter from original source was not stated; EIGA assumed 20% flow area	Hydrogen Fueling Process	EIGA, "Determination of Safety Distances," IGC Doc 75/01/E/rev, 2001
Pipe	Pipe Diameter is between 50 mm and 150 mm	Large Leak	3.00E-07	Per Meter Year	20% of flow area	Chemical Process	Rjinmond, Openbaar Lichaam; Risk Analysis of Six Potentially Hazardous Industrial Objects in the Rijnmond Area, A Pilot Study; COVO; 1982
Pipe	Pipe Diameter Equals 100 mm	Large Leak	6.00E-07	Per Meter Year	Hole diameter from original source was not stated; EIGA assumed 20% flow area	Hydrogen Fueling Process	EIGA, "Determination of Safety Distances," IGC Doc 75/01/E/rev, 2001

Table C- 1. Generic component leakage frequencies.

Component	Specific Component Type	Severity	Frequency	Units	Leak Size Description	Source Type	Source
Pipe	Pipe Diameter Equals 100 mm	Large Leak	7.50E-07	Per Meter Year	Hole diameter from original source was not stated; EIGA assumed 20% flow area	Hydrogen Fueling Process	EIGA, "Determination of Safety Distances," IGC Doc 75/01/E/rev, 2001
Pipe	Pipe Diameter is Less than or Equal to 50 mm	Large Leak	1.00E-06	Per Meter Year	20% of flow area	Chemical Process	Rjinmond, Openbaar Lichaam; Risk Analysis of Six Potentially Hazardous Industrial Objects in the Rijnmond Area, A Pilot Study; COVO; 1982
Pipe	Pipe Diameter Equals 25 mm	Large Leak	2.00E-06	Per Meter Year	Hole diameter from original source was not stated; EIGA assumed 20% flow area	Hydrogen Fueling Process	EIGA, "Determination of Safety Distances," IGC Doc 75/01/E/rev, 2001
Pipe	Pipe Diameter Equals 300 mm	Large Leak	3.00E-06	Per Meter Year	10% cross sectional area	Chemical Process	Cox, A.W., Lees, F.P., Ang, M.L., "Classifications of Hazardous Locations," Institution of Chemical Engineers, 2003
Pipe	Pipe Diameter Equals 100 mm	Large Leak	6.00E-06	Per Meter Year	10% cross sectional area	Chemical Process	Cox, A.W., Lees, F.P., Ang, M.L., "Classifications of Hazardous Locations," Institution of Chemical Engineers, 2003
Pipe	Pipe Diameter Equals 25 mm	Large Leak	1.00E-05	Per Meter Year	10% cross sectional area	Chemical Process	Cox, A.W., Lees, F.P., Ang, M.L., "Classifications of Hazardous Locations," Institution of Chemical Engineers, 2003
Pipe	Pipe Diameter Equals 50 mm	Large Leak	1.00E-05	Per Meter Year	10% cross sectional area	Chemical Process	Cox, A.W., Lees, F.P., Ang, M.L., "Classifications of Hazardous Locations," Institution of Chemical Engineers, 2003
Pipe	Pipe Diameter Equals 100 mm	Rupture	3.00E-08	Per Meter Year	Hole diameter from original source was not stated; EIGA assumed 100% flow area	Hydrogen Fueling Process	EIGA, "Determination of Safety Distances," IGC Doc 75/01/E/rev, 2001
Pipe	Pipe Diameter Equals 450 mm	Rupture	4.20E-08	Per Meter Year	>50 mm	Hydrocarbon Process	Spouge, John, "New Generic Leak Frequencies for Process Equipment, “Process Safety Progress, Vol. 24, No. 4, 2005

Table C- 1. Generic component leakage frequencies.

Component	Specific Component Type	Severity	Frequency	Units	Leak Size Description	Source Type	Source
Pipe	Pipe Diameter Equals 100 mm	Rupture	6.00E-08	Per Meter Year	Hole diameter from original source was not stated; EIGA assumed 100% flow area	Hydrogen Fueling Process	EIGA, "Determination of Safety Distances," IGC Doc 75/01/E/rev, 2001
Pipe	Pipe Diameter Equals 150 mm	Rupture	7.70E-08	Per Meter Year	>50 mm	Hydrocarbon Process	Spouge, John, "New Generic Leak Frequencies for Process Equipment, “Process Safety Progress, Vol. 24, No. 4, 2005
Pipe	No Additional Information	Rupture	8.01E-08	Per Meter Year	>50 gpm (water) or complete failure	Nuclear	Eide, S.A, Khericha, S.T., Calley, M.B., Johnson, D.A., Marteeny, M.L., "Component External Leakage and Rupture Frequency Estimates," EGG-SSRE-9639, Nov 1991.
Pipe	Pipe Diameter Equals 300 mm	Rupture	1.00E-07	Per Meter Year	100% cross sectional area	Chemical Process	Cox, A.W., Lees, F.P., Ang, M.L., "Classifications of Hazardous Locations," Institution of Chemical Engineers, 2003
Pipe	Pipe Diameter is Greater than or Equal to 150 mm	Rupture	1.00E-07	Per Meter Year	100% of flow area	General	Guidelines for quantitative risk assessment. "Purple Book" CPR 18E, ed. 1, 1999
Pipe	Pipe Diameter Equals 100 mm	Rupture	2.30E-07	Per Meter Year	Hole diameter from original source was not stated; EIGA assumed 100% flow area	Hydrogen Fueling Process	EIGA, "Determination of Safety Distances," IGC Doc 75/01/E/rev, 2001
Pipe	No Additional Information	Rupture	2.67E-07	Per Meter Year	No definition of leak size was provided	Chemical Process	Savannah River Site, "Generic Data Base Development," WSRC-TR-93-263, June 1993.
Pipe	Pipe Diameter Equals 100 mm	Rupture	3.00E-07	Per Meter Year	100% cross sectional area	Chemical Process	Cox, A.W., Lees, F.P., Ang, M.L., "Classifications of Hazardous Locations," Institution of Chemical Engineers, 2003
Pipe	Pipe Diameter is between 75 mm to 150 mm	Rupture	3.00E-07	Per Meter Year	100% of flow area	General	Guidelines for quantitative risk assessment. "Purple Book" CPR 18E, ed. 1, 1999
Pipe	No Additional Information	Rupture	3.20E-07	Per Meter Year	>50 gpm (water) or complete failure	Nuclear	Eide, S.A, Khericha, S.T., Calley, M.B., Johnson, D.A., Marteeny, M.L., "Component External Leakage and Rupture Frequency Estimates," EGG-SSRE-9639, Nov 1991.

Table C- 1. Generic component leakage frequencies.

Component	Specific Component Type	Severity	Frequency	Units	Leak Size Description	Source Type	Source
Pipe	Pipe Diameter Equals 25 mm	Rupture	4.60E-07	Per Meter Year	Hole diameter from original source was not stated; EIGA assumed 100% flow area	Hydrogen Fueling Process	EIGA, "Determination of Safety Distances," IGC Doc 75/01/E/rev, 2001
Pipe	Pipe Diameter Equals 25 mm	Rupture	1.00E-06	Per Meter Year	100% cross sectional area	Chemical Process	Cox, A.W., Lees, F.P., Ang, M.L., "Classifications of Hazardous Locations," Institution of Chemical Engineers, 2003
Pipe	Pipe Diameter Equals 50 mm	Rupture	1.00E-06	Per Meter Year	100% cross sectional area	Chemical Process	Cox, A.W., Lees, F.P., Ang, M.L., "Classifications of Hazardous Locations," Institution of Chemical Engineers, 2003
Pipe	Pipe Diameter is Less than 75 mm	Rupture	1.00E-06	Per Meter Year	100% of flow area	General	Guidelines for quantitative risk assessment. "Purple Book" CPR 18E, ed. 1, 1999
Pipe	No Additional Information	Rupture	2.67E-06	Per Meter Year	No definition of leak size was provided	Compressed Gas	Savannah River Site, "Generic Data Base Development," WSRC-TR-93-263, June 1993.
Tubing	No Additional Information	Rupture	2.67E-05	Per Meter Year	No definition of leak size was provided	Compressed Gas	Savannah River Site, "Generic Data Base Development," WSRC-TR-93-263, June 1993.
Pipe	Small Bore Equals 16 mm	Rupture	5.00E-04	Per Meter Year	100% cross sectional area	Chemical Process	Cox, A.W., Lees, F.P., Ang, M.L., "Classifications of Hazardous Locations," Institution of Chemical Engineers, 2003
Pressure Relief Device							
Pressure Relief Device	All types	Inadvertent opening	2.00E-05	Per Year	Maximum release rate	General	Guidelines for quantitative risk assessment. "Purple Book" CPR 18E, ed. 1, 1999
Pressure Relief Device	Safety relief valve	Inadvertent opening	4.45E-03	Per Year	Maximum release rate	Nuclear	NUREG/CR-6928, "Industry-Average Performance for components and Initiating Events at U.S. Commercial Nuclear Power Plants," February 2007
Pressure Relief Device	Pressure relief valve	Inadvertent opening	8.76E-02	Per Year	Maximum release rate	Nuclear	NUREG-75/014, "Reactor Safety Study: An Assessment of Accident Risks in U.S. Commercial Nuclear Power Plants," WASH-1400, Oct 1975
Pump							
Pump	Canned Pumps	Small Leak	5.00E-05	Per Year	10% of connecting pipe diameter (1% of area)	General	Guidelines for quantitative risk assessment. "Purple Book" CPR 18E, ed. 1, 1999

Table C- 1. Generic component leakage frequencies.

Component	Specific Component Type	Severity	Frequency	Units	Leak Size Description	Source Type	Source
Pump	Pumps	Small Leak	5.00E-04	Per Year	10% of connecting pipe diameter (1% of area)	General	Guidelines for quantitative risk assessment. "Purple Book" CPR 18E, ed. 1, 1999
Pump	Motor-driven	Small Leak	1.01E-03	Per Year	1 to 50 gpm (water)	Nuclear	NUREG/CR-6928, "Industry-Average Performance for components and Initiating Events at U.S. Commercial Nuclear Power Plants," February 2007
Pump	Centrifugal	Small Leak	1.80E-03	Per Year	>1 mm	Hydrocarbon Process	Spouge, John, "New Generic Leak Frequencies for Process Equipment, "Process Safety Progress, Vol. 24, No. 4, 2005
Pump	Pumps	Small Leak	3.00E-03	Per Year	1% cross sectional area of connecting pipe	Chemical Process	Cox, A.W., Lees, F.P., Ang, M.L., "Classifications of Hazardous Locations," Institution of Chemical Engineers, 2003
Pump	Reciprocating	Small Leak	3.70E-03	Per Year	>1 mm	Hydrocarbon Process	Spouge, John, "New Generic Leak Frequencies for Process Equipment, "Process Safety Progress, Vol. 24, No. 4, 2005
Pump	Motor-, Turbine-, and Diesel-Driven	Small Leak	8.76E-03	Per Year	No definition of leak size was provided	Chemical Process	Savannah River Site, "Generic Data Base Development," WSRC-TR-93-263, June 1993.
Pump	Pumps	Large Leak	1.00E-04	Per Year	10% cross sectional area of connecting pipe	Chemical Process	Cox, A.W., Lees, F.P., Ang, M.L., "Classifications of Hazardous Locations," Institution of Chemical Engineers, 2003
Pump	Canned Pumps	Rupture	1.00E-05	Per Year	100% of connecting pipe diameter (1% of area)	General	Guidelines for quantitative risk assessment. "Purple Book" CPR 18E, ed. 1, 1999
Pump	Pumps	Rupture	1.00E-05	Per Year	100% cross sectional area of connecting pipe	Chemical Process	Cox, A.W., Lees, F.P., Ang, M.L., "Classifications of Hazardous Locations," Institution of Chemical Engineers, 2003
Pump	Centrifugal	Rupture	2.40E-05	Per Year	>50 mm	Hydrocarbon Process	Spouge, John, "New Generic Leak Frequencies for Process Equipment, "Process Safety Progress, Vol. 24, No. 4, 2005
Pump	Motor-driven	Rupture	7.05E-05	Per Year	> 50 gpm (water)	Nuclear	NUREG/CR-6928, "Industry-Average Performance for components and Initiating Events at U.S. Commercial Nuclear Power Plants," February 2007

Table C- 1. Generic component leakage frequencies.

Component	Specific Component Type	Severity	Frequency	Units	Leak Size Description	Source Type	Source
Pump	Pumps	Rupture	1.00E-04	Per Year	100% of connecting pipe diameter (1% of area)	General	Guidelines for quantitative risk assessment. "Purple Book" CPR 18E, ed. 1, 1999
Pump	Motor-, Turbine-, and Diesel-Driven	Rupture	4.38E-04	Per Year	No definition of leak size was provided	Chemical Process	Savannah River Site, "Generic Data Base Development," WSRC-TR-93-263, June 1993.
Pump	Reciprocating	Rupture	5.20E-04	Per Year	>50 mm	Hydrocarbon Process	Spouge, John, "New Generic Leak Frequencies for Process Equipment, "Process Safety Progress, Vol. 24, No. 4, 2005
Valve							
Valve	Manual, 2 inch diameter	Small Leak	1.40E-05	Per Year	>1 mm	Hydrocarbon Process	Spouge, John, "New Generic Leak Frequencies for Process Equipment, "Process Safety Progress, Vol. 24, No. 4, 2005
Valve	Manual, 6 inch diameter	Small Leak	4.80E-05	Per Year	>1 mm	Hydrocarbon Process	Spouge, John, "New Generic Leak Frequencies for Process Equipment, "Process Safety Progress, Vol. 24, No. 4, 2005
Valve	Solenoid Operated	Small Leak	8.17E-05	Per Year	1 to 50 gpm (water)	Nuclear	NUREG/CR-6928, "Industry-Average Performance for components and Initiating Events at U.S. Commercial Nuclear Power Plants," February 2007
Valve	No Additional Information	Small Leak	8.76E-05	Per Year	<50 gpm (water)	Nuclear	Eide, S.A, Khericha, S.T., Calley, M.B., Johnson, D.A., Marteeny, M.L., "Component External Leakage and Rupture Frequency Estimates," EGG-SSRE-9639, Nov 1991.
Valve	Air Operated	Small Leak	1.13E-04	Per Year	1 to 50 gpm (water)	Nuclear	NUREG/CR-6928, "Industry-Average Performance for components and Initiating Events at U.S. Commercial Nuclear Power Plants," February 2007
Valve	Motor Operated	Small Leak	1.24E-04	Per Year	1 to 50 gpm (water)	Nuclear	NUREG/CR-6928, "Industry-Average Performance for components and Initiating Events at U.S. Commercial Nuclear Power Plants," February 2007
Valve	Hydraulic-operated	Small Leak	1.30E-04	Per Year	1 to 50 gpm (water)	Nuclear	NUREG/CR-6928, "Industry-Average Performance for components and Initiating Events at U.S. Commercial Nuclear Power Plants," February 2007
Valve	Manual, 18 inch diameter	Small Leak	2.20E-04	Per Year	>1 mm	Hydrocarbon Process	Spouge, John, "New Generic Leak Frequencies for Process Equipment, "Process Safety Progress, Vol. 24, No. 4, 2005

Table C- 1. Generic component leakage frequencies.

Component	Specific Component Type	Severity	Frequency	Units	Leak Size Description	Source Type	Source
Valve	Check	Small Leak	2.58E-04	Per Year	1 to 50 gpm (water)	Nuclear	NUREG/CR-6928, "Industry-Average Performance for components and Initiating Events at U.S. Commercial Nuclear Power Plants," February 2007
Valve	Actuated, 6 inch diameter, non-pipeline	Small Leak	2.60E-04	Per Year	>1 mm	Hydrocarbon Process	Spouge, John, "New Generic Leak Frequencies for Process Equipment, "Process Safety Progress, Vol. 24, No. 4, 2005
Valve	Manual	Small Leak	3.91E-04	Per Year	1 to 50 gpm (water)	Nuclear	NUREG/CR-6928, "Industry-Average Performance for components and Initiating Events at U.S. Commercial Nuclear Power Plants," February 2007
Valve	All types	Small Leak	8.76E-04	Per Year	No definition of leak size was provided	Compressed Gas	Savannah River Site, "Generic Data Base Development," WSRC-TR-93-263, June 1993.
Valve	All Sizes	Small Leak	1.00E-03	Per Year	1% cross sectional area	Chemical Process	Cox, A.W., Lees, F.P., Ang, M.L., "Classifications of Hazardous Locations," Institution of Chemical Engineers, 2003
Valve	All types	Small Leak	4.38E-03	Per Year	No definition of leak size was provided	Chemical Process	Savannah River Site, "Generic Data Base Development," WSRC-TR-93-263, June 1993.
Valve	No Additional Information	Small Leak	1.30E-02	Per Year	Gland leak	Hydrogen Fueling Process	EIGA, "Determination of Safety Distances," IGC Doc 75/01/E/rev, 2001
Valve	All Sizes	Large Leak	1.00E-04	Per Year	10% cross sectional area	Chemical Process	Cox, A.W., Lees, F.P., Ang, M.L., "Classifications of Hazardous Locations," Institution of Chemical Engineers, 2003
Valve	Manual, 6 inch diameter	Rupture	4.80E-07	Per Year	>50 mm	Hydrocarbon Process	Spouge, John, "New Generic Leak Frequencies for Process Equipment, "Process Safety Progress, Vol. 24, No. 4, 2005
Valve	No Additional Information	Rupture	8.76E-07	Per Year	>50 gpm (water) or complete failure	Nuclear	Eide, S.A, Khericha, S.T., Calley, M.B., Johnson, D.A., Marteeny, M.L., "Component External Leakage and Rupture Frequency Estimates," EGG-SSRE-9639, Nov 1991.
Valve	Actuated, 6 inch diameter, non-pipeline	Rupture	1.90E-06	Per Year	>50 mm	Hydrocarbon Process	Spouge, John, "New Generic Leak Frequencies for Process Equipment, "Process Safety Progress, Vol. 24, No. 4, 2005

Table C- 1. Generic component leakage frequencies.

Component	Specific Component Type	Severity	Frequency	Units	Leak Size Description	Source Type	Source
Valve	Manual, 18 inch diameter	Rupture	2.30E-06	Per Year	>50 mm	Hydrocarbon Process	Spouge, John, "New Generic Leak Frequencies for Process Equipment, “Process Safety Progress, Vol. 24, No. 4, 2005
Valve	No Additional Information	Rupture	3.50E-06	Per Year	>50 gpm (water) or complete failure	Nuclear	Eide, S.A, Khericha, S.T., Calley, M.B., Johnson, D.A., Marteeny, M.L., "Component External Leakage and Rupture Frequency Estimates," EGG-SSRE-9639, Nov 1991.
Valve	Solenoid Operated	Rupture	5.72E-06	Per Year	> 50 gpm (water)	Nuclear	NUREG/CR-6928, "Industry-Average Performance for components and Initiating Events at U.S. Commercial Nuclear Power Plants," February 2007
Valve	Air Operated	Rupture	7.88E-06	Per Year	> 50 gpm (water)	Nuclear	NUREG/CR-6928, "Industry-Average Performance for components and Initiating Events at U.S. Commercial Nuclear Power Plants," February 2007
Valve	Motor Operated	Rupture	8.62E-06	Per Year	> 50 gpm (water)	Nuclear	NUREG/CR-6928, "Industry-Average Performance for components and Initiating Events at U.S. Commercial Nuclear Power Plants," February 2007
Valve	Hydraulic-operated	Rupture	9.02E-06	Per Year	> 50 gpm (water)	Nuclear	NUREG/CR-6928, "Industry-Average Performance for components and Initiating Events at U.S. Commercial Nuclear Power Plants," February 2007
Valve	All Sizes	Rupture	1.00E-05	Per Year	100% cross sectional area	Chemical Process	Cox, A.W., Lees, F.P., Ang, M.L., "Classifications of Hazardous Locations," Institution of Chemical Engineers, 2003
Valve	Check	Rupture	1.80E-05	Per Year	> 50 gpm (water)	Nuclear	NUREG/CR-6928, "Industry-Average Performance for components and Initiating Events at U.S. Commercial Nuclear Power Plants," February 2007
Valve	Manual	Rupture	2.73E-05	Per Year	> 50 gpm (water)	Nuclear	NUREG/CR-6928, "Industry-Average Performance for components and Initiating Events at U.S. Commercial Nuclear Power Plants," February 2007
Valve	All types	Rupture	4.38E-05	Per Year	No definition of leak size was provided	Compressed Gas	Savannah River Site, "Generic Data Base Development," WSRC-TR-93-263, June 1993.
Valve	All types	Rupture	2.63E-04	Per Year	No definition of leak size was provided	Chemical Process	Savannah River Site, "Generic Data Base Development," WSRC-TR-93-263, June 1993.

Appendix D
Hydrogen Facility Risk Model

This appendix provides the detailed results of the risk assessment for the four example systems modeled in this quantitative risk assessment. Because both the frequency and consequences of leakage events are dependent upon system pressure and leak diameter, the systems were divided into modules to reflect the different operating pressures and piping diameters within the systems. The exposure frequency for a component is the product of the leakage frequency for the component and the probability a person would be exposed to the resulting hydrogen jet. The component leakage frequency for each module is calculated using the leakage frequency data in Table 4-2 and the number of components in each module which is provided in Table B-2. The probability a person would be exposed to a leak from a component is a function of geometry. Table D-1 presents the basis for geometry (exposure) probabilities used in the study.

Table D-2 provides the total exposure frequency for each module in the four systems analyzed in this study. The total exposure frequency for a module is the sum of all the component contributions in the module. The contribution from each component in the modules is presented as a function of four leak diameters which are calculated for the following fractions of the module pipe area (A): 0.001A, 0.01A, 0.1A, and A. The pipe diameter and operating pressure for each module is provided in Table D-2.

The total frequency for two types of leakage sequences modeled in the analysis (jet fires and flash fires) was calculated. The results are shown in Table D-3. The jet fire sequences represent the potential for immediate ignition of a hydrogen jet immediately after the occurrence of a component leak. A flash fire sequence involves a delayed ignition of a hydrogen jet. A person exposed to a hydrogen flame in either sequence is assumed to receive third-degree burns and thus will have a high probability of dying (probability=1.0). Table D-3 also provides the harm distances associated with both jet fire and flash fire sequences. The harm distances provide the distance out to which a fatality is assumed to occur. For the jet fire sequences, the harm distance is equated to the flame length. The harm distance for the flash fire sequences is equated to the 4% hydrogen concentration envelope. Both harm distances were calculated using the Houf and Schefer models described in Appendix A.

Table D-1. Geometry factors used in QRA.

Component	Geometry Factor	Basis
Pipe	0.125	Component can leak in any direction. Target is assumed bounded by a cone of 45E (Geometry Factor = 45E/360E)
Compressor	0.125	Compressors have multiple leak points which can leak in ay direction. Target is assumed bounded by a cone of 45E (Geometry Factor = 45E/360E)
Valves	0.080	Valves can leak from packing or at either end of the fitting. Valve is assumed to be aligned such that one leak path is pointed at the target. Target is assumed bounded by a cone of 90E from each leak path (Geometry Factor = 90E/360E). Geometry Factor is multiplied by 0.333 to reflect probability that leak occurs in location orientated towards target.
Cylinder	0.125	Same as pipe
Elbow Joint	0.125	Target is assumed bounded by a cone of 90E (Geometry Factor =90E/360E). Since one end of the elbow is assumed orientated towards the target, Geometry Factor is multiplied by 0.5.
Tee Joint	0.080	Similar to valves in that leakage can be from three different points.
Union	0.125	Similar to elbow joint
Ball plugs	0.250	Target is assumed bounded by a cone of 90E (Geometry Factor = 90E/360E). Component assumed orientated to leak towards target.
End Caps	0.250	Similar to ball plugs
Hose	0.125	Same as pipe
Rupture Disk	0.125	Same as pipe
Filter	0.125	Same as pipe

Table D-2. Product of module leakage frequencies and geometry factors.

Leak Diameter (mm)	Compressors	Joints	Cylinders	Hoses	Pipes	Valves	Rupture Disks	Filters	Flanges	Total Exposure Frequency (/yr)
1.72 MPa System										
Pressure Control Module 1 (20.68 MPa - 18.97 mm D)										
0.60	0.00E+00	2.48E-06	0.00E+00	0.00E+00	8.57E-07	3.56E-04	0.00E+00	8.60E-07	0.00E+00	3.60E-04
1.90	0.00E+00	5.49E-06	0.00E+00	0.00E+00	3.31E-07	4.62E-05	0.00E+00	1.91E-06	0.00E+00	5.40E-05
6.00	0.00E+00	4.88E-06	0.00E+00	0.00E+00	1.70E-07	1.98E-05	0.00E+00	1.69E-06	0.00E+00	2.65E-05
18.97	0.00E+00	4.36E-06	0.00E+00	0.00E+00	1.06E-07	6.95E-06	0.00E+00	1.51E-06	0.00E+00	1.29E-05
Instrument Module 1 (20.68 MPa - 6.35 mm D))										
0.20	0.00E+00	1.65E-06	0.00E+00	0.00E+00	0.00E+00	4.15E-04	0.00E+00	0.00E+00	0.00E+00	4.17E-04
0.64	0.00E+00	3.66E-06	0.00E+00	0.00E+00	0.00E+00	5.39E-05	0.00E+00	0.00E+00	0.00E+00	5.76E-05
2.01	0.00E+00	3.25E-06	0.00E+00	0.00E+00	0.00E+00	2.31E-05	0.00E+00	0.00E+00	0.00E+00	2.63E-05
6.35	0.00E+00	2.91E-06	0.00E+00	0.00E+00	0.00E+00	8.10E-06	0.00E+00	0.00E+00	0.00E+00	1.10E-05
Pressure Control Module 2 (1.72 MPa - 52.5 mm D)										
1.66	0.00E+00	2.48E-06	0.00E+00	0.00E+00	8.57E-07	1.78E-04	0.00E+00	0.00E+00	0.00E+00	1.81E-04
5.25	0.00E+00	5.49E-06	0.00E+00	0.00E+00	3.31E-07	2.31E-05	0.00E+00	0.00E+00	0.00E+00	2.89E-05
16.60	0.00E+00	4.88E-06	0.00E+00	0.00E+00	1.70E-07	9.89E-06	0.00E+00	0.00E+00	0.00E+00	1.49E-05
52.50	0.00E+00	4.36E-06	0.00E+00	0.00E+00	1.06E-07	3.47E-06	0.00E+00	0.00E+00	0.00E+00	7.94E-06
Instrument Module 2 (1.72 MPa - 12.70 mm D))										
0.40	0.00E+00	3.44E-06	0.00E+00	0.00E+00	0.00E+00	2.37E-04	0.00E+00	0.00E+00	0.00E+00	2.41E-04
1.27	0.00E+00	7.62E-06	0.00E+00	0.00E+00	0.00E+00	3.08E-05	0.00E+00	0.00E+00	0.00E+00	3.84E-05
4.02	0.00E+00	6.78E-06	0.00E+00	0.00E+00	0.00E+00	1.32E-05	0.00E+00	0.00E+00	0.00E+00	2.00E-05
12.70	0.00E+00	6.06E-06	0.00E+00	0.00E+00	0.00E+00	4.63E-06	0.00E+00	0.00E+00	0.00E+00	1.07E-05
Stanchion (20.68 MPa - 18.97 mm D)										
0.60	0.00E+00	2.58E-06	0.00E+00	2.50E-05	8.57E-07	2.37E-04	0.00E+00	0.00E+00	0.00E+00	2.66E-04
1.90	0.00E+00	5.72E-06	0.00E+00	2.19E-05	3.31E-07	3.08E-05	0.00E+00	0.00E+00	0.00E+00	5.87E-05
6.00	0.00E+00	5.08E-06	0.00E+00	1.95E-05	1.70E-07	1.32E-05	0.00E+00	0.00E+00	0.00E+00	3.79E-05
18.97	0.00E+00	4.54E-06	0.00E+00	9.12E-06	1.06E-07	4.63E-06	0.00E+00	0.00E+00	0.00E+00	1.84E-05

Table D-2. Product of module leakage frequencies and geometry factors.

Leak Diameter (mm)	Compressors	Joints	Cylinders	Hoses	Pipes	Valves	Rupture Disks	Filters	Flanges	Total Exposure Frequency (/yr)
Tube Trailer (20.68 MPa - 12.70 mm D)										
0.40	0.00E+00	3.27E-05	1.22E-06	2.50E-04	6.86E-06	7.71E-04	8.60E-06	0.00E+00	0.00E+00	1.07E-03
1.27	0.00E+00	7.24E-05	8.36E-07	2.19E-04	2.65E-06	1.00E-04	1.91E-05	0.00E+00	0.00E+00	4.14E-04
4.02	0.00E+00	6.44E-05	4.83E-07	1.95E-04	1.36E-06	4.29E-05	1.69E-05	0.00E+00	0.00E+00	3.21E-04
12.70	0.00E+00	5.76E-05	2.60E-07	9.12E-05	8.46E-07	1.50E-05	1.51E-05	0.00E+00	0.00E+00	1.80E-04
20.68 MPa System										
Pressure Control Module (20.68 MPa - 19.97 mm D)										
0.60	0.00E+00	4.95E-06	0.00E+00	0.00E+00	1.71E-06	5.34E-04	0.00E+00	8.60E-07	0.00E+00	5.42E-04
1.90	0.00E+00	1.10E-05	0.00E+00	0.00E+00	6.63E-07	6.93E-05	0.00E+00	1.91E-06	0.00E+00	8.29E-05
6.00	0.00E+00	9.76E-06	0.00E+00	0.00E+00	3.41E-07	2.97E-05	0.00E+00	1.69E-06	0.00E+00	4.15E-05
18.97	0.00E+00	8.72E-06	0.00E+00	0.00E+00	2.11E-07	1.04E-05	0.00E+00	1.51E-06	0.00E+00	2.09E-05
Instrument Module (20.68 MPa - 6.35 mm D)										
0.20	0.00E+00	2.75E-06	0.00E+00	0.00E+00	0.00E+00	6.53E-04	0.00E+00	0.00E+00	0.00E+00	6.56E-04
0.64	0.00E+00	6.10E-06	0.00E+00	0.00E+00	0.00E+00	8.48E-05	0.00E+00	0.00E+00	0.00E+00	9.09E-05
2.01	0.00E+00	5.42E-06	0.00E+00	0.00E+00	0.00E+00	3.63E-05	0.00E+00	0.00E+00	0.00E+00	4.17E-05
6.35	0.00E+00	4.85E-06	0.00E+00	0.00E+00	0.00E+00	1.27E-05	0.00E+00	0.00E+00	0.00E+00	1.76E-05
Stanchion (20.68 MPa - 18.97 mm D)										
0.60	0.00E+00	2.58E-06	0.00E+00	2.50E-05	8.57E-07	2.37E-04	0.00E+00	0.00E+00	0.00E+00	2.66E-04
1.90	0.00E+00	5.72E-06	0.00E+00	2.19E-05	3.31E-07	3.08E-05	0.00E+00	0.00E+00	0.00E+00	5.87E-05
6.00	0.00E+00	5.08E-06	0.00E+00	1.95E-05	1.70E-07	1.32E-05	0.00E+00	0.00E+00	0.00E+00	3.79E-05
18.97	0.00E+00	4.54E-06	0.00E+00	9.12E-06	1.06E-07	4.63E-06	0.00E+00	0.00E+00	0.00E+00	1.84E-05
Tube Trailer (20.68 MPa - 12.70 mm D)										
0.40	0.00E+00	3.27E-05	1.22E-06	2.50E-04	6.86E-06	7.71E-04	8.60E-06	0.00E+00	0.00E+00	1.07E-03
1.27	0.00E+00	7.24E-05	8.36E-07	2.19E-04	2.65E-06	1.00E-04	1.91E-05	0.00E+00	0.00E+00	4.14E-04
4.02	0.00E+00	6.44E-05	4.83E-07	1.95E-04	1.36E-06	4.29E-05	1.69E-05	0.00E+00	0.00E+00	3.21E-04
12.70	0.00E+00	5.76E-05	2.60E-07	9.12E-05	8.46E-07	1.50E-05	1.51E-05	0.00E+00	0.00E+00	1.80E-04

Table D-2. Product of module leakage frequencies and geometry factors.

Leak Diameter (mm)	Compressors	Joints	Cylinders	Hoses	Pipes	Valves	Rupture Disks	Filters	Flanges	Total Exposure Frequency (/yr)
51.71 MPa System										
Pressure Control Module including Instruments (51.71 MPa - 7.9 mm D)										
0.25	0.00E+00	7.70E-06	0.00E+00	0.00E+00	1.71E-06	1.19E-03	0.00E+00	8.60E-07	0.00E+00	1.20E-03
0.79	0.00E+00	1.71E-05	0.00E+00	0.00E+00	6.63E-07	1.54E-04	0.00E+00	1.91E-06	0.00E+00	1.74E-04
2.50	0.00E+00	1.52E-05	0.00E+00	0.00E+00	3.41E-07	6.59E-05	0.00E+00	1.69E-06	0.00E+00	8.32E-05
7.92	0.00E+00	1.36E-05	0.00E+00	0.00E+00	2.11E-07	2.32E-05	0.00E+00	1.51E-06	0.00E+00	3.84E-05
Stanchion (20.68 MPa - 18.97 mm D)										
0.60	0.00E+00	2.58E-06	0.00E+00	2.50E-05	8.57E-07	2.37E-04	0.00E+00	0.00E+00	0.00E+00	2.66E-04
1.90	0.00E+00	5.72E-06	0.00E+00	2.19E-05	3.31E-07	3.08E-05	0.00E+00	0.00E+00	0.00E+00	5.87E-05
6.00	0.00E+00	5.08E-06	0.00E+00	1.95E-05	1.70E-07	1.32E-05	0.00E+00	0.00E+00	0.00E+00	3.79E-05
18.97	0.00E+00	4.54E-06	0.00E+00	9.12E-06	1.06E-07	4.63E-06	0.00E+00	0.00E+00	0.00E+00	1.84E-05
High Pressure Storage Module including Compressor (51.71 MPa -7.9 mm D)										
0.25	2.76E-03	1.81E-05	7.34E-07	1.50E-04	3.43E-06	5.34E-04	0.00E+00	0.00E+00	0.00E+00	3.47E-03
0.79	9.92E-04	4.00E-05	5.02E-07	1.31E-04	1.33E-06	6.93E-05	0.00E+00	0.00E+00	0.00E+00	1.23E-03
2.50	2.62E-05	3.56E-05	2.90E-07	1.17E-04	6.81E-07	2.97E-05	0.00E+00	0.00E+00	0.00E+00	2.09E-04
7.92	4.24E-06	3.18E-05	1.56E-07	5.47E-05	4.23E-07	1.04E-05	0.00E+00	0.00E+00	0.00E+00	1.02E-04
Tube Trailer (20.68 MPa - 12.7 mm D)										
0.40	0.00E+00	3.27E-05	1.22E-06	2.50E-04	6.86E-06	7.71E-04	8.60E-06	0.00E+00	0.00E+00	1.07E-03
1.27	0.00E+00	7.24E-05	8.36E-07	2.19E-04	2.65E-06	1.00E-04	1.91E-05	0.00E+00	0.00E+00	4.14E-04
4.02	0.00E+00	6.44E-05	4.83E-07	1.95E-04	1.36E-06	4.29E-05	1.69E-05	0.00E+00	0.00E+00	3.21E-04
12.70	0.00E+00	5.76E-05	2.60E-07	9.12E-05	8.46E-07	1.50E-05	1.51E-05	0.00E+00	0.00E+00	1.80E-04
103.42 MPa System										
Pressure Control Module including Instruments (103.42 MPa - 7.16 mm D)										
0.23	0.00E+00	7.70E-06	0.00E+00	0.00E+00	1.71E-06	1.19E-03	0.00E+00	8.60E-07	0.00E+00	1.20E-03
0.72	0.00E+00	1.71E-05	0.00E+00	0.00E+00	6.63E-07	1.54E-04	0.00E+00	1.91E-06	0.00E+00	1.74E-04
2.26	0.00E+00	1.52E-05	0.00E+00	0.00E+00	3.41E-07	6.59E-05	0.00E+00	1.69E-06	0.00E+00	8.32E-05
7.16	0.00E+00	1.36E-05	0.00E+00	0.00E+00	2.11E-07	2.32E-05	0.00E+00	1.51E-06	0.00E+00	3.84E-05

Table D-2. Product of module leakage frequencies and geometry factors.

Leak Diameter (mm)	Compressors	Joints	Cylinders	Hoses	Pipes	Valves	Rupture Disks	Filters	Flanges	Total Exposure Frequency (/yr)
Stanchion (20.68 MPa - 18.97 mm D)										
0.60	0.00E+00	2.58E-06	0.00E+00	2.50E-05	8.57E-07	2.37E-04	0.00E+00	0.00E+00	0.00E+00	2.66E-04
1.90	0.00E+00	5.72E-06	0.00E+00	2.19E-05	3.31E-07	3.08E-05	0.00E+00	0.00E+00	0.00E+00	5.87E-05
6.00	0.00E+00	5.08E-06	0.00E+00	1.95E-05	1.70E-07	1.32E-05	0.00E+00	0.00E+00	0.00E+00	3.79E-05
18.97	0.00E+00	4.54E-06	0.00E+00	9.12E-06	1.06E-07	4.63E-06	0.00E+00	0.00E+00	0.00E+00	1.84E-05
High Pressure Storage Module including Compressor (103.42 MPa - 7.16 mm D)										
0.23	2.76E-03	1.81E-05	7.34E-07	1.50E-04	3.43E-06	5.34E-04	0.00E+00	0.00E+00	0.00E+00	3.47E-03
0.72	9.92E-04	4.00E-05	5.02E-07	1.31E-04	1.33E-06	6.93E-05	0.00E+00	0.00E+00	0.00E+00	1.23E-03
2.26	2.62E-05	3.56E-05	2.90E-07	1.17E-04	6.81E-07	2.97E-05	0.00E+00	0.00E+00	0.00E+00	2.09E-04
7.16	4.24E-06	3.18E-05	1.56E-07	5.47E-05	4.23E-07	1.04E-05	0.00E+00	0.00E+00	0.00E+00	1.02E-04
Tube Trailer (20.68 MPa - 12.7 mm D)										
0.40	0.00E+00	3.27E-05	1.22E-06	2.50E-04	6.86E-06	7.71E-04	8.60E-06	0.00E+00	0.00E+00	1.07E-03
1.27	0.00E+00	7.24E-05	8.36E-07	2.19E-04	2.65E-06	1.00E-04	1.91E-05	0.00E+00	0.00E+00	4.14E-04
4.02	0.00E+00	6.44E-05	4.83E-07	1.95E-04	1.36E-06	4.29E-05	1.69E-05	0.00E+00	0.00E+00	3.21E-04
12.70	0.00E+00	5.76E-05	2.60E-07	9.12E-05	8.46E-07	1.50E-05	1.51E-05	0.00E+00	0.00E+00	1.80E-04

Table D-3. Sequence frequencies and harm distances.

	Jet Fire Sequence				Flash Fire Sequence				
Total Exposure Frequency[1] (/yr)	**Immediate Ignition Probability**	**Jet Fire Sequence Frequency[2] (/yr)**	**Cumulative Jet Fire Frequency[3] (/yr)**	**Harm Distance - Flame Length[4] (m)**	**Probability of No Immediate Ignition[5]**	**Delayed Ignition Probability**	**Flash Fire Sequence Frequency[6] (/yr)**	**Cumulative Flash Fire Frequency[7] (/yr)**	**Harm Distance - 4% H2[4] (m)**
1.72 MPa System									
Pressure Control Module 1 (20.68 MPa - 18.97 mm D)									
3.60E-04	0.008	2.88E-06	4.21E-06	1.06	0.992	0.004	1.43E-06	2.08E-06	2.57
5.40E-05	0.008	4.32E-07	1.33E-06	3.36	0.992	0.004	2.14E-07	6.50E-07	8.09
2.65E-05	0.008	2.12E-07	8.97E-07	10.63	0.992	0.004	1.05E-07	4.36E-07	25.55
1.29E-05	0.053	6.85E-07	6.85E-07	33.59	0.947	0.027	3.31E-07	3.31E-07	80.77
Instrument Module 1 (20.68 MPa - 6.35 mm D)									
4.17E-04	0.008	3.34E-06	4.59E-06	0.36	0.992	0.004	1.65E-06	2.27E-06	0.87
5.76E-05	0.008	4.61E-07	1.25E-06	1.13	0.992	0.004	2.29E-07	6.15E-07	2.72
2.63E-05	0.008	2.11E-07	7.94E-07	3.56	0.992	0.004	1.04E-07	3.86E-07	8.56
1.10E-05	0.053	5.84E-07	5.84E-07	11.25	0.947	0.027	2.82E-07	2.82E-07	27.05
Pressure Control Module 2 (1.72 MPa - 52.5 mm D)									
1.81E-04	0.008	1.45E-06	2.22E-06	0.92	0.992	0.004	7.20E-07	1.10E-06	2.22
2.89E-05	0.008	2.31E-07	7.72E-07	2.92	0.992	0.004	1.15E-07	3.77E-07	7.01
1.49E-05	0.008	1.20E-07	5.40E-07	9.22	0.992	0.004	5.93E-08	2.62E-07	22.16
7.94E-06	0.053	4.21E-07	4.21E-07	29.14	0.947	0.027	2.03E-07	2.03E-07	70.08
Instrument Module 2 (1.72 MPa - 12.70 mm D)									
2.41E-04	0.008	1.93E-06	2.96E-06	0.22	0.992	0.004	9.56E-07	1.46E-06	0.54
3.84E-05	0.008	3.08E-07	1.03E-06	0.71	0.992	0.004	1.53E-07	5.05E-07	1.70
2.00E-05	0.008	1.60E-07	7.26E-07	2.23	0.992	0.004	7.92E-08	3.53E-07	5.36
1.07E-05	0.053	5.66E-07	5.66E-07	7.05	0.947	0.027	2.73E-07	2.73E-07	16.96
Stanchion (20.68 MPa - 18.97 mm D)									
2.66E-04	0.008	2.13E-06	3.87E-06	1.06	0.992	0.004	1.05E-06	1.91E-06	2.57
5.87E-05	0.008	4.70E-07	1.75E-06	3.36	0.992	0.004	2.33E-07	8.54E-07	8.09
3.79E-05	0.008	3.03E-07	1.28E-06	10.63	0.992	0.004	1.51E-07	6.21E-07	25.55
1.84E-05	0.053	9.75E-07	9.75E-07	33.59	0.947	0.027	4.70E-07	4.70E-07	80.77

Table D-3. Sequence frequencies and harm distances.

	Jet Fire Sequence				Flash Fire Sequence				
Total Exposure Frequency[1] (/yr)	**Immediate Ignition Probability**	**Jet Fire Sequence Frequency[2] (/yr)**	**Cumulative Jet Fire Frequency[3] (/yr)**	**Harm Distance - Flame Length[4] (m)**	**Probability of No Immediate Ignition[5]**	**Delayed Ignition Probability**	**Flash Fire Sequence Frequency[6] (/yr)**	**Cumulative Flash Fire Frequency[7] (/yr)**	**Harm Distance - 4% H2[4] (m)**
Tube Trailer (20.68 MPa - 12.70 mm D)									
1.07E-03	0.008	8.57E-06	2.40E-05	0.71	0.992	0.004	4.25E-06	1.18E-05	1.72
4.14E-04	0.008	3.31E-06	1.54E-05	2.25	0.992	0.004	1.64E-06	7.52E-06	5.42
3.21E-04	0.008	2.57E-06	1.21E-05	7.11	0.992	0.004	1.27E-06	5.88E-06	17.11
1.80E-04	0.053	9.54E-06	9.54E-06	22.49	0.947	0.027	4.60E-06	4.60E-06	54.08
20.68 MPa System									
Pressure Control Module (20.68 MPa - 19.97 mm D)									
5.42E-04	0.008	4.33E-06	6.43E-06	1.06	0.992	0.004	2.15E-06	3.18E-06	2.57
8.29E-05	0.008	6.63E-07	2.10E-06	3.36	0.992	0.004	3.29E-07	1.03E-06	8.09
4.15E-05	0.008	3.32E-07	1.44E-06	10.63	0.992	0.004	1.65E-07	6.98E-07	25.55
2.09E-05	0.053	1.11E-06	1.11E-06	33.59	0.947	0.027	5.34E-07	5.34E-07	80.77
Instrument Module (20.68 MPa - 6.35 mm D)									
6.56E-04	0.008	5.24E-06	7.24E-06	0.36	0.992	0.004	2.60E-06	3.58E-06	0.87
9.09E-05	0.008	7.27E-07	1.99E-06	1.13	0.992	0.004	3.61E-07	9.75E-07	2.72
4.17E-05	0.008	3.33E-07	1.27E-06	3.56	0.992	0.004	1.65E-07	6.15E-07	8.56
1.76E-05	0.053	9.32E-07	9.32E-07	11.25	0.947	0.027	4.50E-07	4.50E-07	27.05
Stanchion (20.68 MPa - 18.97 mm D)									
2.66E-04	0.008	2.13E-06	3.87E-06	1.06	0.992	0.004	1.05E-06	1.91E-06	2.57
5.87E-05	0.008	4.70E-07	1.75E-06	3.36	0.992	0.004	2.33E-07	8.54E-07	8.09
3.79E-05	0.008	3.03E-07	1.28E-06	10.63	0.992	0.004	1.51E-07	6.21E-07	25.55
1.84E-05	0.053	9.75E-07	9.75E-07	33.59	0.947	0.027	4.70E-07	4.70E-07	80.77
Tube Trailer (20.68 MPa - 12.70 mm D)									
1.07E-03	0.008	8.57E-06	2.40E-05	0.71	0.992	0.004	4.25E-06	1.18E-05	1.72
4.14E-04	0.008	3.31E-06	1.54E-05	2.25	0.992	0.004	1.64E-06	7.52E-06	5.42
3.21E-04	0.008	2.57E-06	1.21E-05	7.11	0.992	0.004	1.27E-06	5.88E-06	17.11
1.80E-04	0.053	9.54E-06	9.54E-06	22.49	0.947	0.027	4.60E-06	4.60E-06	54.08

Table D-3. Sequence frequencies and harm distances.

	Jet Fire Sequence				Flash Fire Sequence				
Total Exposure Frequency[1] (/yr)	**Immediate Ignition Probability**	**Jet Fire Sequence Frequency[2] (/yr)**	**Cumulative Jet Fire Frequency[3] (/yr)**	**Harm Distance - Flame Length[4] (m)**	**Probability of No Immediate Ignition[5]**	**Delayed Ignition Probability**	**Flash Fire Sequence Frequency[6] (/yr)**	**Cumulative Flash Fire Frequency[7] (/yr)**	**Harm Distance - 4% H2[4] (m)**
51.71 MPa System									
Pressure Control Module (51.71 MPa - 7.9 mm D)									
1.20E-03	0.008	9.58E-06	1.37E-05	0.67	0.992	0.004	4.75E-06	6.75E-06	1.62
1.74E-04	0.008	1.39E-06	4.09E-06	2.11	0.992	0.004	6.89E-07	2.00E-06	5.07
8.32E-05	0.008	6.65E-07	2.70E-06	6.64	0.992	0.004	3.30E-07	1.31E-06	15.98
3.84E-05	0.053	2.04E-06	2.04E-06	20.99	0.947	0.027	9.83E-07	9.83E-07	50.48
Stanchion (20.68 MPa - 18.97 mm D)									
2.66E-04	0.008	2.13E-06	3.87E-06	1.06	0.992	0.004	1.05E-06	1.91E-06	2.57
5.87E-05	0.008	4.70E-07	1.75E-06	3.36	0.992	0.004	2.33E-07	8.54E-07	8.09
3.79E-05	0.008	3.03E-07	1.28E-06	10.63	0.992	0.004	1.51E-07	6.21E-07	25.55
1.84E-05	0.053	9.75E-07	9.75E-07	33.59	0.947	0.027	4.70E-07	4.70E-07	80.77
High Pressure Storage Module (51.71 MPa -7.9 mm D)									
3.47E-03	0.008	2.77E-05	4.47E-05	0.67	0.992	0.004	1.38E-05	2.21E-05	1.62
1.23E-03	0.008	9.87E-06	1.69E-05	2.11	0.992	0.004	4.90E-06	8.33E-06	5.07
2.09E-04	0.008	1.67E-06	7.07E-06	6.64	0.992	0.004	8.31E-07	3.43E-06	15.98
1.02E-04	0.053	5.39E-06	5.39E-06	20.99	0.947	0.027	2.60E-06	2.60E-06	50.48
Tube Trailer (20.68 MPa - 12.7 mm D)									
1.07E-03	0.008	8.57E-06	2.40E-05	0.71	0.992	0.004	4.25E-06	1.18E-05	1.72
4.14E-04	0.008	3.31E-06	1.54E-05	2.25	0.992	0.004	1.64E-06	7.52E-06	5.42
3.21E-04	0.008	2.57E-06	1.21E-05	7.11	0.992	0.004	1.27E-06	5.88E-06	17.11
1.80E-04	0.053	9.54E-06	9.54E-06	22.49	0.947	0.027	4.60E-06	4.60E-06	54.08
103.42 MPa System									
Pressure Control Module (103.42 MPa - 7.16 mm D)									
1.20E-03	0.008	9.58E-06	1.37E-05	0.79	0.992	0.004	4.75E-06	6.75E-06	1.93
1.74E-04	0.008	1.39E-06	4.09E-06	2.49	0.992	0.004	6.89E-07	2.00E-06	6.02
8.32E-05	0.008	6.65E-07	2.70E-06	7.87	0.992	0.004	3.30E-07	1.31E-06	18.94

Table D-3. Sequence frequencies and harm distances.

	Jet Fire Sequence				Flash Fire Sequence				
Total Exposure Frequency[1] (/yr)	**Immediate Ignition Probability**	**Jet Fire Sequence Frequency[2] (/yr)**	**Cumulative Jet Fire Frequency[3] (/yr)**	**Harm Distance - Flame Length[4] (m)**	**Probability of No Immediate Ignition[5]**	**Delayed Ignition Probability**	**Flash Fire Sequence Frequency[6] (/yr)**	**Cumulative Flash Fire Frequency[7] (/yr)**	**Harm Distance - 4% H2[4] (m)**
3.84E-05	0.053	2.04E-06	2.04E-06	24.88	0.947	0.027	9.83E-07	9.83E-07	59.82
Stanchion (20.68 MPa - 18.97 mm D)									
2.66E-04	0.008	2.13E-06	3.87E-06	1.06	0.992	0.004	1.05E-06	1.91E-06	2.57
5.87E-05	0.008	4.70E-07	1.75E-06	3.36	0.992	0.004	2.33E-07	8.54E-07	8.09
3.79E-05	0.008	3.03E-07	1.28E-06	10.63	0.992	0.004	1.51E-07	6.21E-07	25.55
1.84E-05	0.053	9.75E-07	9.75E-07	33.59	0.947	0.027	4.70E-07	4.70E-07	80.77
High Pressure Storage Module (103.42 MPa - 7.16 mm D)									
3.47E-03	0.008	2.77E-05	4.47E-05	0.79	0.992	0.004	1.38E-05	2.21E-05	1.93
1.23E-03	0.008	9.87E-06	1.69E-05	2.49	0.992	0.004	4.90E-06	8.33E-06	6.02
2.09E-04	0.008	1.67E-06	7.07E-06	7.87	0.992	0.004	8.31E-07	3.43E-06	18.94
1.02E-04	0.053	5.39E-06	5.39E-06	24.88	0.947	0.027	2.60E-06	2.60E-06	59.82
Tube Trailer (20.68 MPa - 12.7 mm D)									
1.07E-03	0.008	8.57E-06	2.40E-05	0.71	0.992	0.004	4.25E-06	1.18E-05	1.72
4.14E-04	0.008	3.31E-06	1.54E-05	2.25	0.992	0.004	1.64E-06	7.52E-06	5.42
3.21E-04	0.008	2.57E-06	1.21E-05	7.11	0.992	0.004	1.27E-06	5.88E-06	17.11
1.80E-04	0.053	9.54E-06	9.54E-06	22.49	0.947	0.027	4.60E-06	4.60E-06	54.08

Notes:

[1] Total exposure frequency includes leakage contribution from all components in each module and geometry (exposure) probability.

[2] Jet fire sequence frequency = total exposure frequency x immediate ignition probability.

[3] Cumulative jet fire frequency = sum of jet fire sequence frequencies for all sequences in this module below this entry.

[4] Harm distances were calculated using the Houf and Schefer model described in Appendix A.

[5] Probability of no immediate ignition = 1 – immediate ignition probability.

[6] Flash fire sequence frequency = total exposure frequency x probability of no immediate ignition x probability of delayed ignition.

[7] Cumulative flash fire frequency = sum of flash fire sequence frequencies for all sequences in this module below this entry.

Distribution

1	MS 0899	Technical Library, 9536 (electronic copy)


Sandia National Laboratories